Molecular Analysis of Oomycete Pathogens to Identify and Translate Novel Resistance Mechanisms to Crops

Kevin Erwin Fedkenheuer

Dissertation submitted to the faculty of the Virginia Polytechnic Institute and State University in partial fulfillment of the requirements for the degree of

Doctor of Philosophy

In

Plant Pathology, Physiology, and Weed Science

John M. McDowell

Mohammad A. Saghai-Maroof

Bingyu Zhao

Boris A. Vinatzer

05/18/2016

Blacksburg, VA

Keywords: *Glycine max*, Soybean, *R* genes, effector-directed breeding, RXLR proteins, *Phytophthora sojae*

Molecular Analysis of Oomycete Pathogens to Identify and Translate Novel Resistance Mechanisms to Crops

Kevin Erwin Fedkenheuer

ABSTRACT

Disease outbreaks caused by oomycetes can be catastrophic. The first part of this dissertation describes development of a system to identify potential new and durable resistance (*R)* genes against *P. sojae* in soybean germplasm. We developed a system to screen soybean germplasm for genes that recognize core *Phytophthora sojae* RXLR effectors that are conserved within the pathogen species and essential for virulence. *R* genes that recognize these effectors will likely be effective and durable against diverse *P. sojae* isolates. We developed a system to deliver individual *P. sojae* effectors by Type III secretion into soybean using the bacterium *Pseudomonas*, and we screened 12 core effectors on a collection of 30 *G. max* lines that likely contain new resistance genes against *P. sojae*. We identified candidate *R* genes against 10 effectors. Genetic segregation ratios from crosses indicated that three of these genes have a simple inheritance pattern and would be amenable to breeding into elite cultivars. The second part of the dissertation involves use of a model plant-oomycete system to study the genetic basis of susceptibility to oomycete diseases. We compared host transcriptomes from a resistant and a susceptible infection of *Arabidopsis thaliana* by the downy mildew pathogen *Hyaloperonospora arabidopsidis* (*Hpa*). We identified five gene clusters with expression patterns specific to the susceptible interaction. Genes from each cluster were selected and null mutants were tested for altered susceptibility to virulent *Hpa*. Most *A.*

thaliana null mutants showed enhanced disease susceptibility, suggesting their involvement in pattern-triggered immunity (PTI). A knockout mutant in the *At*Gcn5 gene was completely resistant to *Hpa* Emco5 suggesting that the gene/protein is necessary for *Hpa* to successfully colonize the plant. This study provided new molecular insights into plant-oomycete interaction and revealed a plant gene that could potentially be engineered to provide enhanced resistance to oomycete pathogens.

TABLE OF CONTENTS

LIST OF FIGURES

LIST OF TABLES

ACKNOWLEDGMENTS

I would like to thank the many people who have helped me develop scientifically at Virginia Tech. I would like to thank my family and my friends who helped me develop into a responsible professional. I would like to acknowledge funding sources which include USDA-NIFA, NSF, and the TPS program at Virginia Tech. The scientific advisory board which advised our USDA funded work provided necessary technical advice. Francine Govers at Wageningen University and Research Center gave useful scientific insight into the project design and presentation.

I would like to specifically acknowledge Mike G. Fedkenheuer and John M. McDowell for their leadership roles in many projects. The work would not be possible without their valuable contributions. Colin L. Davis should be recognized for his ability to take a leadership role. I would like to thank Joel L. Shuman for his help with disease assays and with organization/travel. I would like to thank Bhadra Gunesekera for her tireless help in making the lab run smoothly.

I would like to recognize M. A. Saghai Maroof for his breeding expertise and for his collaborative spirit. I would like to thank Brett M. Tyler. Brett has made significant revisions to manuscripts and to experimental design. He shares important scientific results freely with us on a weekly basis. Lastly, I would like to thank the committee members who will review my work.

ATTRIUBTIONS

Projects Managed and Maintained by Graduate Students:

Kevin E Fedkenheuer[1]

Michael G Fedkenheuer[1]

Colin L. Davis[2]

Projects Designed and Advised by PhD Advisors:

John M. McDowell[1]

M. A. Saghai Maroof[2]

Brett M. Tyler[3]

[1]Department of Plant Pathology, Physiology, and Weed Science, Virginia Polytechnic Institute, Blacksburg, VA, [2]Department of Crop and Soil Environmental Sciences, Blacksburg, VA, [3]Department of Botany and Plant Pathology, Corvallis, OR

Chapter 1

Recent Advances in Integrated Management of Phytophthora *Root and Stem Rot Disease of Soybean*

Kevin E. Fedkenheuer[1] and John M. McDowell[1*]

[1]Department of Plant Pathology, Physiology, and Weed Science, Virginia Polytechnic Institute, Blacksburg, VA

[*]for correspondence, johnmcd@vt.edu

In preparation for submission to *Phytopathology*.

Some information in this article is available on the Plant Management Network (PMN) as an educational webcast. The PMN is an online plant science network of journals and applied plant information. It provides this information primarily for extension professionals and their audiences. Our webcast, "A Role for Oomycete Biology in the Development of Disease Resistant Soybean", can be viewed at:

http://www.plantmanagementnetwork.org/infocenter/topic/focusonsoybean/ [1]

Author Contributions: KF developed and wrote the manuscript with advice from JM.

Abstract

Oomycete plant pathogens have been identified as a global threat to food security. *Phytophthora sojae*, the causal agent of *Phytophthora* root and stem rot, causes significant yield reduction in soybean annually. This article focuses on recent advances in strategies to mitigate this disease with an emphasis on new tools provided by genome information from the host and the pathogen. For example, it has become clear that *P. sojae* secretes effector proteins into soybean cells to subvert host immunity. Resistance to *Phytophthora sojae* (*Rps*) genes can be used to recognize *P. sojae* and trigger immunity. This is the most cost-effective approach for managing *P. sojae*; however, genetically diverse *P. sojae* can overcome *Rps*-mediated resistance. New *Rps* genes *Rps*8, *Rps*UN1, and *Rps*UN2 have been characterized and will be deployed in the future. Recently, we characterized three potential *Rps* loci in *G. max* and one potential *Rps* locus in *G. soja* using an effectoromics strategy. These loci will likely provide broader and more durable resistance when compared with *Rps* genes that were identified solely with pathogen-based screens. Extension agents from the Midwest USA have all noted a surprising increase in *P. sojae* genetic diversity. Molecular diagnostics are needed to better describe diverse *P. sojae* isolates. By monitoring this diversity in the field with DNA-based diagnostics for fungicide resistance or for loss of *Avr* genes, growers will be able to choose the best tools to manage the pathogen populations in their fields.

Introduction to Oomycete Plant Pathogens

Impact of Oomycetes on Food Security

Plant diseases substantially reduce agricultural productivity. On average, pathogens, animals, and weeds are estimated to reduce global agricultural productivity by 20% - 40% [2]. Diseases can be difficult to manage and unpredictable outbreaks can exacerbate the current food supply deficit [3]. Savary et al. argued that indirect losses due to disease (e.g., post-harvest quality loss and toxin accumulation) drive true yield losses even higher [2]. As global populations grow and as demand for food increases, researchers must develop unique disease management options. These must be robust to pathogens that have demonstrated substantial potential to co-evolve and adapt to current control measures. In this article, we discuss traditionally effective and newly described controls against *Phytophthora sojae*, a destructive oomycete pathogen of one of the world's most important crops.

Oomycetes can cause disease on many plant species [4]. In 2012 and 2014, fungi and oomycetes were labeled by Bebber et al. as the largest threat to global food security [5]. They further suggested that plant monoculture is indirectly selecting for prolific and evolvable microbes [5]. The most notorious oomycete, *Phytophthora infestans*, caused the Irish Potato Famine in the eighteenth century [6, 7]. This blight created a historic food shortage that directly or indirectly afflicted millions, and even today causes an estimated 5 to 6 billion dollars (15% of production) in annual, global losses [8]. Oomycete pathogens can negatively impact trees and ornamentals as well [9]. For example, *Phytophthora ramorum* causes sudden oak death disease and is killing forest oaks in California [7, 9]. It is clear that oomycete diseases are predicted to remain a top threat to global agricultural markets in upcoming years [5].

Classification of Oomycetes

Oomycetes, commonly referred to as water molds, were traditionally classified as phycomycetes or "lower fungi" [6]. Despite similarities in osmotrophic nutrition and filamentous growth, oomycetes and fungi are not closely related [6]. Oomycetes are diploid organisms with cell walls comprised of β-glucan and cellulose [6, 10]. Fungi can be haploid or dikaryotic and their cell walls are composed mainly of chitin [6]. Additionally, fungi and oomycetes differ in reproduction strategies and in spore formation [6]. Many oomycetes produce motile spores called zoospores [4]. Oomycete zoospores have an anterior "tinsel" flagellum and a posterior "whiplash" flagellum [4]. The Chytridiomycota (chytrids) is the only phylum of true fungi to produce zoospores, and chytrid zoospores are generally propelled by a single posterior flagellum [11]. These distinctions supported oomycete placement in the kingdom Chromalveolata [4, 6]. This was validated by DNA analysis of intergenic regions [12]. In a distance based analysis of multiple DNA sequences, oomycetes were found to be genetically dissimilar to fungi [12]. Widely supported, these results validated morphological evidence which supported the oomycete and fungi separation [12].

The class Oomycota (oomycetes) belong to the phylum *Heterokontophyta* or *Stramenopila* [4]. In the order *Leptomitales*, the *Aphanomycetes*, *Pythiaceae*, *Albuginaceae*, and *Peronosporaceae* families contain the majority of oomycete plant pathogen species [7, 13, 14]. *Pythiaceae* include the important genera *Pythium* and *Phytophthora* [14]. The *Albuginaceae* is comprised of white rusts, and downy mildews are represented in the *Peronosporaceae* [14]. Nearly all oomycete plant pathogens form a monophyletic subclass, the *Peronosporomycetidae*, indicating that pathogenicity on plants likely evolved from an ancestor of the class [7].

The genus of most oomycete plant pathogens can be identified by microscopic examination of asexual reproductive structures [13]. Species can be determined by morphological differences in sexual structures and/or by DNA sequencing of target regions [13, 15]. Numerous primers have been designed to amplify internal transcribed spacer (ITS), large subunit of rRNA (LSU), and small subunit of rRNA (SSU) [13, 15]. A list of experimentally validated diagnostic primers are listed in Table 1 [16-18].

Phytophthora ***Root and Stem Rot Disease on Soybean***

Soybean Production

Cultivated soybean, *Glycine max*, was likely domesticated in China 6,000 to 9,000 years ago [19]. It is commonly accepted that *G. max* diverged from *G. soja* but some mysteries still surround the divergence [19, 20]. Soybean is harvested for the abundant quantities of oil and protein in its seed [21]. After the soybeans are crushed and oil is extracted, the cake-like remains are marketed as soybean meal, which is an important food source for animals and fish [22].

In 2014, the US devoted 31% of its cropping area to soybean, and remained the top producer of soybean [23]. The USA has historically led soybean production and export [23]. However, the steady growth of emerging soybean markets in Brazil and Argentina during the 1990s decreased the USA share in world soybean production [24]. An estimated 93% of global soybean production is transgenic for herbicide tolerance (Roundup Ready, or RR) [25]. A combination of RR and no-tillage systems make large-scale soybean production an attractive land use option [22]. However, scale-up in soybean production has had negative effects particularly in developing nations. These include the assimilation of traditional farming systems and deforestation, as exemplified by the impact of soybean production on rainforests in South

America [22]. Thus, it is essential to develop tools through which soybean production is efficient and environmentally sustainable.

History of Phytophthora *Root and Stem Rot*

The first documented outbreak of *Phytophthora* root and stem rot occurred c. 1954 [26]. *Phytophthora sojae* was formerly known as *Phytophthora cactorum*, *Phytophthora Megasperma* Drechsler var. s*ojae*, and *Phytophthora Megasperma* f.sp. *glycinea*. The designations "var." and "f. sp." refer to variety and *forma specialis* respectively. The variety designation typically describes virulence on a compatible host. *Forma specialis*, implies a taxonomic distinction based on morphological differences. Little is known about the origin of *Phytophthora* root and stem rot [27]. Because *P. sojae* was first identified during large-scale soybean deployment in the Midwest, it was likely a pathogen indigenous to the United States of America (USA) [27]. Since its identification, *P. sojae* has been reported in nine soybean-growing countries [28]. *P. sojae* has been described as a pathogen of lupines [29]. Common in the USA, lupines are flowering plants from the legume family *Fabracea* [29]. This suggests that *P. sojae* had the potential to exist on lupines in the Midwest prior to the introduction of cultivated soybean, *Glycine max*.

Agronomic Impact

To examine disease impact on soybean over time, Wrather et al. summarized yield suppression in the USA from 1996 to 2007 [30]. In all years, soybean cyst nematode (SCN) disease was the most severe disease [30]. In seven out of the twelve years, *P. sojae* was the second strongest yield suppressor [30]. Yield suppression by *P. sojae* was consistent over twelve years [30]. In comparison, SCN yield suppression decreased over time [30]. Wrather et al. estimated 2006 soybean yield loss from *Phytophthora* root and stem rot disease at 1.46 million metric tonnes (million t.) in the USA and 2.32 million t. worldwide [31]. Soybean production

was 83.4 million t. and 220.4 million t. in the USA and worldwide, respectively [31]. Thus, *P. sojae* is estimated to be responsible for a yield reduction of 1.75% in the USA and 1.05% worldwide. If annual yield losses remain constant, *Phytophthora* root and stem rot will cost global soybean markets billions of dollars over time. New and durable disease resistance would obviously benefit producers and consumers.

To determine the most important oomycete plant pathogens, Kamoun et al. surveyed oomycete biologists worldwide [32]. They recorded 263 votes from 62 scientists across 15 countries to determine the top ten oomycete plant diseases based on scientific and economic importance [32]. The vote suggested 33 important species [32]. *P. sojae* ranked fifth for its agronomic importance and utility as a model oomycete pathogen [32].

Disease Progression and Plant Resistance

P. sojae *Life Cycle*

P. sojae overwinters in soil and plant debris as oospores that can persist in the soil for years [33, 34]. When conditions are permissive, oospores germinate directly as hyphae or to produce sporangia [33, 34]. Sporangia contain asexual zoospores [33, 34]. Zoospores swim toward soybean root exudates and encyst [35]. Encysted zoospores penetrate root tissue as intercellular hyphae [33-35]. In a compatible infection, *P. sojae* emerges from the host producing sporangia [33, 34]. Asexual reproduction will dominate until the end of the growing season [34]. An early-season *P. sojae* outbreak will cause seedling rot and damping-off [34]. A late-season *P. sojae* outbreak will cause root and/or stem rot on mature plants [34]. The visual symptoms include a stem rot lesion which precedes foliar symptoms [28]. A severe infection may cause plants to wilt and die [28].

Soybean Pattern-Triggered Immunity

Most plants have three layers of defense against prospective pathogens. The first comprises pre-formed barriers such as a waxy leaf surface, hairs, or cell walls [36]. The next layer of plant defense is referred to as pattern-triggered immunity (PTI) [37]. PTI is a generic immune response that is activated when plant pattern recognition receptors (PRRs) recognize pathogen-associated molecular patterns (PAMPS) [38]. PAMPs are conserved molecules such as bacterial flagellin, elongation factor Tu (EF-Tu), chitin, and β-glucan [38]. Many oomycete PAMPs such as cellulose binding elicitor lectins (CBELs) are secreted proteins [38]. PTI cellular responses at the infection site include callose deposition at the cell walls, reactive oxygen species (ROS) production, and secretion of defense compounds [36-39].

The first identified oomycete PAMP was a beta-glucan fragment from *P. soja* cell walls which elicited phytoalexin (antibiotic) accumulation in soybean [40]. During early infection, soybean β-1,3 glucanase attacks the pathogen cell wall, releasing active β-glucan elicitors (GE) that stimulate phytoalexin production [41]. *P. sojae* GE was reported to interact with a GE-binding protein (GEBP) in soybean root cells [41]. The second oomycete PAMP was identified as a 13 amino acid peptide (Pep-13) from a *P. sojae* which elicited a defense response in parsley [42]. Pep-13 is a surface-exposed fragment within the calcium-dependent transglutaminase (TGase) protein GP42 [42, 43]. Pep-13 is conserved among *Phytophthora* TGases and can activate defense responses in potatoes and parsley [43]. This suggests Pep-13 may activate both host and non-host resistance [43].

P. sojae *Subverts Soybean Immunity by Secreting Effector Proteins*

P. sojae enters root tissue of developing seedlings [34]. When growing inside the host as intercellular hyphae, *P. sojae* interacts with soybean cells using specialized feeding structures called haustoria [33, 36, 39]. A haustorium is formed when pathogen hyphae invaginate the host cell wall [36, 39]. *P. sojae* extracts nutrients and secretes virulence proteins at this interface [36, 39]. If successful, this effector-triggered susceptibility (ETS) leads to a compatible interaction [36].

P. sojae virulence proteins are referred to as effectors. By definition, effector proteins are secreted from the pathogen and serve virulence functions on the outside or inside of plant cells. One of the most important findings from oomycete functional genomics is that oomycete plant pathogens contain large repertoires of effector-encoding genes in their genome. Effector-encoding genes can be grouped into superfamilies based on representative sequence motifs [44]. The best-studied effector superfamily is referred to as “RXLR”, after the motif Arg-(any amino

acid)-Leu-Arg. [44]. RXLR effectors have an N-terminal signal peptide that is followed by a RXLR motif, a short "dEER" region of acidic amino acids, and a domain which executes specific virulence functions of each protein [45]. *Phytophthora* RXLR effectors are secreted from haustoria, to the extrahaustorial matrix, and finally to the plant plasma membrane [45]. This trafficking is likely mediated by the N-terminal RXLR-dEER [44, 45].

Research on *P. sojae* has been at the forefront of this emerging area. In 2008, the first genome-wide inventory of RXLR genes for any oomycete was provided by Tyler et al. They identified 385 candidate RXLR effectors in *P. sojae* which were named as "avirulence homologs (*Avh*)" [44]. These *Avh* genes are located in areas of the genome which are rapidly evolving and are often located near synteny break points [44]. Interestingly, no *P. sojae Avh* gene showed greater than 30-50% sequence homology to *Phytophthora ramorum*, providing the first demonstration of the rapidity with which RXLR effectors can evolve [44]. *Avh* genes appear to have undergone extensive gene duplication and divergence [44]. Many *P. sojae Avh* effectors contain W, Y, and L motifs that are predicted to play a role in effector function [44, 46]. The positioning of RXLR effectors in the genome promotes rapid evolution of effectors by re-arrangement of WY motifs.

A large number of candidate *P. sojae* effectors were differentiated by transcription and sequence variation [47]. About 12% of effector genes showed a high degree of polymorphism and evidence of positive selection [47]. Many of the 169 tested effectors suppressed an exogenously applied elicitor of cell death [47]. Two classes of early expressed effectors were identified [47]. One set that was expressed immediately upon infection suppressed cell death caused by other early expressed effectors [47]. The other set suppressed the cell death elicitor

[47]. Wang et al. suggests that these differentially expressed effectors function in different defense response pathways [47].

Crinkler (CRN) effectors were first identified in *Phytophthora infestans* for causing leaf-crinkling when exogenously expressed [48]. CRNs have an effector domain and a conserved N-terminal motif, FLAK [49, 50]. The FLAK motif is predicted to translocate CRN effectors into host cells [49]. Recently, Stam et al. discovered that many of the 84 full length Phyt*ophthora capsici* CRN likely target host nuclear processes [51]. In *P. sojae*, *Ps*CRN63 and *Ps*CRN115 were identified [52]. Despite sequence similarities, *Ps*CRN63 elicits cell death and *Ps*CRN115 suppressed cell death elicitors in *N. benthamiana* [52]. In 2014, Rajput et al. characterized *Ps*CRN70 suppression of all known cell death elicitors in *N. benthamiana* [53]. This suggests *Ps*CRN70 may be a broad suppressor of cell death [53]. Similar to most CRNs, *Ps*CRN63, *Ps*CRN115, and *Ps*CRN70 localize to the plant cell nucleus [52, 53]. The virulence function of CRN effectors is predicted to interfere with host nuclear processes [53].

It is commonly accepted that the RXLR motif is involved in cell entry but this process is not fully understood [54]. In 2007, Whisson et al. used the *Avr/R* interaction between *Phytophthora infestans Avr*3a and the potato *R* gene *R3a* as a proxy for effector entry into host cells [55]. The *Avr*3a RXLR-dEER domain was mutagenized and constructs were inoculated on *R3a* for comparison to WT *Avr*3a on *R3a* [55]. Amino acid mutations in the RXLR-dEER of *Avr*3a prevented recognition by *R3a* [55].

In 2008, Dou et al. exploited the *Avr/R* interaction between *P. sojae* effector *Avr*1b and soybean *Resistance to Phytophthora sojae* (Rps) 1b [56]. Differences between the two *Avr*1b domains suggested that sequences surrounding the RXLR were important for effector entry [56]. To visualize cell entry, soybean roots were exposed to high levels of *Avr*1b-GFP and shown to

uptake the protein. Mutations in the RXLR and dEER prevented protein uptake into soybean roots [56]. In total, their results suggest that the RXLR-dEER translocate effectors into host cells [56]. In the same year, Dou et al. published that mutations in the W and Y motifs can reduce or abolish *Avr*1b cell death suppression [57]. These motifs are likely important in diverse effector functions [57].

Functional testing with *P. sojae* effectors *Avr*1k and *Avr*1b suggest that the RXLR domain is important for effector entry into soybean cells [44]. When the RXLR domain was deleted from *Avr*1k or *Avr*1b, the effectors could no longer trigger a HR on soybean leaves containing cognate *R* genes *Rps*1k or *Rps*1b, respectively [44]. In 2010, Kale et al. reported that RXLR motifs enable binding to phosphatidylinositol-3-phosphate (PI3P) [58]. An abundant quantity of PI3P was discovered on the plant cell membrane [58]. They suggested effector entry into plant cells by lipid raft-mediated endocytosis [58].

In 2011, Yaeno et al. disputed Whisson et al., Dou et al., and Kale et al. They found that mutations in the RXLR domain does not abolish *Avr*3a binding to *R3a* [59]. Instead, they implicate a positively charged patch of amino acids in the effector domain for binding phosphatidyl inositol monophosphates (PIPs) [59]. They suggest the mechanism for Avr3a entry into host cells by PIP [59]. In 2012, Wawra et al., suggested that *Avr*3a produces homodimers and that mutations in the *Avr*3a RXLR domain attenuate dimerization and entry into host cells [60]. They suggest that the effector domain likely guides entry into host cells [60].

The debate surrounding effector entry into host cells is incomplete. The mechanism of Avr3a entry into host cells remains unclear, and only indirect evidence was reported which disputes *Avr*1b RXLR mediated effector entry into host cells. Effector entry into host cells is likely a complex process that will require community-wide effort to solve.

Disease Management

Introduction to Effector-Triggered Immunity

Plant *R* proteins recognize pathogen effectors [36, 39]. A recognition event produces a robust immune response which is characterized by localized cell death (i. e. hypersensitive response, HR). This robust response is referred to as effector-triggered immunity (ETI), and it impedes pathogen growth [36, 39]. ETI thereby comprises the third and most powerful layer of plant defense. ETI also represents the molecular basis for the genetic term "gene-for-gene resistance", in which plant resistance genes ("*R* genes") provide resistance to pathogens that contain cognate avirulence genes ("*Avr* genes"). Known *Avr/R* interactions are commonly used to validate effector function and to determine complex molecular mechanisms.

Resistance to Phytophthora sojae *(*Rps*) Genes*

Genetic resistance can provide full protection against *P. sojae* in the field, without additional input from the grower. This is a key component of integrated disease management. Twenty-four *Rps* genes have been documented within *G. max* [33, 34, 44, 61]. These comprise *R* genes that conform to the predictions of the aforementioned "gene-for-gene" model. Seven *Rps* genes are available in commercial cultivars (*Rps*1a, *Rps*1b, *Rps*1c, *Rps*1k, *Rps*3a, *Rps*6, and *Rps*8) [34]. The cognate *P. sojae* Avr genes for six of these seven genes (excepting *Rps*8) have been identified as RXLR genes [34]. *Avr*1a, *Avr*1b, *Avr*1c, *Avr*1k, *Avr*3a/5, *Avr*3b, *Avr*3c, and *Avr*4/6 are recognized *P. sojae* RXLR effectors [33]. Unfortunately, a single *Rps* gene does not protect against all *P. sojae* isolates [33, 34, 61]. Due to pathogen co-evolution, *Rps* genes become ineffective 8 to 15 years following significant geographic deployment [62].

In 2003, Burnham et al. identified that the *Rps*8 locus was contained in South Korean germplasm [63]. When the accession containing *Rps*8 was crossed with susceptible cultivar

Williams, the authors noted an intense segregation distortion [64]. The accession containing *Rps*8 was crossed to a PI containing multiple *R* genes [64]. In populations derived from this cross, the locus segregated by Mendelian genetics [64]. Ortega and Dorrance mapped the *Rps*8 locus to a 2.23 Mb region which is located on chromosome thirteen in 2011 [64]. The segregation distortion caused by crossing the *Rps*8 accession with Williams was possibly due to meiotic abnormalities in the offspring of the cross used for mapping [64].

In 2013, *Rps*UN1 and *Rps*UN2 were identified [65]. An accession with robust resistance against *P. sojae* resistance was crossed with susceptible cultivar Williams [65]. From this cross, they generated 245 F2 individuals and 403 $F_{2:3}$ families [65]. *Rps*UN1 mapped to a 6.5 cM region on the *Rps*1 locus on chromosome three and *Rps*UN2 mapped to a 3.0 cM region upstream of *Rps*2 on chromosome sixteen [65]. A screen with sixteen *P. sojae* isolates indicated that *Rps*UN1 is likely a novel allele at the *Rps*1 locus and *Rps*UN2 is likely a novel *Rps* gene.

The first soybean *Rps* gene which recognizes two *P. sojae Avr* effectors was recently described [66]. *Avr*1k and *Avr*1b silencing and overexpression constructs were transformed into *P. sojae* [66]. The transformed isolates were tested for virulence on *Rps*1k [66]. *P. sojae* isolates with both mutant alleles in *Avr*1k and in *Avr*1b were able to evade recognition by *Rps*1k [66]. These observations show that *Rps*1k recognizes *Avr*1k and *Avr*1b [66]. Therefore, we should not expect every *R* gene to work in a single "gene-for-gene" interaction [66].

Genomic information can be exploited to improve and accelerate disease resistance breeding [67]. Effector-directed breeding uses effector(s) to probe diverse germplasm for *Avr/R* interactions, typically characterized by a HR [67]. This strategy can accelerate disease resistance breeding against many plant pathogens [68]. Using this method, non-host plants are amenable to

screening. It is applicable to any pathogen with a sequenced genome and with identifiable effectors [69]. Specific effectors can be targeted by this approach [69].

Research on a different soybean disease helped lay the foundation for this approach, when Staskawicz et al. determined *Pseudomonas syringae pathovar glycinea* (*Psg*) race compatibility on soybean in the 1980s [70, 71]. They successfully characterized two *Avr* genes from *Psg* race 0 and race 1, *Avr*B and *Avr*C [71]. The discovery of *Avr*B1 provided evidence of an *Avr/R* interaction between *Avr*B1 and the *Resistance to Pseudomonas syringae pv glycinea* (*Rpg*) 1 locus [71]. In 1991, Keen and Buzzell suggested that *Rpg*4 was likely providing soybean immunity to *Pseudomonas* carrying *Avr*D [72]. These results suggest that *R* genes may confer non-host resistance.

The first example of effector-directed breeding against an oomycete disease was reported in 2008 by Vleeshouwers et al. They used effectoromics to identify new *R* genes against potato late blight [67]. Agrobacterium-mediated transient transformation was used to deliver 54 *Phytophthora infestans* effectors to wild *Solanum* [67]. The RXLR family IpiO produced a HR on three related wild *Solanum* species [67]. Using a heterologous system in *Nicotiana benthamiana*, an *Avr/R* interaction between *Avr*-blb1 and *Rpi*-blb1 was uncovered [67]. These new *R* genes are currently being developed for commercial deployment in potato, for which new sources of late blight resistance are urgently needed.

Most recently, we used effector-directed breeding to identify potential *Rps* genes against core *P. sojae* effectors [69]. By definition, core effectors are highly expressed in early infection, conserved in field isolates, and necessary for virulence [69]. A *Rps* gene against a core *P. sojae* effector will likely be more durable and more effective against field isolates when compared to a

conventional *R* gene [69]. *P. sojae* effectors *Avh*16, *Avh*180, and *Avh*240 best fit the core effector criteria [69].

We developed a bacterial *Pseudomonas* system to deliver individual *P. sojae* effectors by Type III secretion into soybean leaf cells [69]. Soybean germplasm that developed a HR in response to core *P. sojae* effector(s) were crossed with *P.sojae*-susceptible cultivar Williams [69]. Gm32 likely contains *R* genes that recognize *Avh*16 and *Avh*240 [69]. Gm326 likely contains an *R* gene that recognizes *Avh*180 [69]. Our screen also uncovered potential *R* genes against seven additional core effectors. We intend to map these loci in RI lines by assessing *Avr/R* interactions in effector and pathogen assays [69].

To uncover additional sources of *P. sojae* resistance, we optimized this system for use in wild soybean, *Glycine soja* [73]. By screening *P. sojae* resistant *G. soja* germplasm, we observed additional *Avr/R* interactions [73]. Gs2292 likely contains an *R* gene that recognizes *Avh*240 [73]. Gs2763, gs730, and gs727 were incompatible with *Psg* race 4 which suggests new *Rpg* loci [73]. Traditional breeding can be used to transfer loci between sexually compatible *G. max* and *G. soja* [73]. These results suggest that wild soybean is a valuable source of disease resistance [73]. Effector-directed breeding offers long term disease management against diverse *P. sojae* isolates.

Cultural Practices and Chemical Controls for Managing Phytophthora *Root and Stem Rot*

Integrated management strategies which utilize host resistance, good cultural practice, and chemical treatment are the most effective for disease control [34]. An effective cultural practice is to improve soil drainage with drain tiles and tillage [34]. Tillage is expensive, time consuming, and increases soil erosion [74]. Since tillage offers little yield improvement, it is not typically recommended for soybean [74]. However, tillage is a useful tool for pathogen

management [74]. An understanding of field conditions is essential for determining when tillage is appropriate [74].

P. sojae infects soybean optimally in the range of 25 to 30°C [75]. Thus, early planting can lead to increased incidence of seedling disease in field settings [75]. Early planting often creates a scenario that favors pathogen virulence and negatively effects plant health [75]. Because *P. sojae* produce oospores, it is not recommended to leave plant material in the field, a common practice in conservation tillage [75]. Seed treatments are most effective against *P. sojae* infection [34]. Mefenoxam, metalaxyl, and ethaboxam are the most effective seed treatments [34]. Although effective at preventing early season damping-off, these treatments are not effective against mid-season disease [34]. These chemicals are frequently used as seed treatments [34]. Increasing the concentration of these chemicals produces higher levels of resistance to *P. soja* [34]. Oomycete pathogens have demonstrated the ability to adapt to chemical control mechanisms [34]. *P. sojae* was intolerant to Mefenoxam or metalaxyl throughout an intensive four year survey between 2001 and 2005 [34]. However, *P. sojae* isolates with resistance against these fungicides will likely emerge. Identification and management of resistant races will become easier as fungicide resistance genes are cloned using functional genomics, and DNA assays are designed to identify resistant races. By combining chemical treatment and good cultural practice with genetic resistance, growers can more effectively manage disease outbreaks.

P. sojae *Genetic Diversity*

Pathotype and Race

In 1984, 37 different *P. sojae* races have been described [27]. Over the last 20 years, more than 50 new races of *P. sojae* have been discovered [76]. *P. sojae* genetic structure has been traditionally determined by testing isolate virulence on soybean *Rps* cultivars [34]. Each isolate is assigned a pathotype to designate which *Rps* genes it defeated [34]. For example, an isolate which defeated *Rps*1k, *Rps*1b, and *Rps*7 would be given the pathotype *1k, 1b, 7* [34].

After determining pathotype, a race number is assigned [34]. The race designation is a numerical code used to simplify pathotype designations [34]. The race distinction is useful to characterize a few well-known *P. sojae* isolates [34]. If too much complexity is added, the race system loses its value. Before this happens, a community decision should be made to describe isolates by pathotype or by a unique metric. One option is to phenotype *P. sojae* isolates on less *Rps* cultivars. This would decrease pathotype and race complexity. The most practical and informative *Rps* cultivars may be sufficient for virulence phenotyping. Another option is to develop a molecular diagnostic that produces relevant isolate information.

For *P. sojae* detection, Rojas et al. designed one genus-specific and two species-specific qPCR probes which bind mitochondrial DNA from *Phytophthora* [77]. Species specific probes can be used to identify *P. sojae* [77]. These probes were validated to diagnose *P. sojae* and other *Phytophthora* from symptomatic plants [77]. Although useful for *P. sojae* identification, additional molecular tools are required to distinguish isolates at the race level [77].

Diversity in the Midwest USA

It is important to understand the genetic diversity of *P. sojae* in the field to determine proper management options. This data informs us which *Rps* cultivars will be effective against future disease outbreaks. In the USA, *P. sojae* diversity has been examined in detail in Ohio, Iowa, Illinois, and Michigan.

Schmitthenner et al. analyzed pathogen diversity in Ohio [62]. They determined that the efficacy of *Rps* resistance in Ohio, mediated by *Rps*1k, has deteriorated over ten years [62]. Isolates which defeated *Rps*1k were isolated and pathotyped. They reported an increase in isolates which overcome *Rps*1k-mediated resistance from 1978 to 1991 [62]. *P. sojae* race 7 and race 3 were the most prevalent during the 1980s and early 1990s, respectively.

During the 1990s, Yang et al. characterized *P. sojae* pathotypic diversity in Iowa. *P. sojae* race 3 and race 1 were the most prevalent isolates found on diseased plants and in soil samples respectively [78]. In 1997, Leitz et al. reported a majority of *P. sojae* races 1, 3, and 4 in soil samples from Illinois [79]. They noted more pathotypic diversity and characterized new isolates, one of which defeated *Rps*1k mediated resistance [79].

In 2001, R. C Kaitany characterized virulence of Michigan isolates [80]. He reported *P. sojae* races 2, 25, 41, and 44 which were identified for the first time in Michigan [80]. To better manage the disease in Michigan, he suggested incorporating *Rps1b, Rps1k, Rps3a, Rps3b,* and *Rps6* into cultivars with good field tolerance [80]. All of these studies note a surprising increase in *P. sojae* diversity. In the future, we may be able to use molecular markers, to quickly determine *P. sojae* genetic diversity. This information can tell us which soybean *Rps* cultivar(s) will be most effective.

Figures and Tables

Table 1.1 Experimentally validated diagnostic primers that target ITS and LSU regions are listed. Primer pairings include: ITS1 and ITS2 (ITS-1 region), ITS1 and ITS4 (ITS-1 and ITS-2 regions), ITS3 and ITS4 (ITS-2 region), UN-up18S42 and UN-lo28S1220 (ITS and LSU regions), and UN-up18S42 and UN-lo28S22 (ITS region).

Primer	Sequence (5' to 3')
ITS1	TCCGTAGGTGAACCTGCGG
ITS2	GCTGCGTTCTTCATCGATGC
ITS3	GCATCGATGAAGAACGCAGC
ITS4	TCCTCCGCTTATTGATATGC
UN-up18S42	CGTAACAAGGTTTCCGTAGGTGAAC
UN-lo28S1220	GTTGTTACACACTCCTTAGCGGAT
UN-lo28S22	GTTTCTTTTCCTCCGCTTATTGATATG

Chapter 2

Effector-Directed Screens for New Disease Resistance Genes against the Soybean Root and Stem Rot Pathogen Phytophthora sojae

Kevin E Fedkenheuer[1], Michael G Fedkenheuer[1], Colin L. Davis[2], Joel L. Shuman[1], Nick A. Dietz[1], Brett M. Tyler[3], M. A. Saghai Maroof[2], and John M. McDowell[1*]

[1]Department of Plant Pathology, Physiology, and Weed Science, Latham Hall, Virginia Tech. Blacksburg, VA 24060-0390

[2]Department of Botany and Plant Pathology, Oregon State University, Corvallis, OR

[3]Department of Crop, Soil, and Environmental Sciences, Latham Hall, Virginia Tech, Blacksburg, VA 24060-0390

[*]for correspondence, johnmcd@vt.edu

In preparation for submission to *New Phytologist*

Author Contributions: KF wrote and developed this manuscript with advice from JM, BT, MF, and CD. JM, BT, and SM advised this project. JS helped with plant maintenance and *P. sojae* culture advice. KF developed the *Pseudomonas* effector delivery system in soybean. KF trained MF and CD in the procedure. MF and CD helped optimize this procedure for screening

segregating $F_{2:3}$ populations. KF, MF, CD, and ND screened the $F_{2:3}$ populations used in this study. MF developed a scoring system to analyze segregating populations.

Abstract

Phytophthora root and stem rot disease suppresses global soybean production. We developed a system to screen soybean germplasm for *Resistance to Phytophthora sojae* (*Rps*) genes that recognize core *Phytophthora sojae* RXLR effectors. New *Rps* genes that target core effectors will likely be effective and durable against diverse *P. sojae* isolates. We developed a system using the bacterium *Pseudomonas* to deliver individual *P. sojae* effectors into soybean by Type III secretion. If the delivered effector is recognized by a resistance (*R*) gene, a visual hypersensitive response (HR) is produced. We used *P. sojae* avirulence (*Avr*) effectors to validate that this approach can recapitulate known *Avr/R* interactions. We delivered core *P. sojae* effectors *Avh*16, *Avh*180, and *Avh*240 into disease-resistant *Glycine max* germplasm. *G. max* accessions that produced a HR in response to core effector(s) were selected for crosses with *P. sojae*-susceptible cultivar Williams. We assayed genetic segregation of the response to three effectors in $F_{2:3}$ progeny derived from crosses of resistant X susceptible soybean. In all cases, we observed a simple, genetically dominant inheritance pattern that is consistent with gene-for-gene resistance and suggestive of amenability to breeding. A screen with additional core *P. sojae* effectors suggested that the resistant germplasm likely contains many potential new *Rps* genes. We will characterize and breed these potential *Rps* loci for commercial deployment this destructive disease.

Introduction

Phytophthora sojae, an oomycete pathogen, is the causal agent of *Phytophthora* root and stem rot disease on cultivated soybean, *Glycine max* [34, 81]. The United States of America (USA) is the world leader in soybean production, devoting 29% and 31% of its cropping area to soybean in 2013 and 2014 respectively [23]. Soybeans are crushed to extract valuable oil. The crushed remainder is processed into soybean meal [22]. Soybean meal is marketed globally as a food source for animals and fish [22]. In 2006, soybean crop losses due to *Phytophthora* root and stem rot were estimated at 1.46 million metric tons in the USA and over 2.32 million metric tons worldwide [31]. This was a loss of 1.75% of all soybean produced during that year in the USA [31]. Robust management options are needed to mitigate these losses.

P. sojae overwinters in dried plant tissue and soil, typically as oospores [33, 34]. Germinating oospores can infect seedlings directly, or can produce sporangia, containing asexual zoospores [33, 34]. Once released, zoospores will swim towards root exudates, encyst, and invade root tissue with filamentous hyphae [35]. *P. sojae* hyphae grow intercellularly and produce feeding structures, called haustoria, which penetrate the cell wall and interface with the plant cell membrane [82]. *P. sojae* secretes effector proteins into soybean cells at this interface to suppress plant immunity and to promote virulence [33, 34, 82]. A compatible infection is propagated asexually during the soybean growing season [33, 34].

Pests and pathogens secrete effectors to subvert plant immunity [36]. The genome sequence of *P. sojae* revealed hundreds of genes encoding candidate effectors [83-86]. One large effector family, RXLR effectors, can enter plant cells [36]. These effectors contain an N-terminal signal peptide, RXLR-dEER motif, and an effector domain [45]. The *P. sojae* genome contains nearly 400 genes encoding candidate RXLR effectors [47]. Many effector genes have variable

sequence and expression in diverse *P. sojae* isolates [47, 83]. If a *P. sojae* effector is recognized by a soybean *Rps* gene (effector-triggered immunity or ETI), the plant produces localized cell death (i.e., a Hypersensitive Response or HR) [33]. These gene-for-gene interactions trigger a robust immune response which impedes pathogen growth [36].

Gene-for-gene resistance has been effective at controlling *Phytophthora* root and stem rot under field conditions [33, 34, 87]. A total of 24 genes has been identified. Of these, seven (*Rps*1a, *Rps*1b, *Rps*1c, *Rps*1k, *Rps*3a, *Rps*6, and *Rps*8) have been commercially deployed to manage this disease [34, 87]. Because *R* gene function is dependent on effector(s) recognition, *Rps* genes can be defeated when *P. sojae* genetic diversity includes isolates for which *Avr* effectors are mutated or silenced [34, 87]. *P. sojae* isolates that defeat all commercial *Rps* genes have been described [34]. The average effectiveness of a soybean *R* gene in the field was estimated at 8-15 years, underscoring the need to identify new sources of genetic resistance against *P. sojae* [88].

Effectors have been identified that interact with all of these *Rps* genes except for *Rps*8 [34]. In every case (*Avr*1a, *Avr*1b, *Avr*1c, *Avr*1k, *Avr*3a/5, *Avr*3b, *Avr*3c, and *Avr*4/6), all recognized effectors are from the RXLR family [33]. With the exception of *Avr*3b, these effectors make minor contributions to *P. sojae* virulence on soybean [33]. Non-essential *P. sojae* effector genes can be silenced, deleted, or mutated in response to *Rps*-mediated selective pressure with little or no fitness cost to the pathogen. These mechanisms for evading host immunity can subvert conventional *R* genes, rendering the *R* gene useless for disease control.

Effector-directed breeding strategies (termed “effectoromics”) can accelerate disease resistance breeding against plant pathogens [68]. For example, effectoromics has been successfully applied to improve potato resistance against potato late blight [67]. Vleeshouwers et

al assayed 54 effectors from *Phytophthora infestans* for *Avr* activity on wild *Solanum* [67]. The RXLR family lpiO induced a HR on three species which revealed the *Rpi*-blb1 *R* gene. They identified the cognate effector *Avr*-blb1 by transiently expressing IpiO and *Rpi*-blb1 in a heterologous *Nicotiana benthamiana* system [67].

We chose to search for novel *Rps* genes which recognize core *P. sojae* effectors. We define core effectors as highly expressed in early infection, conserved amongst diverse isolates, and necessary for virulence based on reverse genetic criteria. *Rps* genes against core *P. sojae* effectors will likely be more durable and more effective against genetically diverse isolates when compared to traditional *Rps* genes, because *P. sojae* cannot easily discard a core effector without a major fitness penalty. In this study, we designed a system for delivering oomycete effectors from *Pseudomonas* into soybean. This system was used to screen soybean germplasm for potential new *Rps* genes against numerous core *P. sojae* effectors. *G. max* accessions with potential new *Rps* genes were crossed with susceptible cultivar Williams. Inheritance of three candidate *Rps* genes in $F_{2:3}$ populations suggested single, dominant loci, indicating that the effectors are recognized by R proteins that can be easily bred into elite soybean cultivars.

Results

Overview of the Screen

Our approach tests *G. max* for a localized cell death (hypersensitive response or HR) against specific pathogen effectors, when the effector is delivered to the inside of plant cells by a bacterial surrogate. A visual HR suggests the presence of a *R* gene in a tested population. To identify novel and durable *R* genes, we assayed *P. sojae* resistant soybean germplasm for HRs against core *P. sojae* effectors. *G. max* accessions which contained predicted *R* genes were crossed with susceptible Williams. *Avr* activity was assessed in $F_{2:3}$ populations to determine gene inheritance. An overview of the strategy is provided in Figure 2.1.

Identification of Resistant Soybean Germplasm

In a recently published study, Matthiesen et al. screened 1,019 Glycine accessions with a mixture of three *P. sojae* isolates which defeat 13 commercial *Rps* genes [89]. They predicted that 17% of the *G. max* accessions contained novel *Rps* loci [89]. We used these accessions in our screen with core effectors. We listed the *G. max* accession IDs and its corresponding plant introduction (PI) number for tested *G. max* germplasm in Table 2.1.

Identification of Core Effectors from P. sojae

This work will be described in a forthcoming manuscript [90]. In this study, Wise et al. identified 30 RXLR effectors (from ~400 predicted RXLR genes [56]) which are highly expressed at early time points in the infection and which are genetically monomorphic amongst four *P. sojae* reference [90]. These isolates collectively encompass much of the *P. sojae* genetic diversity in the USA [47]. RNA silencing of effector genes was used to test whether seventeen effectors are important for virulence [90]. The results indicated that three effectors have major effects on virulence, four have no effect, and the remaining ten have intermediate effects [90].

The three essential effectors (*Avh*16, *Avh*180 and *Avh*240) were subsequently silenced in an additional three reference isolates and were shown to be essential in all three isolates [90]. *Avh*16, *Avh*180 and *Avh*240 were shown to be highly expressed in all four *P. sojae* reference isolates [90]. These results suggest that *Avh*16, *Avh*180 and *Avh*240 are broadly important across the species, and we therefore selected them as the first effectors for our screen [90]. Germplasm was tested with nine additional effectors: *Avh*53, *Avh*137, *Avh*261, *Avh*488, *Snel*1, *Avh*94, *Avh*241, *Avh*23, or *Avh*110 [90]. This second set of effectors was chosen for screening based on gene expression and sequence conservation [90]. RNA interference experiments indicate that *Avh94* and *Avh241* make major contributions to virulence and that *Avh110* and *Avh23* only make moderate contributions to virulence. The remaining genes have not yet been tested with RNAi.

Development of a Bacterial System for Transient Effector Delivery

Our primary objective was to develop a system for delivering *P. sojae* effectors, one at a time, to the interior of plant cells so that recognition of the effector by an *R* protein would trigger a visible cell death response. The screens with *P. infestans* effectors were accomplished using *Agrobacterium*-mediated transient transformation [67]. This approach works well in tomato and related species, but soybean is recalcitrant to *Agrobacterium*-mediated transient transformation (K. Fedkenheuer, data not shown). Therefore, we decided to focus on developing a system through which the effectors could be delivered by the *Pseudomonas* Type III secretion system. Effector delivery was accomplished using the effector-detector vector (pEDV6) that provides a Type III secretion system (T3SS) signal [91]. Cloning into pEDV6 produces a *AvrRps*4-RXLR fusion product [91]. The bacterial *AvrRps*4 leader sequence enables secretion of the construct through the T3SS into plant cells [91]. This approach has proven useful when screening for

virulence or avirulence activity of *Hyaloperonospora arabidopsidis* RXLR effectors in *Arabidopsis* [91].

We chose several *Pseudomonas* strains to evaluate for the ability to deliver *P. sojae* effectors into soybean. *Pseudomonas syringae pathovar tomato DC3000* is a widely used reference strain. D28E is a mutant version of the reference strain *Pst DC3000* in which 28 Type III effectors have been removed by targeted deletions [92]. D28E (*Avr*PtoB) is D28E with the *Pst DC3000* effector *Avr*PtoB, which can potentially suppress PTI [92]. *Pseudomonas syringae* pathovar *glycinea* (*Psg*) race 4 is a virulent pathogen on soybean [71]. *Pseudomonas fluorescens (Pf0*) is a soil bacterium that is non-pathogenic and does not contain Type III effectors nor a T3SS [93]. *Pf0* strain EtHAN contains a transgenic, stably integrated operon of genes encoding the *Pst DC3000* Type III secretion components [93].

First, we tested whether these strains provoke a HR in soybean. *Pst DC3000* produced a visual HR on all tested soybean cultivars. No visual HR was observed on leaves in response to infiltration with *Pst DC3000* D28E, *Pst DC3000* D28E (*Avr*PtoB), *Psg* race 4, or *Pf0* EtHAN. Next, we tested whether these strains could deliver *P. sojae* effectors into soybean. We cloned *P. sojae Avr* effectors *Avr*1k, *Avr*1b, and *Avr*4/6 into pEDV6 and transformed the five *Pseudomonas* strains with these constructs. For each strain, we challenged cultivars containing *Rps*1k, *Rps*1b, and *Rps*4 with their cognate effectors. Each *Pseudomonas* strain was evaluated for its ability to produce a visual HR on *Rps* cultivars in known *Avr/R* interactions.

We performed *in vivo* bacterial growth assays following infiltrations of *Psg*-*Avr*1k and EtHAN-*Avr*1k. We did not recover any *Psg race 4* carrying the pEDV6-*Avr*1k plasmid at 5 DPI (Figure 2.2). EtHAN carrying *Avr*1k grew only 1 log $(cfu/cm)^2$ at 5 DPI in the presence *Rps*1k (Figure 2.2). The unexpected absence of *P. s. glycinea*-*Avr*1k bacteria at 5 DPI led us to test the

stability of the pEDV6-effector constructs in our five *Pseudomonas* strains. We performed an experiment in which the strains were assayed for a loss of the plasmid prior to inoculation into soybean. The strains were grown in King's Broth (KB) media with antibiotic selection and were re-suspended in 10 mM $MgCl_2$. The cells were incubated at 28ºC and were assayed for presence of the pEDV6-effector construct by plating the bacteria on selective and non-selective media. The results indicated that, in all strains except EtHAN, pEDV6-effector constructs were rapidly lost during a 15 minute incubation in 10 mM $MgCl_2$ (Table 2.2). This suggests that the pEDV6-effector construct is lost from all *Pseudomonas* strains except EtHAN when selective pressure is removed (Table 2.2).

We hypothesized that *P. sojae* effectors could be toxic to virulent *Pseudomonas* strains and potentially to non-pathogenic EtHAN. To test this possibility, we measured the growth rate of strains in minimal media with antibiotic selection to force plasmid retention. All three *P. sojae* effectors were mildly toxic to *P. s. glycinea* and to EtHAN, reducing WT growth rates (Figure 2.3). Despite mild sensitivity to *P. sojae* effectors, EtHAN was selected as the only candidate because it did not eject pEDV6-effector constructs (Table 2.2 and Figure 2.3).

Optimization of the Growth of EtHAN in planta

To improve HR consistency and intensity, we explored options to enhance effector delivery in EtHAN. We hypothesized that increasing the *in planta* growth of EtHAN might improve visual signal in response to *P. sojae* effectors. This hypothesis was based on prior work by Keen et al. that demonstrated that the *in planta* growth of *P. fluorescens* could be improved by co-infiltration with a virulent strain of *Psg* [94].

We confirmed these results by assaying the growth of EtHAN in soybean leaves with and without *Psg* race 4. The addition of *Psg* race 4 by co-infiltration improved the *in planta* growth

of EtHAN two-fold in a compatible interaction (Figure 2.4). In an incompatible interaction, the addition of *Psg* race 4 augments the growth of EtHAN tenfold (Figure 2.4). This was seen in incompatible interactions of EtHAN delivering *Avr*1k, *Avr*1b, or *Avr*4/6 on soybean cultivars *Rps*1k, *Rps*1b, and *Rps*4 respectively (Figure 2.4). Based on these results, we chose to use *P. s. glycinea* race 4 to augment the growth of EtHAN for screening soybean germplasm. There are no known *R* genes against *P. s. glycinea* race 4 [71]. We confirmed that our starting germplasm was susceptible to this race by pre-screening accessions with this *P. s. glycinea* race 4.

Optimization of Plant Growth

We optimized several aspects of plant growth to achieve consistent results with our system. We found that a light intensity of 250-300 µM to be key for the production of consistent macroscopic HRs during screening. It is critical that plants are consistently watered. Drought stress will cause early senescence of the unifoliate leaves. Flats were watered with 1.5 L of H_2O per flat every 36-48 hours or more frequently as needed. Humidity was held at 80% RH.

Approximately 12-14 days post planting, *G. max* cultivars will begin producing immature trifoliate leaves. This is described as the V2 growth stage for soybean [95]. Because results are scored seven days post infiltration, senescence of the unifoliate leaves can interfere with data collection. We discovered that pruning the first set of trifoliate leaves causes a reprogramming of the unifoliate leaves (Figure 2.5): After two days the unifoliate leaves become thicker, darker, and resilient (Figure 2.5). By removing trifoliate leaves at the stalk apex, unifoliate leaves are exposed to more direct light as they are unshaded. In *Avr/R* interactions, effector-responses were stronger and more consistent on unifoliate leaves from pruned plants compared to unifoliate leaves from unpruned plants.

A Facile Assay for P. sojae *Virulence*

We also developed an assay to determine *P. sojae* virulence on detached trifoliate leaves. Mycelial plugs from *P. sojae* race 2 produced large lesions on trifoliate leaves from susceptible cultivars which were wounded at the plug site (leaf center): Williams and Harosoy (Figure 2.6). This isolate did not produce an expanded lesion on the resistant control cultivar Haro 15 (Figure 2.6). Using this technique, we confirmed *P. sojae* resistance in *G. max* accessions, accession 32 (gm32) and gm326 (Figure 2.6).

Validation of the Pseudomonas*/EDV Delivery System*

After optimizing plant growth, the next step was to test whether *Avr*1k, *Avr*1b, and *Avr*4/6 can elicit a strong and consistent HR when delivered by EtHAN to soybean cultivars *Rps*1k, *Rps*1b, and *Rps*4 respectively (Figure 2.7). We quantified the consistency of the macroscopic HR as a percentage of infiltration sites. *Avr1k* had the highest percent HR on *Rps*1k and *Avr4/6* had the lowest percent HR on *Rps*4 (Figure 2.7b). We produced similar results using *Rps* cultivars in the Williams background (Table 2.3). EtHAN alone, or with *P. s. glycinea race 4*, did not produce a HR on any tested soybean cultivar (Table 2.4).

To quantify cell death, we measured ion leakage from the soybean leaves into water using a conductivity meter. Infiltration of strains carrying *Avr*1k, *Avr*1b, and *Avr*4/6 into cultivars containing a cognate *R* gene produced higher levels of ion leakage (20-30% higher) when compared with the Harosoy control (Figure 2.8). Co-infiltration of EtHAN and *Psg* race 4 produced some background cell death (Figure 2.8). These results indicate that the *Pseudomonas* delivery system is suitable for screening *G. max* germplasm to find novel gene-for-gene interactions.

Screening of Resistant G. max *Germplasm with* P. sojae *Core Effectors*

To identify potential new *R* genes, we screened 32 *G. max* accessions which are predicted to contain novel *Rps* loci [89]. Our first set of screens utilized EtHAN strains carrying the three most promising core effectors, *Avh16*, *Avh180*, and *Avh240*. From the 32 *P. sojae*-resistant *G. max* accessions, six accessions responded to *Avh*16 with a visible HR, six accessions responded to *Avh*180, and six accessions responded to *Avh*240 (Table 2.5). *Avh*7a, a homolog of *Avh*16, produced a HR on the same accessions that responded to *Avh*16 (Table 2.6). Three accessions responded to two effectors, and one accession responded to all three effectors (Table 2.5). Seventeen accessions did not respond to these three effectors. Additionally, six *G. max* accessions with partial resistance against *P. sojae* were included as blind negative controls and did not respond to effector treatment.

Screening Resistant G. max *Germplasm with Additional Effectors*

The positive results from screens with *Avh*16, *Avh*180, and *Avh*240, encouraged us to screen the same 32 *G. max* accessions with a second set of core *P. sojae* effectors, namely *Avh*53, *Avh*137, *Avh*261, *Avh*488, *Snel*1, *Avh*94, *Avh*241, *Avh*23, and *Avh*110 (Table 2.7). These effectors were selected by the same criteria as *Avh*16, *Avh*180 and *Avh*240, except that their function in P7076, P7074 and P7063 was not tested by silencing. We found that many *G. max* accessions respond to one or more of these effectors (Table 2.7). *Avh*23 and *Avh*110 did not provoke a HR on any tested accessions.

Genetic Segregation of Effector Response in $F_{2:3}$ Populations

Seven effector-responsive accessions were selected for crossing with susceptible Williams (Table 2.8). We chose to breed resistant accessions with Williams because it has a sequenced genome [96] and no *Rps* genes [64]. A sequenced genome enables us to design single

nucleotide polymorphism (SNP) chips which are essential for soybean locus mapping. A SNP is a nucleotide variation at a genomic position within a population and these chips can assay multiple SNPs concurrently [97]. Williams was chosen for breeding based on maturity group as well. The maturity group refers to the cultivar development period which is characterized by growth stages [95]. Soybean producers use maturity group information to accurately time chemical treatments. Williams' 3.9 maturity group is ideal for growth in the Midwest.

We analyzed $F_{2:3}$ seed for two crosses, accession 32 (gm32) x Williams and gm326 x Williams. Because most known *R* genes segregate as single, genetically dominant loci, we predicted that the HR response to the effectors would segregate similarly, producing a 1:2:1 phenotypic ratio in segregating $F_{2:3}$ populations.

We tested segregating $F_{2:3}$ families for *Avr* activity using the effector delivery system. For gm32, we observed a phenotypic ratio not significantly different ($x > 0.05$) than 1:2:1 in response to *Avh*16 and in response to *Avh*240 (Table 2.9). For gm326, we observed a phenotypic ratio not significantly different ($x > 0.05$) than 1:2:1 in response to *Avh*180 (Table 2.9). We conclude that gm32 likely contains two dominant *R* genes and gm326 likely contains one dominant *R* gene. Was Fig 2.9 discussed at all?

Discussion:

Phytophthora root and stem rot disease on soybean was first described in 1954 by soybean farmers in southwestern Ontario and in the Midwest [26]. *P. sojae* owes its "success" as a crop pathogen to a plastic genome which supports rapid evolution. *P. sojae* isolates have been described which defeat all commercial *Rps* genes. To mitigate this disease in the future, we need new and robust disease management options. Genetic resistance is the most economic tool, but most *R* genes against *Phytophthora* pathogens are not durable because they recognize effectors that do not play essential roles in virulence.

Our strategy is based on screening for novel *R* genes against core *P. sojae* effectors and to breed these *R* genes for commercial deployment. To probe soybean germplasm recognition for core *P. sojae* effectors, we first needed a flexible system for transient expression in soybean. We exploited the *Pseudomonas* T3SS for effector delivery into soybean, drawing from early work by Staskawicz et al., who produced visual cell death symptoms by transforming *P. s. glycinea* race 1, race 4, and race 5 with molecular components from *P. s glycinea* race 6 [70]. AvrB1 was shown to produce an HR on Rpg1 [71]. While analyzing the *Rpg*2, *Rpg*3, and *Rpg*4 loci in 1991, Keen and Buzzell transformed *P. s. glycinea* race 4 with *Avr*D from *Pst* and observed visual incompatibility [72]. They suggested that *Rpg*4 may be responsible for *G. max* resistance against *Pseudomonas* carrying *Avr*D [72]. These experiments demonstrate that *P. s glycinea* is capable of delivering exogenous, plasmid borne effectors to soybean leaves in sufficient quantity to produce *Avr* activity in *Avr/R* interactions. Using this information, we constructed a *Pseudomonas* system for transient expression in soybean.

Our system uses Type III secretion by *Pseudomonas fluorescens* strain EtHAN to deliver *P. sojae* effectors. A critical component of effector delivery to *G. max* by EtHAN is the addition

of *P.s. glycinea* race 4 to the inoculum. We hypothesize that *P. s. glycinea* race 4 improves the growth of EtHAN *in planta* by suppressing plant immunity. To validate this system, we exploited known *Avr/R* interactions between *P. sojae Avr* effectors and *G. max R* proteins. When *Avr*1k, *Avr*1b, and *Avr*4/6 were delivered to *G. max* cultivars which contained a cognate *R* gene, we observed visual HRs. We confirmed cell death symptoms using an ion leakage assay. This new system gave us the unique ability to study oomycete effectors in soybean. Importantly, the bacterial system recapitulated the same gene-for-gene specificity as is seen in experiments with *P. sojae* containing the same *Avr* genes. In fact, the previously documented strength of resistance was recapitulated in our system: The response to *Avr*1K was strongest and the response to *Avr*4/6 was weakest, mirroring the strength of the responses in either *P. sojae*-based assays or when the effectors are delivered by biolistics [98, 99]. Thus, this system was validated for studying oomycete effectors in soybean. The broad applicability of EtHAN as an effector-screening system is further underscored by recent reports of its successful use in monocot wheat leaves [100, 101].

We tested 12 core effectors, and observed that ten produced a visual HR on at least one of the 32 tested *G. max* accessions. Six accessions responded to one effector, twelve accessions responded to two effectors, seven accessions responded to three effectors and one accession responded to four effectors. By selecting for *P. sojae* resistant germplasm and by then selecting for accessions with no known resistance, we likely enriched our germplasm with accessions containing new *Rps* genes.

We selected seven accessions which produced a HR in response to a core effector(s) for breeding with susceptible Williams. We observed *Avr* activity in $F_{2:3}$ progeny from crosses, gm32 x Williams and gm326 x Williams. In $F_{2:3}$ populations, a 1:2:1 phenotypic ratio was

expected and observed suggesting dominant inheritance. We concluded that gm32 likely contains *Rps* genes which recognize core *P. sojae* effectors *Avh*16 and *Avh*240. Gm326 likely contains one dominant *Rps* gene which targets *Avh*180.

In addition to resistance loci *Rps*1 to *Rps*6 for which *Avr* effectors have been identified, twelve additional *Rps* loci have been described [87]. These uncharacterized resistance loci may explain some of our *Avr* activity. In 2013, Lin et al. independently mapped two *R* genes in PI567139B, *Rps*Un1 and *Rps*Un2 [65]. We independently identified effector-responses in PI567139B against *Avh*16 and *Avh*240. This effector-response may correlate to *Rps*Un1 and *Rps*Un2. It is unlikely that effector-responses were due to effector-toxicity in soybean leaves because effector-responses were accession specific and were similar to effector-responses by *Rps* cultivars in known *Avr/R* interactions.

Effector-directed breeding provides many advantages over classical pathogen-based breeding. Effector-directed breeding allows for the identification of potential *R* genes which recognize core pathogen effectors. This approach can be applied to find potential *R* genes against any pathogen with a sequenced genome and identifiable effectors. Non-host plants can be screened for effector recognition as well. Effector-directed breeding can facilitate stacking *R* genes.

We suggest using both effector-directed breeding and pathogen-based screening to identify novel, durable R genes. This may help to eliminate accidental duplication of *R* loci during resistance breeding. Mapping the same population using both *Avr* activity and pathogen screens will create a multidimensional map to more accurately determine resistance mechanisms. For this reason, we have developed a technique to detect *Avr* activity in simultaneous effector

and pathogen assays. This system will yield effector data and pathogen data for a single individual.

In principle, our effector delivery system could be used to screen any host plant for *R* genes against a pathogen for which effectors are characterized. EtHAN was used to successfully deliver effectors to wheat leaves [100, 101]. This demonstrates that EtHAN may be useful for effector delivery in a broad range of systems. Our immediate goal is to use effector data and pathogen data to map potential *Rps* genes in soybean RI lines. In the future, we hope to introduce new and durable *Rps* genes to soybean growers for protection against *Phytophthora* root and stem rot.

Materials and Methods

Effector Plasmid Clones

Clones encoding RXLR effectors were cloned into pENTR using the pENTR™/D-TOPO® Cloning Kit – ThermoFischer Scientific or they were provided by the Tyler lab at Oregon State University. The coding region of the ORF began with a methionine codon, followed by the first codon following the signal peptide cleavage site as predicted by SignalP. An LR reaction was used to clone the effector genes into the destination vector pEDV6 [93]. Constructs were transformed into10 *E. coli*. Single colonies were selected on KB agar containing Gentamycin (10 µg/µl) and were screened for the desired plasmid by PCR, using a pEDV6 forward (F) primer and a gene specific reverse (R) primer. Positive transformants were maintained at 37 °C under Gentamycin selection.

Transformation of EtHAN by Tri-Parental Mating

P. fluorescens strain EtHAN was provided by the Chang lab at Oregon State University [93]. EtHAN was transformed using tri-parental mating as follows: Bacterial strains RK600, EtHAN, and positive transformants in top10 *E. coli* were streaked onto KB agar plates with the proper selection. Onto one King's Broth (KB) agar plates, we streaked our positive transformants in top10 then the helper strain RK600 followed by EtHAN. The plates were incubated for three days at 28 °C. Following the incubation, colonies were streaked onto KB agar containing Chloramphenicol (10 µg/µl), Nitrofurantoin (20 µg/µl), and Gentamycin (10 µg/µl). Single colonies were screened by PCR using the pEDV6 F primer and a gene specific R primer. All bacterial strains are described in Table 2.10. A list of primers used for cloning can be found in Table 2.11.

Culture Preparation

Bacterial cultures were prepared from single colonies and inoculated in 5 mL aliquots of KB media containing the appropriate antibiotic selection. The cultures were incubated at 28 °C for 18-22 h. The bacteria was pelleted and re-suspended in 10 mM $MgSO_4$. EtHAN and EtHAN-effector constructs were prepared at an OD = 0.6. For co-infiltration, EtHAN and *Psg* were mixed for at ODs = 0.6 and ODs = 0.3, respectively for a final OD = 0.9.

Plant Growth Conditions

G. max was planted in Fafner P2 potting media. About 1.5 kg Fafard P2 potting media was hydrated with 2 L of water with Cal-Mag fertilizer. 4 inch pots were packed firmly with media. 5 seeds were sown per pot and covered with about 2-3 cm of loosely packed potting media. The top soil was treated with Marathon insecticide, put into flats (8 plants per flat), and covered with clear plastic lids to maintain humidity during germination. After 24-36 h, the lids were removed from the flats. Germination rates were >95% for all *G. max* tested. *G. max* were germinated and maintained under diurnal light (16 h light at 22 ^{0}C; 6 h dark at 20 ^{0}C). Light intensity was maintained between 250-300 μM for all experiments.

Effector Infiltrations

Plants were infiltrated after 15-17 days (3 days post pruning). Bacterial solutions were prepared 1 hour prior to infiltration. *G. max* unifoliates from pruned plants infiltrate best 1 h after the lights turn on. Needless syringes were used to pressure infiltrate unifoliate leaves. Each unifoliate received 4 infiltrations of 100-200 uL of bacterial solution. The identical process is performed on the adjacent unifoliate. Co-infiltration of EtHAN and *Psg* did not produce a visible HR on any tested *G. max* cultivar. The best negative control is to co-infiltrate EtHAN-effector

and *Psg* into *G. max* cultivars which contain no *R* gene against the cloned effector. A list of soybean cultivars which were used for these experiments is detailed in Table 2.12.

Scoring

Seven days post infiltration (DPI), the unifoliate leaves were detached, imaged, and scored. A plant scored positive if ≥ 5/8 infiltration spots produced a visual HR on both unifoliate leaves (Figure 2.9b). Plants were scored as negative if ≤2/8 infiltration spots produced a visible HR (Figure 2.9b). Plants that fell between 3-4/8 were scored as ambiguous (Figure 2.9b). Any data, scored as ambiguous, was discarded, and the experiment was repeated until the appropriate sample size was reached. To calculate % HR, we used the equation, $\% HR = (\#\ of\ responding\ plants) \div (\#\ of\ infiltrated\ plants)$.

If too much pressure is applied during infiltration, the damage may induce a cell death response around edges of infiltration sites (Figure 2.9a). This can make scoring weak HRs more difficult. If the cell death response is weak, the infiltration site will turn brown with very small HRs throughout the site (Figure 2.9a). Cell death can occur on negative control plants if disease or insects are present (Figure 2.9c). The Compendium of Soybean Diseases was used as a reference to identify disease [95].

Determination of R *Gene Inheritance in $F_{2:3}$ Populations*

Plants from segregating $F_{2:3}$ families were screened with a single effector at a time. Prior to screening, we determined the background cell death each effector produced on Williams. $F_{2:3}$ families were tested with an average sample size c. 15 individuals per family or line. Seed was limited.

Determining $F_{2:3}$ Phenotypic Ratios

After compiling the results, we analyzed the data as % HR with variation represented as standard deviation (σ). We determined our range for homozygous dominant using the equation, $RR = 100\%\ to\ (100\% - 1\ parental\ \sigma)$. We determined our range for homozygous recessive using the equation, $rr = 0\%\ to\ (Williams\ \%\ HR + 1\ Williams\ \sigma)$. Families that fell within the two ranges are considered to be segregating.

In planta *Bacterial Growth Curves*

All bacterial strains were grown at 28 °C on KB agar containing the appropriate antibiotic selection. Single colonies were inoculated in 5 mL liquid KB media containing antibiotic selection. The cultures were incubated at 28 °C for 18-22 h. Bacterial cultures were then pelleted by centrifugation at 2,000 x g for 15 minutes and resuspended in 3-5 mL 10 mM $MgSO_4$. Optical densities (OD) were calculated by measuring absorbance at 600nm (OD_{600}). Bacterial solutions were then diluted to appropriate ODs with 10 mM $MgSO_4$. In bacterial growth assays containing only one strain of bacteria, solutions were pressure infiltrated into soybean unifoliates using a needless syringe at an OD_{600} = 0.01. In the case of co-infiltration experiments, the target strain (EtHAN) for the assay was infiltrated at an OD =0.01 while the non-target strain (*Psg*) was infiltrated at an OD = 0.3. Leaf disks were collected at 0 days post inoculation (0 DPI) and 5 days post inoculation (5 DPI). Leaf disks were homogenized in 200 µL 10 mM $MgSO_4$ using 1 mm glass beads in a bead beater. Samples were transferred to a sterile 96 well plate and diluted 1:10 serially. The dilution series was plated on KB agar containing the appropriate antibiotic selection. Plates were placed at 28 °C for 2 days at which point colony forming units (CFU) were counted (n = 5 plants / 10 leaves per replicate). Three biological replicates were performed.

Ion Leakage Assay

Soybean leaves were inoculated according to the methods for the visual hypersensitive response assay. After seven days, six circular leaf punches (1 cm in diameter) were taken from inoculated areas. Leaf disks were then floated in 45 mL sterile ddH_20 to reduce background ion leakage from cutting. After one hour, leaf disks were transferred to new tubes with 5 mL of water. After a three hour incubation, the water was removed and transferred to a 10 mL beaker. A handheld conductivity meter was used to measure the ions in solution. After conductivity readings were taken, the water was added back to the sample tubes. Samples were then boiled for 8 minutes to release all of the ions from the leaf disks. New conductivity readings were then taken to measure total ion leakage. To determine percent ion leakage, the initial conductivity reading was divided by the total ion leakage. Three biological replicates were performed (n = 3 plants / 6 leaf punches per replicate).

In vitro *and* in planta *Plasmid Ejection Assay*

Plasmid ejection of pEDV6 containing *P. sojae* avirulence genes *Avr*1K, *Avr*1B, or *Avr*4/6 was measured in all *Pseudomonas* strains used in this study. Bacterial colonies were grown in a 5 mL liquid KB cultures containing the appropriate antibiotic selection. Bacteria were pelleted and resuspended in 10 mM $MgSO_4$. For the *in vitro* assay, the bacterial solution was left to incubate at 28 °C and 10 µL aliquots were plated every 15 minutes onto KB agar containing an antibiotic to select for the bacteria and Gentamycin to select for the pEDV6-effector plasmid. Three independent biological replicates were performed (n = 3 cultures per replicate). The plates were then incubated for two days at 28 °C and CFU were counted. The *in planta* bacterial growth curve described above was used to observe plasmid ejection after

pressure infiltration of the culture into soybean leaves. For the *in planta* assay, time points were at 0 DPI and 3 DPI.

Effector Toxicity Assay

In order to test the toxicity of effector proteins *Avr*1K, *Avr*1B, and *Avr*4/6 on EtHAN and on *Psg*, bacterial cultures were grown in 5 mL liquid KB cultures containing the appropriate antibiotic selection. Cells were pelleted by centrifugation and diluted to an OD_{600}= 0.1 in 5 mL minimal media (50 mM KH_2PO_4, 5 mM K_2HPO_4, 1.7 mM $MgCl_2$*$6H_2O$, 7.6 mM $(NH_4)2SO_4$, 1.7 mM NaCl, 10 mM mannitol, and 10 mM fructose, filter sterilized) maintaining proper antibiotic selection. We measured OD_{600} at 5 hour intervals to assess effector impact on bacterial growth. Effector impact on growth was measured for each strain separately and compared to an untransformed control. Three independent biological replicates were performed (n = 5 cultures per replicate).

P. sojae *Mycelium Plug Infection Assay on Detached Trifoliate Leaves*

P. sojae was maintained on a PARP V8 plate. Three weeks prior to infection, a mycelium plug is transferred from a PARP V8 plate to a V8 plate. After three weeks, the culture should colonize most of the V8 plate. Contaminated plates should be discarded. Fresh mycelium plugs should be taken from freshly colonized V8 plates for the best results.

At 14 days post planting, trifoliate leaves should appear expanded. Per plant, remove each trifoliate and place each leaf in a wetted petri dish with a piece of filter paper. Experimental design will depend on leaf and culture sample size. On average, each petri dish will contain three leaves from three different individual plants. This allows for testing individuals with multiple pathogen isolates during a single replicate.

When ready to infect, scar each leaf in the center and place a 1cm mycelium plug on top of the scarred area. Parafilm the plates to maintain high humidity. Disease symptoms will begin at about 48 hours post infection. The symptoms conclude after seven days. Each culture should be passage every 1.5 months to maintain virulence.

Figures and Tables

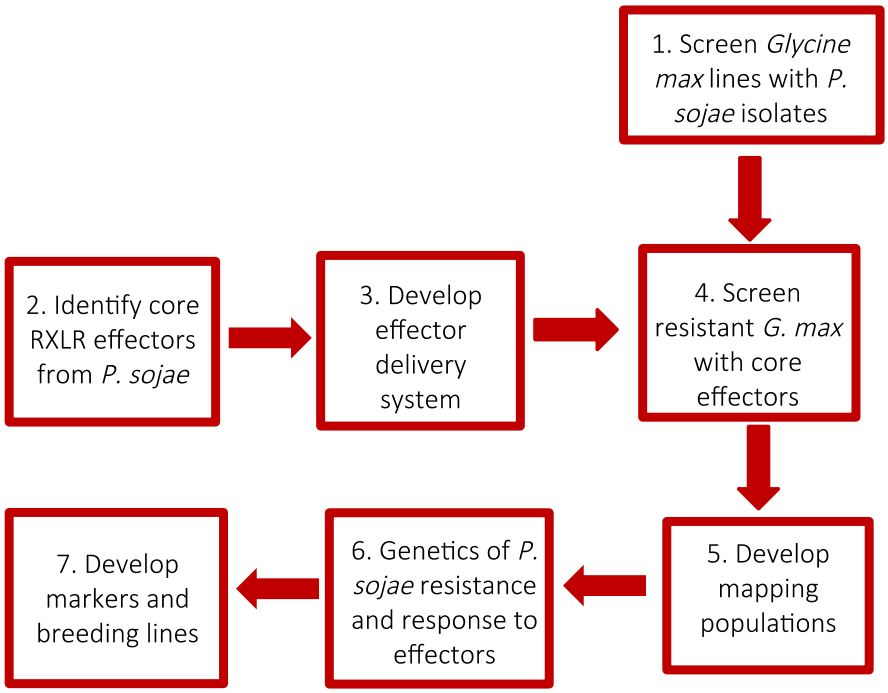

Figure 2.1 An overview of effector-directed breeding in soybean. This summarizes the development of soybean lines with *R* genes that recognize core *P. sojae* effectors. *Glycine max* germplasm is screened with a collection of isolates that collectively break all commercially available *Rps* genes. 2. Core effectors are identified with functional genomics tools. 3. A bacterial system to deliver those effectors individually to plants is developed. 4. The *P. sojae*-resistant germplasm from Step 1 is screened with the core effectors. 5. Lines with putative *R* genes against the effectors are crossed to a susceptible line, and progeny from the cross are used to develop mapping populations. 6. Genetic analysis is used to validate the phenotypes and identify lines in which effector recognition and pathogen resistance are conferred by the same locus. 7. Such lines will be used to develop breeding lines.

Table 2.1 The PI numbers for all referenced accessions are listed.

G. max **Parental Accession**	**PI Number**
gm13	PI407985
gm20	PI408319C
gm31	PI398440
gm32	PI567139B
gm41	PI200553
gm48	PI274508
gm78	PI398666
gm92	PI398775
gm94	PI398791
gm96	PI398946
gm98	PI398996
gm99	PI399004
gm106	PI399036
gm121	PI408287
gm123	PI423741
gm144	PI424477
gm291	PI399079
gm314	PI408015
gm315	PI408020A
gm317	PI408029
gm320	PI408097
gm321	PI408111
gm326	PI408132

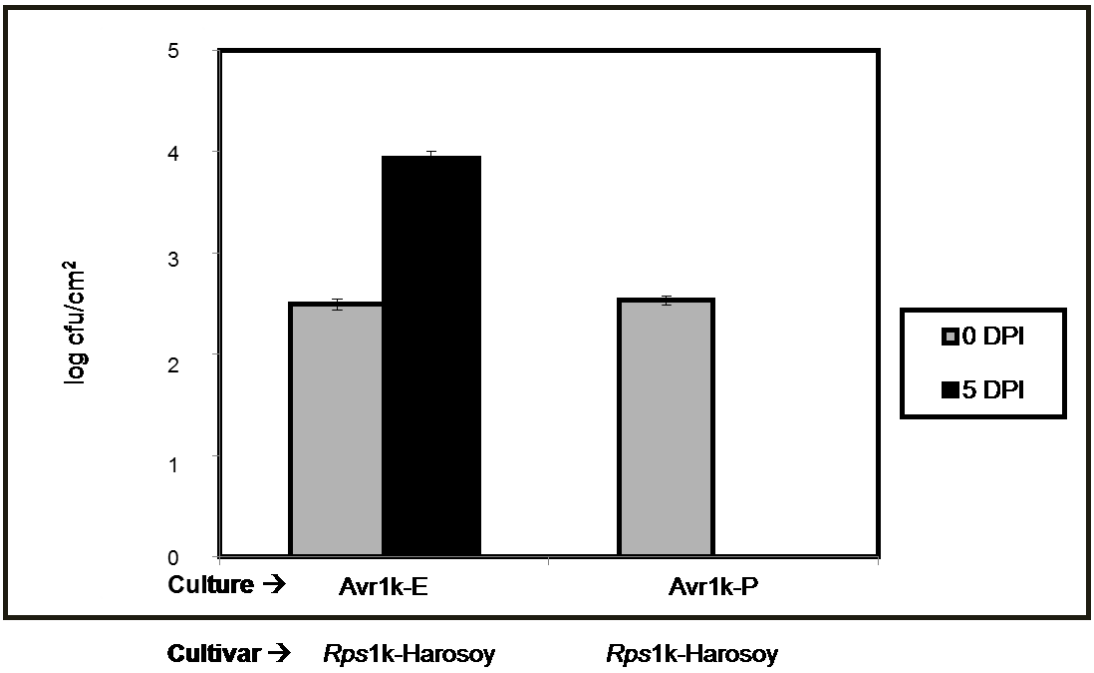

Figure 2.2 *Psg* likely ejects the *Avr*1k-pEDV6 plasmid prior to or during effector infiltration. *In planta* growth assay with *Psg* race 4 carrying *Avr*1k (*Avr*1k-P) and EtHAN carrying *Avr*1k (*Avr*1k-E) on HARO15. We recovered no *Avr*1k-P at 5 DPI. This data was produced from one biological replicate (n = 5 plants / 10 leaves per culture). The standard deviation represents leaf-to-leaf variation. Two other biological replicates produced similar results.

Table 2.2 EtHAN is the only strain that does not eject pEDV6 containing *Avr*1k, *Avr*1b, or *Avr*4/6. After a 15 minute incubation in 10mM $MgSO_4$, strains were plated onto selective media. Only *P. f.* EtHAN retained the plasmids. Grey shading indicates plasmid ejection. Black indicates plasmid retention. This data was produced from three independent biological replicates (n = 3 cultures per replicate).

Pseudomonas **Strains**	**Plasmid Ejection**		
	***Avr*1k**	***Avr*1b**	***Avr*4/6**
P. f. EtHAN			
P. syringe DC3000			
P. syringe DC3000 D28E			
P. syringe DC3000 D28E + AvrPtoB			
P. s. glycinea race 4			

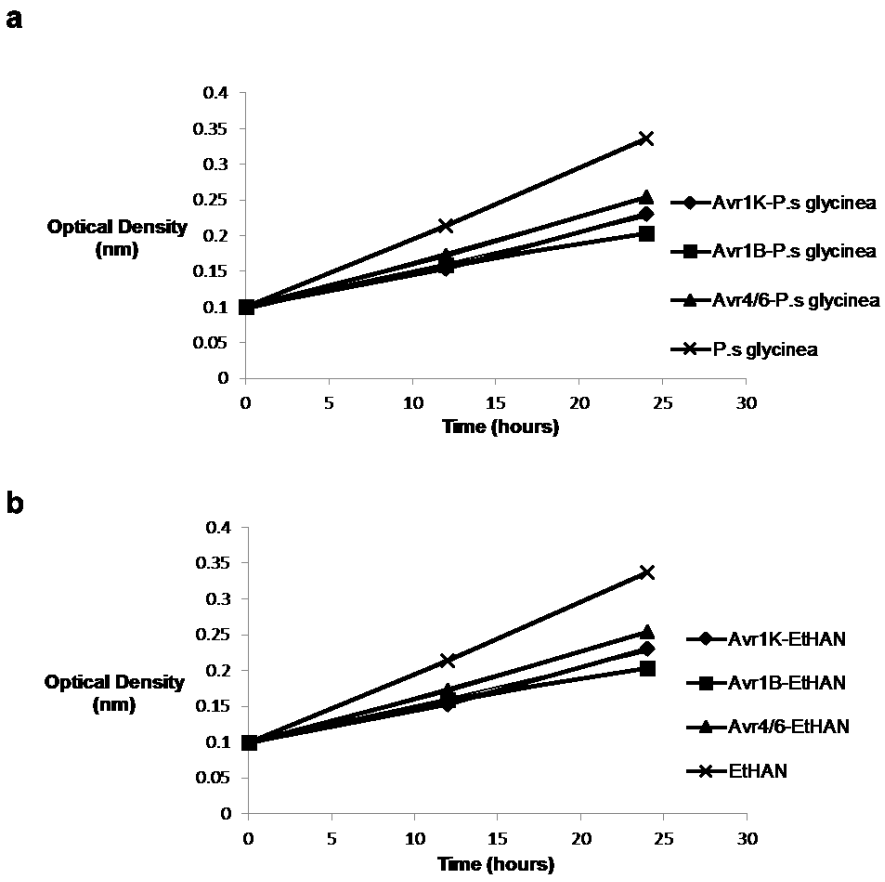

Figure 2.3 *P. sojae* effector toxicity on *Pseudomonas*. Bacterial strains carrying *Avr*1k, *Avr*1b, or *Avr*4/6 were cloned into pEDV6 and were grown in minimal media with antibiotic selection for 24 hours. Minimal media stress activates effector production and antibiotic selection forces plasmid retention. *P. sojae* effector expression inhibited the growth of a) *Psg* and b) *P. f.* EtHAN. This data was produced from one replicate (n = 5 cultures per replicate). Two other biological replicates produced similar results.

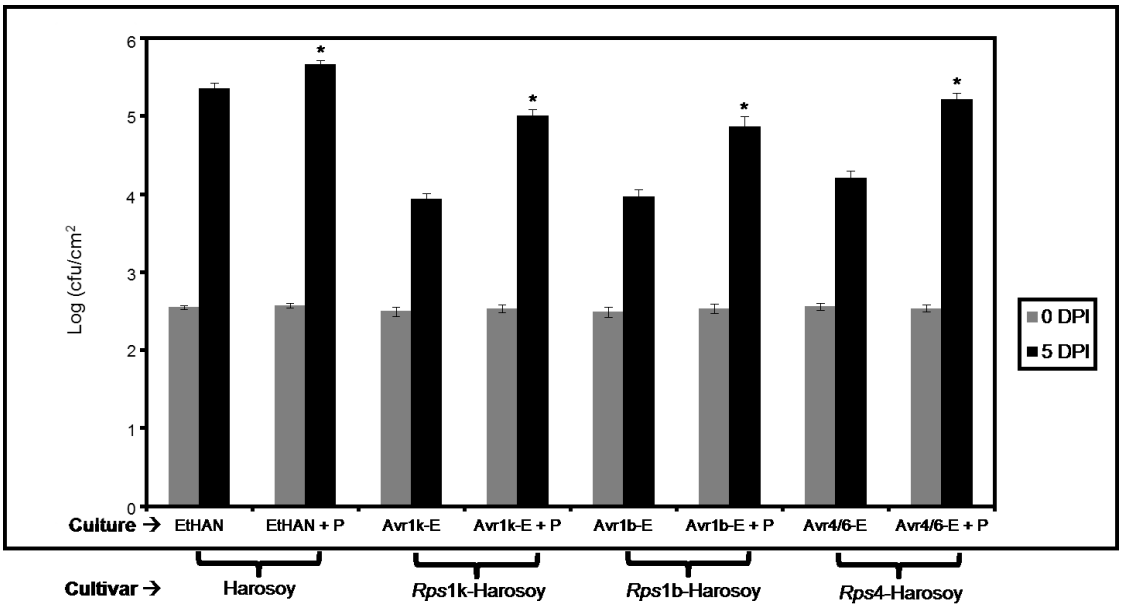

Figure 2.4 Co-infiltration with virulent *Psg* race 4 improves the growth of EtHAN *in planta*. EtHAN or EtHAN with the indicated *Avr* genes was infiltrated into the indicated plant cultivars that carry *R* genes against the cognate *Avr* effector proteins. The addition of *Psg* race 4 to a culture is indicated by a "+ P". These data were produced from one biological replicate (n = 5 plants / 10 leaves per culture). Standard deviation represents leaf-to-leaf variation. Statistical significance of *Avr-Psg* race 4 CFU was determined by a pairwise t-test against the cognate *Avr-P. f.* EtHAN CFU ($p < 0.05$) and is denoted by an *. Two additional biological replicates produced similar results.

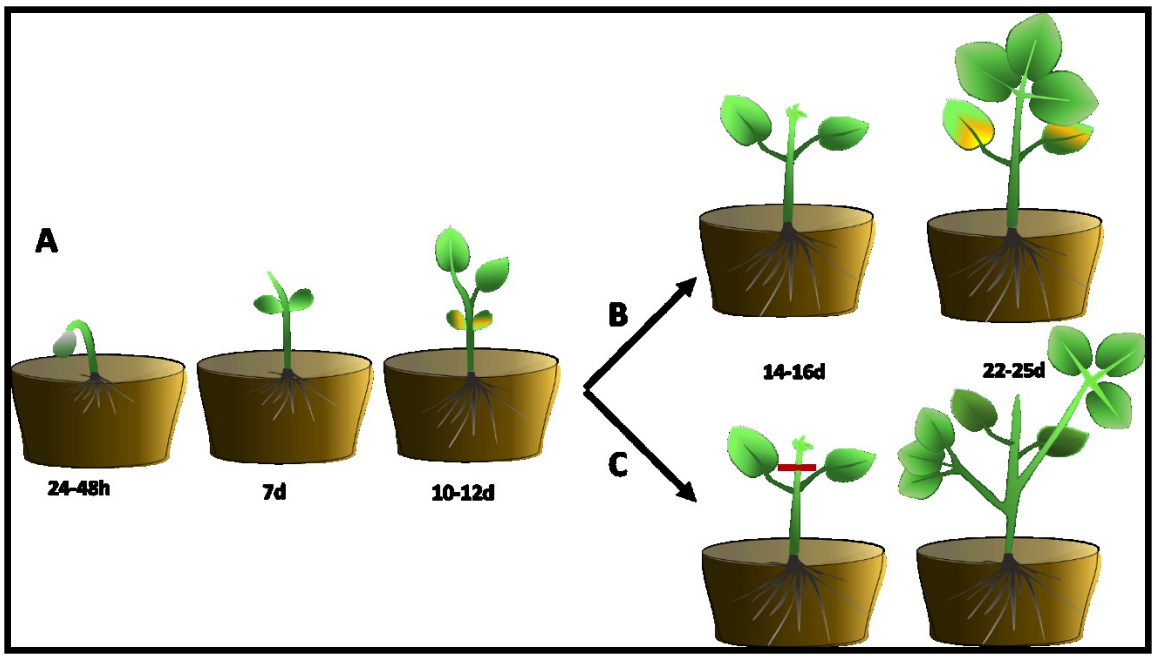

Figure 2.5 Soybean growth and pruning techniques for optimizing effector-response. *G. max* plants germinate, first producing cotyledons. **a)** Unifoliate leaves emerge after 10-12 days at which point the cotyledons senesce. **b)** The plant will then begin producing trifoliate leaves which will mature, leading to senescence of unifoliate leaves. **c)** If the immature trifoliate leaves are pruned between days 14-16 (Red Hash Mark) the unifoliate leaves will become thicker and darker. New inflorescence will be generated below the point of pruning.

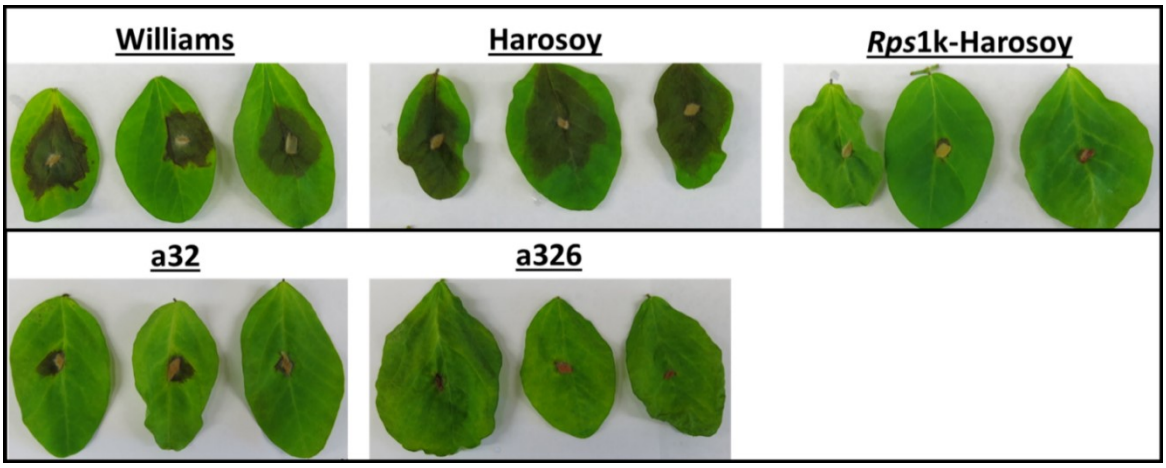

Figure 2.6 A simple *P. sojae* mycelial plug assay for testing detached soybean leaves. We detach trifoliate leaves after the V2 growth stage. These trifoliate leaves are inoculated with *P. sojae* plug. The infection is scored at 7 DPI. *P. sojae* produced large brown/black legions on susceptible cultivars Williams and Harosoy in all cases. *Rps*1k-Harosoy is included as a positive control for resistance against *P. sojae* race 2 and showed no expanded disease legion. *P. sojae* race 2 did not produce expanded disease legions on gm32 or gm326 suggesting that they are resistant to this isolate. This figure was produced from one biological replicate (n = 3 plants / 3 leaves per replicate). Two additional biological replicates produced similar results.

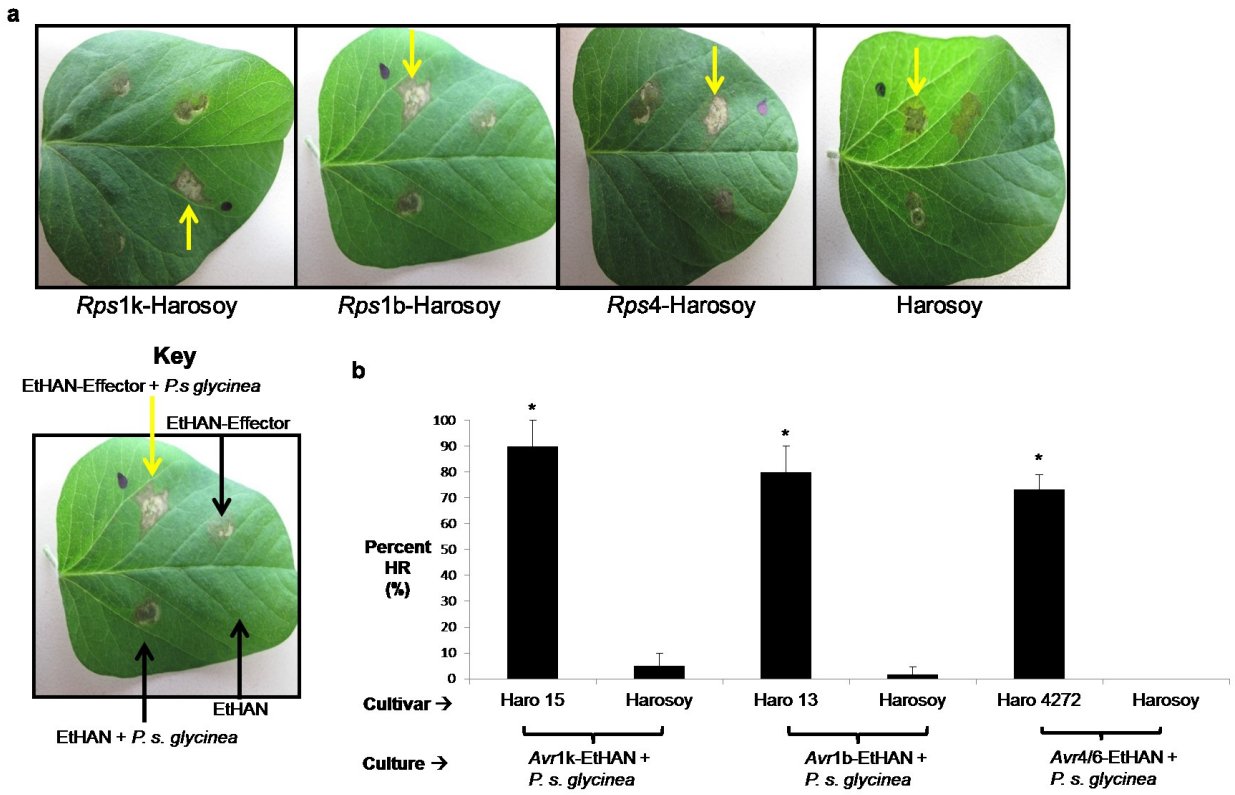

Figure 2.7 Validating the *Pseudomonas* effector delivery system using known *Avr/R* interactions. **a)** *P. sojae* avirulence proteins trigger gene-for-gene resistance when delivered from *P. fluorescens* by Type III secretion. The key depicts the infiltration strategy. The yellow arrow indicates the sites at which EtHAN expressing the avirulence effector was co-infiltrated with *Psg* race 4. The adjacent infiltration is EtHAN expressing the avirulence effector without *P. s. glycinea* race 4. The negative controls for each treatment were infiltrated on the opposite side of the leaf. **b)** The graph quantifies the amount of times a visual HR was produced on a cultivar, represented as % HR. Harosoy was used as a negative control. The error bars depict standard deviation between the three biological replicates (n = 10 plants/ 20 leaves per replicate). Statistical significance was determined by a pairwise t-test against Harosoy ($p < 0.05$) and is represented by an asterisk.

Table 2.3 Validating effector delivery using *Avr*1k, *Avr*1b, and *Avr*4/6 on *Rps* cultivars in the Williams background. These effectors produce about 30% background cell death on cultivar Williams. Three independent biological replicates were performed (n = 10 plants / 20 leaves per replicate). Standard deviation was calculated between the three replicates.

G. max Cultivar	**% HR *Avr*1k**	**% HR *Avr*1b**	**% HR *Avr*4/6**
Williams82	84 ± 11	28 ± 14	30 ±6
L77-1863	46 ± 7	72 ± 16	28 ± 11
L85-2352	22 ± 8	27 ± 6	68 ± 18
Williams	34 ± 11	25 ± 6	32 ± 6

Table 2.4 A EtHAN and *Psg* race 4 mixture of bacteria do not produce a HR on tested cultivars. Three independent biological replicates were performed (n = 10 plants / 20 leaves per replicate). Standard deviation was calculated between the three replicates.

Isoline	**Resistance Gene**	**EtHAN + *Psg* race 4**
Williams 82	*Rps*1k	8 ± 2
Haro 15	*Rps*1k	4 ± 1
L77-1863	*Rps*1b	12 ± 5
Haro 13	*Rps*1b	2 ± 1
L85-2352	*Rps*4	13 ± 3
Haro 4272	*Rps*4	0

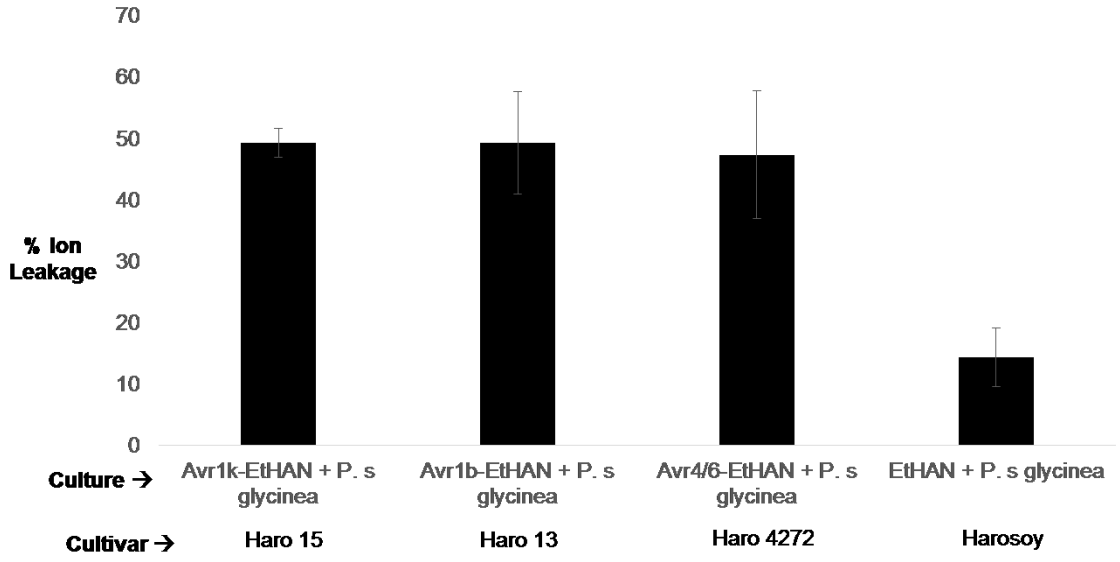

Figure 2.8 Ion leakage assay to quantify cell death symptoms in visual assays. *Avr*1k, *Avr*1b, and *Avr*4/6 were inoculated onto cultivars which contained a cognate *R* gene. EtHAN + *Psg* race 4 on Harosoy was used to measure background cell death. Three independent biological replicates were performed (n = 3 plants / 6 leaf punches per replicate). Standard deviation was calculated between the three replicates.

Table 2.5 Soybean germplasm respond to core *P. sojae* effectors, *Avh*16, *Avh*180, and *Avh*240. Responses of 30 *G. max* accessions to core effectors *Avh*16, *Avh*180, and *Avh*240. Data are presented as percentage of infiltration sites responding with a macroscopic HR, with standard deviation between the three biological replicates (n = 10 plants / 20 leaves per replicate).. Statistical significance was determined by pairwise t-test against Harosoy ($p < 0.05$). No background cell death was recorded for the *P. sojae* resistant *G. max* germplasm.

G. max **Parental Accession**	***Avh*16** **% HR**	***Avh*180** **% HR**	***Avh*240** **% HR**	***Avh*16** **T-Test (p)**	***Avh*180** **T-Test (p)**	***Avh*240** **T-Test (p)**
99	54 ± 7	0	0	P<0.001	0	0
321	51 ± 28	0	0	P<0.04	0	0
48	67 ± 31	0	0	P<0.03	0	0
144	70 ± 24	0	0	P<0.02	0	0
31	0	86 ± 4	0	0	P<0.0003	0
326	0	86 ± 16	0	0	P<0.005	0
314	0	70 ± 10	0	0	P<0.003	0
20	0	0	60 ± 10	0	0	P<0.004
13	0	0	73 ± 21	0	0	P<0.01
32	88 ± 11	0	93 ± 7	P<0.001	0	P<0.0006
291	0	73 ± 15	77 ± 15	0	P<0.005	P<0.006
78	0	90 ± 10	91 ± 9	0	P<0.002	P<0.001
320	68 ± 16	63 ± 6	97 ± 6	P<0.008	P<0.001	P<0.0005
Harosoy	3	0	0	0	0	0

Table 2.6 Homologous effectors, *Avh*16 and *Avh*7a, provoke similar response patterns in resistant germplasm. We identified *Avh*7a as a homolog of *Avh*16. Resistant *G. max* accessions which responded to *Avh16* with a HR, were tested with *Avh7a* as well. We obtained similar results in responding cultivars. This data was produced from three biological replicates (n = 10 plants / 20 leaves per replicate). Standard deviation was calculated between the three replicates.

***G. max* Parental Accession**	***Avh*16 % HR**	***Avh*7a %HR**
99	54 ± 7	87 ± 6
321	51 ± 28	100 ± 0
48	67 ± 31	67 ± 6
144	70 ± 24	63 ± 12
32	88 ± 11	93 ± 6
320	68 ± 16	100 ± 0

Table 2.7 Response of *G. max* germplasm to twelve core *P. sojae* effectors. Blank cells indicate that the accession did not respond to the corresponding effector with an HR % >30. The delivery of *Avh*23 and *Avh*110 to the resistant germplasm did not produce a HR on any accession. Three independent biological replicates were performed (n = 5 plants / 10 leaves per replicate). Standard deviation was calculated between the three replicates.

***G. max* Parental Accession**	**Response to Core *P. sojae* Effectors**									
	***Avh*16**	***Avh*180**	***Avh*240**	***Avh*53**	***Avh*137**	***Avh*261**	***Avh*488**	**Snel1**	***Avh*94**	***Avh*241**
13			73 ± 21						55 ± 16	84 ± 10
20			60 ± 10							
31		86 ± 4		82 ± 8					71 ± 16	
32	88 ± 11		93 ± 7							
40				83 ± 10			85 ± 8			
41				85 ± 8	81 ± 14					
48	67 ± 31								86 ± 4	
78		90 ± 10	91 ± 9							
92					77 ± 7					
94				55 ± 6	62 ± 10	81 ± 6				
96					81 ± 6	84 ± 15				
98									72 ± 10	
99	54 ± 7									
106				86 ± 8	60 ± 24					
121				78 ± 6		62 ± 14				80 ± 10
123				54 ± 26		76 ± 14				
144	70 ± 24									
291		73 ± 15	77 ± 15		56 ± 10		66 ± 14			
314		70 ± 10			83 ± 6					

315									77 ± 12	
317								84 ± 8		60 ± 24
320	68 ± 16	63 ± 6	97 ± 6							
321	51 ± 28				62 ±14					
326		86 ± 16					66 ± 20			

Table 2.8 *G. max* accession which responded to core effectors were bred with susceptible Williams. We tested multiple individuals from segregating $F_{2:3}$ populations for a response to the effector with a HR. The tested $F_{2:3}$ populations have a * next the cross name.

Cross	ID	*Avh*16	*Avh*180	*Avh*240	Maturity Group
32(R) x Williams(S)*	cr32				V
326(R) x Williams(S)*	cr326				IV
144(R) x Williams(S)	cr144				IV
284(R) x Williams(S)	cr284				IV
291(R) x Williams(S)	c291				IV
13(R) x Williams (S)	cr13				IV
320(R) x Williams(S)	cr320				IV

Table 2.9 Effector-response phenotypic ratios in $F_{2:3}$ populations. We screened segregating $F_{2:3}$ families for the phenotype of response to an effector with a HR. We observed a 1:2:1 phenotypic ratio in all crosses. Four independent biological replicates were performed (n = 5 plants / 10 leaves per replicate). Statistical significance of our observed ratio was determined using a chi-squared test against a 1:2:1 expected ratio ($x > 0.05$). The observed ratios are not statistically significant suggesting that the response to the effector is provided by a single, dominant locus.

Effector	Cross	Number of F3 Families			Expected Ratio	x^2 value (2 df)
		HmR	Seg	HS		
*Avh*180	*G. max* 326(R) x Williams(S)	14	27	13	1:2:1	0.071
*Avh*16	*G. max* 32(R) x Williams(S)	21	45	23	1:2:1	0.101
*Avh*240	*G. max* 32(R) x Williams(S)	19	47	17	1:2:1	1.56

Table 2.10 Bacterial strains and their corresponding selectable markers are listed. All *Psuedomonas* strains were grown at 28°C and all *E. coli* strains were grown at 37°C.

Bacterial Strain	**Selectable Marker**	**Temperature (°C)**
Top 10 *E. coli*	None	37
P. fluorescens, EtHAN	Chloramphenicol	28
E. coli, RK600	Chloramphenicol	37
P. s pv glycinea race 4	Riffampicin	28
P. syringae DC3000	Tetracyclin	28
P. s DC3000, D28E	Riffampicin / Spectinomicin	28
P. s DC3000, D28E + *Avr*PtoB	Riffampicin / Spectinomicin	28

Table 2.11 The diagnostic primers used screen for positive transformants into pEDV6 are listed. In all cases, the pEDV6 F primer was used with a gene specific *R* primer to confirm the insert and proper directionality.

Primer	**Sequence (5'-3')**
pEDV6 F	GGCACCCCAGGCTTTACACTTTATG
*Avr*1K R	TCAGATAATCATGATGCTGT
*Avr*1B R	CCGGTGAAAGGTGTATCCGTTGTAG
*Avr*4/6 R	CGTTAGGTGGTGTAGTCCGACGGAC
*Avh*16 R	CCATCTTCTTTGCTTCCTTAGC
*Avh*7a R	CTACAAGCCGTCCGTGTTCATGCCCA
*Avh*180 R	CTAAGCGATGTTCGTCTG
*Avh*240 R	CTAGTTTGCGGGTTGG
*Avh*23 R	TCATGCATTGTCGGAAAGTTTGAAGT
*Avh*110 R	TTATCCTACGCGGACACTCGCTACGC
*Avh*53 R	GTTATTTTCGTTAGCCCCATA
*Avh*137 R	CGGGTAAATGTATCCCTCAAG
*Avh*261 R	AATGTGATTTTGCGGGTTGTC
*Avh*488 R	CGGCGACTGGCCCATGCGAGC
Snel1 R	CGATCGCCGGTGCTGACGACT
*Avh*94 R	CTAAGCGGTGTCCTCCTCCTCC
*Avh*241 R	GTTCAGCTCGTGCCACTTGAA
*Avh*7a R	CTACAAGCCGTCCGTGTTCATGCCCA

Table 2.12 Williams and Harosoy isolines are listed.

Resistance Gene	Cultivar	Isoline
Rps1k	Williams	Williams 82
Rps1k	Harosoy	Haro 15
Rps1b	Williams	L77-1863
Rps1b	Harosoy	Haro 13
Rps4	Williams	L85-2352
Rps4	Harosoy	Haro 4272

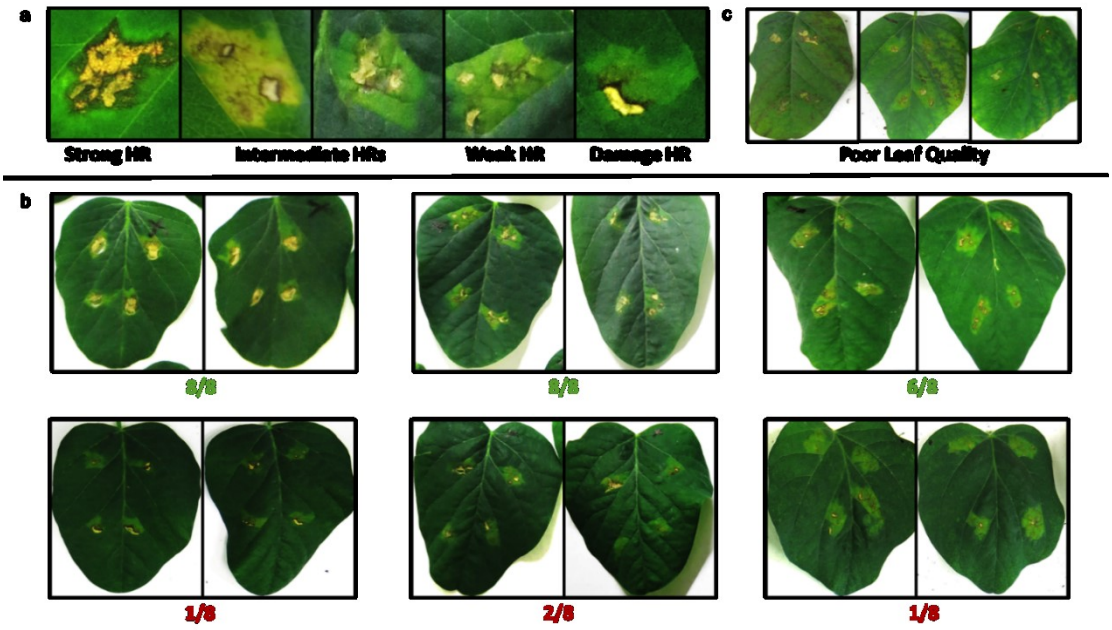

Figure 2.9 Effector-response was scored by presence or absence of a HR. **a)** The strength of the effector response (aka Strong/Medium/Weak) was not recorded for individual infiltration site. **b)** During all screens, each plant received 8 effector inoculations, 4 per unifoliate leaf. Each of the 8 infiltration spots were scored as either 1 or 0 for the presence or absence of a HR. If ≥5 individual sites produced a HR, the plant was considered a positive responder. If ≤2 spots produced a HR the plants were negative. If between 3-4 infiltration spots responded, the data was considered too ambiguous to score.

Chapter 3

Development of an Effector-Based Screening System to Identify Novel R *Genes in a Wild Relative of Cultivated Soybean*

Michael G. Fedkenheuer[1], Kevin E. Fedkenheuer[1], Colin L. Davis[1], Brett M. Tyler[2], M. A. Saghai-Maroof[3], and John M. McDowell[1*]

[1]Department of Plant Pathology, Physiology, and Weed Science, Latham Hall, Virginia Tech. Blacksburg, VA 24060-0390

[2]Department of Botany and Plant Pathology, Oregon State University, Corvallis, OR

[3]Department of Crop, Soil, and Environmental Sciences, Latham Hall, Virginia Tech, Blacksburg, VA 24060-0390

[*]for correspondence, johnmcd@vt.edu

In preparation for submission to *MPMI*

Author Contributions: MF wrote and developed this manuscript with advice from JM and KF. JM, BT, and SM advised this project. The majority of effector-based screening data was generated by MF. KF helped with development of effector-based screening in *G. soja* by providing technical expertise throughout experiments for troubleshooting and optimization. CD was involved with screening the segregating population and helped develop the batch style scarification technique.

Abstract

*T*he oomycete *Phytophthora sojae* causes a destructive root and stem rot disease of cultivated soybean (*Glycine max*). Over time, commercial cultivars with available resistance (*R*) genes are losing efficacy against *P. sojae*. We hypothesized that *Glycine soja*, a sexually compatible wild relative of *Glycine max*, could be exploited as a useful source of new *R* genes against soybean pathogens. We developed a system to screen *G. soja* with core RXLR effectors from *P. sojae* to identify novel *R* genes. We focused our screening on conserved RXLR effectors that are essential for virulence. *R* genes that recognize core effectors are expected to be durable, because mutations in the effector genes will result in a fitness penalty for the pathogen. We screened 24 *P. sojae*-resistant *G. soja* accessions with individual RXLR effectors delivered by *Pseudomonas fluorescens* Type III secretion. We identified several *G. soja* accessions for which delivery of one or more core effectors triggered a localized cell death, suggestive of effector-triggered immunity. We developed a segregating population from a cross of one *G. soja* line with a susceptible *G. max* line, to track inheritance of the *R* gene. Response to the effector *Avh*240 segregated in a 1:2:1 phenotypic ratio in the $F_{2:3}$ generation suggesting that this line contains one dominant *R* gene against the core *P. sojae* effector *Avh*240. These results indicate that an effector-based screening approach can be utilized to identify useful new *R* genes from a wild relative of soybean.

Introduction

Soybean is an important crop which accounts for 60% of world oilseed production [102]. The United States is a world leader in the production of various soybean products such as oil, crush, and meal [103]. Soybean production and trade continues to increase globally and in the US [103]. *Phytophthora* root and stem rot is one of the most destructive disease affecting soybean yield [104]. In 2006, losses associated with *Phytophthora* root and stem rot in the United States were 1,464 metric tons, equivalent to nearly $500 million USD [104].

Phytophthora sojae (*P. sojae*), the causal agent of this disease, is responsible for pre- and post-emergence damping off of susceptible seedlings [33]. On mature soybean plants, *P. sojae* causes root and stem browning and leaf chlorosis [95]. The disease symptoms generally appear 1 to 2 weeks after heavy rainfall [33]. *P. sojae* produces sporangia and oospores during infection. Sporangia release motile zoospores that swim to root exudates through wet soil. Zoospores then encyst and penetrate roots, producing hyphae that grow in the spaces between cells [105]. The filamentous hyphae create specialized feeding structures, known as haustoria, that draw nutrients out of the cell [82]. Additionally, these structures function as an interfaces where virulence factors, called effectors, are secreted to subvert immunity and reprogram the cell for feeding [82]. Oospores are thick-walled sexual structures produced in plant tissue that can survive for many years dominant in the soil and endure winter frosts. Oospores germinate in the spring and infect emerging seedlings. Heavy rains will induce oospore germination making this disease very volatile in seasons with extended periods of flooding, which typically initiates disease epidemics [105].

P. sojae secretes several different types of effector proteins to subvert plant immunity and alter host cell structure and function [44, 46]. The best-studied effector protein superfamily,

called RXLR effectors, are defined by an N-terminal secretion signal, followed by the consensus amino acid motif RXLR [106]. The RXLR motif is often, but not always, followed by a short motif enriched for acidic amino acids ("DEER") and by so-called "W" and "Y" domains that form helical "WY folds" which are unique to RXLR effectors in the *Phytophthora* and downy mildew families [44, 107]. These domains can be arranged to form complex folds, which make the WY fold a highly evolvable platform that supports structured surface polymorphisms upon rearrangement [46]. Virulence targets of RXLR proteins have been validated as key regulators of immunity, and it is becoming increasingly clear that RXLR proteins play a major role in promoting virulence of oomycetes in the *Phytophthora* genus [108].

Despite their importance for virulence, RXLR proteins can also be detrimental to the pathogen if recognition of an RXLR effector by a plant *R* protein leads to gene-for-gene resistance (more recently termed "effector triggered immunity" or ETI [109]). Indeed, every case of ETI against *Phytophthora* species, characterized at the molecular level, involves recognition of an RXLR protein by a nucleotide-binding, leucine-rich repeat immune receptor protein [46]. ETI is often characterized by localized cell death (termed the hypersensitive response or HR) which impedes pathogen growth [109]. This type of resistance is generally regarded as one of the most cost-effective tools to manage diseases caused by *Phytophthora* pathogens.

In soybean, there are 24 known Resistance to *Phytophthora sojae* (*Rps*) genes that provide gene-for-gene resistance against *P. sojae* infection. Seven of these genes have been commercially deployed with varying degrees of effectiveness against the most common *P. sojae* pathotypes [34, 110]. Unfortunately, even the most effective *Rps* genes are now being overcome by pathogen co-evolution. This co-evolution produces diverse *P. sojae* strains ("pathotypes") characterized by different patterns of pathogenicity on *Rps* soybean cultivars. In other words, a

soybean cultivar containing a *R* gene against *P. sojae* may be resistant to one pathotype and susceptible to a different pathotype [34]. It would be desirable to identify *R* genes with resistance to most or all of the *P. sojae* pathotypes encountered in field situations.

Genome analyses of oomycete phytopathogens is revealing the mechanisms behind the rapid evolution of pathotype diversity. *Phytophthora* genomes contain large, variable collections of RXLR-encoding genes which in turn has given rise to multiple *P. sojae* pathotypes [110]. Pathogen genomes are often organized by a bipartite distribution of fast and slow evolving genetic elements. It is hypothesized that pathogens create a two 'speed-speed genome' to modulate the evolutionary speeds of genes [111]. Effector genes are located in a part of the genome where rates of polymorphisms, copy-number variation, and recombination are extremely high [112]. Effector genes can be deleted or altered to avoid *R* gene detection. Due to genomic instability, expression of effectors is often variable. Transcriptional changes can cause effectors expression to fall below detection thresholds [46]. Polymorphisms that affect the coding sequence can cause effectors to have variability or off target catalytic activity. By this mechanism effector function can be changed or modulated to achieve new virulence mechanisms [46]. The proximity of RXLR effectors to transposable elements suggest a potential epigenetic adaptation to globally silence a group of RXLR effectors under environmentally favorable conditions [113]. These silencing events could potentially be reversed if the environmental pressures for the silencing are reduced, thereby providing the pathogen with a powerful mechanism for rapid co-evolution. Altogether, these mechanisms illustrate why host resistance to *Phytophthora* species is short-lived, and underscore the challenges of breeding soybean with durable resistance to *P. sojae* field isolates with diverse pathotypes, as are frequently encountered in the field [114].

Wild relatives of domesticated crop species often contain useful agronomic traits such as tolerance to abiotic stresses, yield enhancement, and disease resistance [115]. These traits can be bred into commercial cultivars by conventional breeding if the relative is sexually compatible with the crop or if somatic cell hybrids and bridge species can be used to circumvent compatibility issues. Working with sexually compatible species is advantageous because it simplifies the breeding process. There have been successful reports of breeding resistance from wild relatives into commercial varieties. One of the first examples of introgression of resistance from a wild species was in potato [116]. Since then, disease resistance traits have been introgressed from wild species in most major crop plants.

Soybean was domesticated 6,000-9,000 years ago in Eastern Asia [20]. Although many aspects of domestication remain unclear, *Glycine soja* (*G. soja*) is accepted as the closest known wild relative to *G. max* [20]. *G. max* seed contains about 17% more oil than *G. soja* seed. *G. max* germinates consistently to produce uniform plants with large seed and thin seed coats. *G. soja* produces small, vine-like plants with small seed and thick seed coats. Despite these phenotypic differences, *G. max* and *G. soja* are sexually compatible [95], such that useful traits from *G. soja* can, in principle, be bred into soybean cultivars. Many studies of soybean genetic diversity suggest that most landraces of *G. max* are monophyletic, and *G. soja* germplasm is reported to contain more genetic diversity than *G. max* germplasm. Wen et al. and Joshi et al. both hypothesized six *G. soja* genetic subgroups [117, 118]. The subgroups are separated geographically and correspond to Japan, Korea, Russia, northeast China, southern China, and the Huanghuai Valleys in China. Long-term seed dispersal is rare and does not appear to impact population structure of native populations.

Resistance against soybean cyst nematode [119], soybean mosaic virus [120], and *Phytophthora* root and stem rot [89] have been reported in *G. soja*. There are no reports of using directed breeding to intentionally introgress disease resistance traits from *G. soja* to *G. max*. Using molecular diagnostics, *G. soja* can be exploited as a source of resistance genes against *P. sojae*. Our goal is to identify novel and durable *R* genes against *P. sojae* in *G. soja* accessions, using an approach that combines traditional, pathogen-based screens with effector-based screen in which plant germplasm is probed for immunity triggered by delivery of individual effectors. This effector-based approach was pioneered against *Phytophthora infestans* [67]. 54 RXLR effectors from *P. infestans* were assayed for avirulence activity, by delivering effectors one-at-a-time to *Solanum* germplasm via *Agrobacterium*-mediated transient expression. In this system, *Agrobacterium* suspensions were infiltrated into plant leaves, which were then screened for a macroscopic cell death response that could result from hypersensitive cell death triggered by recognition of the effector. Vleeshouwers et al. used wild *Solanum* species to identify the *Rpi*-blb1 *R* gene using this approach. The avirulence response was triggered by the IpiO RXLR family [67]. More recently, Oh et al. bred novel *R* genes *Rpi*-blb1 and *Rpi*-blb2 against potato late blight from a wild *Solanum* species into potato [121]. Efforts are now underway to commercialize these genes in potato. This example illustrates how useful *R* genes were discovered by probing wild *Solanaceae* with RXLR effectors.

Following the *P. infestans* example, our approach is based on screening with RXLR effectors; however we focused our approach on "core effectors" that are highly expressed early in infection, conserved and monomorphic among the four most common *P. sojae* pathotypes, and required for virulence. By focusing on effectors that are conserved and contribute most to virulence, we hope to find resistance genes that target the pathogen's most static or most

vulnerable points. This would make it more difficult for the pathogen to evolve quickly by mutating or silencing the gene and activating genes with redundant functions. In addition, *R* genes that recognize conserved effectors are more likely to provide recognition and resistance to a broad range of field isolates.

This study builds on a recent effort in which comparative genomics and transcriptomics were used to identify RXLR effector genes in *P. sojae* which were highly expressed early in infection and conserved among the four most common *P. sojae* pathotypes [122, 123]. Then, transient gene silencing was used to suppress expression of candidate core *P. sojae* effectors. The silencing of core *P. sojae* effectors *Avh*16, *Avh*180, and *Avh*240 greatly reduced pathogen growth on the susceptible cultivars, while the silencing of 7 other effectors *Avh*53, *Avh*137, *Avh*23, *Avh*110, *Avh*488, SNEL1 and *Avh*241showed moderately reduced pathogen growth. These are the effectors that we used in the current study.

Our screening strategy was based on an effector-based screening approach that was developed in *G .max* (Chapter 2). Importantly, this study developed an alternative system for effector delivery (see below). We were able to effectively optimize techniques developed in this study for use in wild soybean. After normalizing the variables of germination and growth stage in wild soybean we found that the effector-based screening was suitable for use with minor technical modifications. Using effector-based screening we were able to identify putative resistance genes in accessions containing novel resistance to *P. sojae*. Additionally, we were able to confirm simple inheritance of one putative *R* gene in segregating populations. This suggests that this technique can be used to identify *R* genes in *G. soja* and is sensitive enough to map resistance in crosses between *G. soja* and *G. max*, thereby validating its utility for disease resistance breeding.

Results

Overview of the Strategy

Our approach for delivering effectors was based on a screening system described in Fedkenheuer et al. 2016 (Chapter 2). Because *Agrobacterium*-mediated transient transformation is not efficient in soybean, we developed a system for delivering effectors via Type III secretion from *Pseudomonas*. Trials with different *Pseudomonas* species revealed that the best strain for delivery in soybean is the soil bacterium *P. fluorescens*, EtHAN. EtHAN contains an artificially engineered type III secretion system which can be utilized to deliver individual effectors. *P. sojae* effectors were cloned into the Effector Detector Vector (pEDV6) that contains the bacterial *AvrRps*4 promoter and leader sequence which guides proteins through the type III secretion system [93]. We co-infiltrated EtHAN with *P. syringae pathovar glycinea* (*Psg*) for effector-based screens to improve signal intensity. *Psg* has been shown to improve the growth of EtHAN *in planta* presumably by suppressing host immunity (Chapter 2). Consequential to improved growth, more effector protein is likely delivered. If a host *R* gene recognizes the delivered effector, a macroscopic HR is triggered that can be scored visually.

In this study, we validated that the EtHAN-effector system efficiently delivers core *P. sojae* effectors into *G. soja* unifoliate leaves. Recently, Matthiesen et al. screened ~1,000 Glycine accessions with a mixture of three *P. sojae* isolates which defeat 13 commercial *Rps* genes [89]. From these accessions, we chose 24 *G. soja* accessions for effector-based screening. These resistant lines are likely to contain novel *R* gene loci or new alleles at known loci. The effector-based approach described below provides a mechanism through which to sort and prioritize these genes for breeding.

Optimizing the Screening System

The first objective of this study was to optimize growth conditions for *G. soja*, because our experience with this screen in *G. max* demonstrated that robust plant health is of key importance to obtaining reliable results from bacterial inoculations. This required several modifications of the protocols developed for the *G. max* screen. *G. soja* seeds are small and are coated with a thick outer wall. Germination of *G. soja* seed requires removal of the seed coat (scarification). We found that *G. soja* seeds germinated best when scarified in 100% H_2SO_4. We determined that 5 minutes in these conditions was sufficient to remove all seed coats. Immediately following chemical treatment, seeds were removed and rinsed with diH_2O to remove all traces of acid.

Another complication is that vegetative growth and development is more variable in *G. soja* than in cultivated soybean. Unlike *G. max*, *G. soja* must be germinated at 100% humidity to achieve consistent germination. Another important step was to prune off the first set of trifoliates leaves at three days after germination. This allowed us to standardize growth stage prior to effector infiltration. This is critical when screening diverse accessions of *G. soja* because timing of unifoliate leaf maturity is often variable among accessions. Pruning of trifoliate leaves also improves unifoliate leaf quality. After pruning, unifoliate leaves became thicker and acquired a darker green color. In plants treated in this manner, resistance responses are stronger and the infiltration zone is more clearly visible. When scoring for visual HRs, it is important to judge the spread of cell death outside of the zone where the syringe interfaced with the leaf surface. This is done to avoid false positives caused from damage induced by the infiltration process. The negative control and the effector treatment must be done on different plants because a strong effector response can trigger cell death in the negative control (a priming effect). Individuals

were subjected to only one treatment for this reason. When screening individual effectors, the experimental treatment can be treated as a negative control on non-responding accessions. When recognition does not occur, levels of cell death are often below those of the untransformed control (Figure 3.1).

Screening G. soja *accessions with 3* P. sojae *pathotypes*

As mentioned above, our screen focused on *G. soja* accessions identified in a previous study to be resistant to a combination of *P. sojae* pathotypes which collectively overcome all known *Rps* genes. Table 3.1 lists the relevant accession information including PI numbers and geographic origin. To confirm disease resistance responses we performed disease screening on *G. soja* germplasm using individual isolates rather than the combination of three used in the previous study. We believed it was important to look at infections on an individual level because it is impossible to predict the complexity of interactions when using isolates in combination. For example, a strong immune response to one pathotype may override the virulence mechanisms of another pathotype. We optimized infectivity of our cultures at monthly intervals by passaging isolates through infected soybean (cv. Williams). The process of refreshing *P. sojae* cultures is essential to maintain strong infection. A loss in virulence over time was observed in all isolates during stem and leaf inoculation assays.

We developed a disease assay in which trifoliate leaves were inoculated with agar plugs from each of three virulent accessions: Pt1005, Pt2004, and Race 7 (Figure 3.2). This assay is reproducible, convenient, and allows the same plants to be scored simultaneously for pathogen resistance and effector response. Wounding of the leaf prior to inoculation was essential for reproducibility. After 5-7 days, resistance versus susceptibility was very clear, and we scored the plants as resistant or susceptible without taking measurements of disease lesions. The *G. max*

accession Williams was used as a control for susceptibility. We confirmed that many of the *G. soja* accessions were resistant to all three isolates; however, several accessions were partially susceptible to one or two pathotypes. No accessions were susceptible to all three isolates. Hypocotyl inoculations were done to confirm instances of susceptibility in foliar assays. In all cases, we observed perfect agreement between hypocotyl and leaf inoculation. The major technical challenge of these assays is providing a consistently moist infection site for pathogen infection following inoculation. This refined pathotype information will be important for prioritizing accessions for further characterization and for accurately mapping pathogen resistance loci in segregating populations. Hypocotyl inoculations were laborious and had limited throughput when compared to the trifoliate assay.

Three G. soja *Accessions Contain Novel Resistance to* Psg *race 4, a Bacterial Pathogen of Soybean*

As mentioned above, our effector delivery system is based on co-inoculation with EtHAN (containing the effector transgene) and *Psg* race 4 (to boost growth of the EtHAN strain). Thus, it was necessary to pre-screen *G. soja* accessions for immune responses to *Psg* race 4 that would interfere with effector delivery during the co-inoculation with EtHAN + *Psg*. This was important to eliminate false positives from our screens that could occur from ETI triggered by the native effectors secreted by *Psg* race 4. We found three *G. soja* accessions (gs2763, gs730, and gs727) that produced a HR when pressure infiltrated with *Psg* race 4 (Figure 3.3 and Table 3.2). Visual HRs were apparent one to two days post inoculation (DPI). Gs2763 and gs730 produced strong HRs. Accession gs727 produced a weak and inconsistent visual HR against *Psg*. Thus, we were unable to screen for effector-specific HRs in these accessions due to the immune

interaction with the helper strain *Psg*. However, these accessions likely contain potentially useful resistance genes against *Psg*.

Effector-based screening

Our first screen of 20 *P. sojae*-resistant *G. soja* accessions was conducted with three of the most promising core *P. sojae* effectors: *Avh*16*, Avh*180, and *Avh*240. These effectors are strongly expressed and make major contributions to virulence in all four of the reference *P. sojae* accessions, so *R* genes against any of these effectors could be very effective. Effectors were delivered individually for each of the 20 accessions via co-infiltration with EtHAN and *Psg* race 4, as described in Figure 3.1. We scored responses to these effectors with a HR as a percentage (%HR). We observed 3 accessions (gs2777, gs2514, and gs2292) that produced HRs against *Avh*16, *Avh*180, and *Avh*240 respectively (Figure 3.4). Effector responses in these accessions were strong and extremely specific (Table 3.3). Gs2292 produced a HR against *Avh*240 in 95% of individuals tested. Accessions gs2777 and gs2514 produced HRs against *Avh*16 and *Avh*180 respectively in 90% of individuals tested. These accessions produce strong and consistent HRs against their corresponding effectors and display no background cell death from our internal control of untransformed EtHAN co-infiltrated with *Psg*.

A second round of screens was performed with core effectors *Avh53*, *Avh*137, *Avh*23, *Avh*110, *Avh*488, *Snel*1 and *Avh*241. *Avh*53 and *Avh*137 elicited resistance responses in many accessions from multiple subgroups (Figure 3.5). Additionally, we observed paired responses to effectors *Avh*53 and *Avh*137 only in accessions collected in Primorsky, Russia. This observed geographic distribution suggests that these accessions share common resistance loci. *Avh*23 and *Avh*110 did not produce a visual HR on any tested *P. sojae*-resistant *G. soja* accession (Table 3.4 A-G). We compiled effector screening data and accession information in Table 3.5

Determining the Inheritance of Potential R *Genes in a Segregating $F_{2:3}$ Population*

Root and stem rot disease resistant *G. soja* accessions which responded with a HR to a core *P. sojae* effector were crossed with the susceptible *G. max* cultivar Williams as part of our breeding program. In order to test the viability of using effector-based screening to map a resistance gene, we looked at the inheritance of a potential *R* gene in a segregating $F_{2:3}$ population (Figure 3.6). We analyzed the cross, gs2292 (R) x Williams (S), for the phenotype of response to core *P. sojae* effector *Avh*240 with a HR. Figure 3.7 B describes the screening and scoring individuals within segregating $F_{2:3}$ populations. We collected data from 89 $F_{2:3}$ families with a sample size n>10. Because most *R* genes segregate as major-effect, genetically dominant loci, we expected a 1:2:1 phenotypic ratio. HR strength was variable throughout biological replicates, however the presence or absence of visual HRs was extremely consistent. As expected, we observed a 1:2:1 phenotypic ratio in the $F_{2:3}$ progeny of a cross between gs2292 (R) x Williams (S) (Figure 3.7 and Table 3.6). By analyzing this population, we determined that effector-based screening is both sensitive and accurate enough to identify resistance responses on an individual plant basis. Additionally, the response to *Avh*240 in this accession appears to segregate as a single locus, easily amenable to introgression into *G. max* cultivars.

Discussion

Soybean is harvested for oil and protein, and ranked second for area planted in the US in 2014 [124]. In 2015, 55% of vegetable oil consumed in the United States of America (USA) came from soybean, underscoring the importance of this crop. *Phytophthora* root and stem rot substantially affects the profitability of soybean by reducing soybean harvests in pathogen suited environments across the world [104]. In the USA, *Phytophthora* root and stem rot is most severe in the Midwest, and resistance to *P. sojae* can be broken by many factors [114]. In the past, soybean *Rps* genes were reported to confer full resistance against most *P. sojae* pathotypes. Unfortunately, *P. sojae* is evolving to evade recognition by soybean *Rps* genes, and the average effectiveness of an *Rps* gene in the field is 8-15 years [88]. Thus, it is important to identify novel *R* genes against *P. sojae* which are durable in the field and which recognize the potentially broad diversity of isolates encountered in field situations.

We began by assessing *G. soja* germplasm for resistance to *P. sojae* to confirm and extend the results from Matthiesen et al. [89]. We used the same three pathotypes, which collectively overcome all known *Rps* resistance genes except Rps8, that were used by [89]. We developed a trifoliate infection assay to complement our new effector based screening system. Agar plugs were used to infect a wounded trifoliate leaf. Our trifoliate agar plug infection assay can be used to measure quantitative resistance by measuring lesion diameter, or it can be used to measure qualitative resistance by assaying for the presence or absence of disease lesions in pronounced examples. We used specialized tools to quickly generate uniform agar chunks, greatly increasing throughput and consistency. Most importantly, this assay can be used in combination with effector-based screening since trifoliates are removed during the pruning process. Using this disease screening technique, we evaluated *G. soja* germplasm for novel

resistance to *P. sojae*. Screening with pathotypes individually versus in combination generated uniquely complimentary data. For example, the individual isolate approach generates a more accurate pathotype profile; while screening in combination allows us to infer the strength of the resistance response. Resistance observed in screening with a combination of pathotypes indicate that resistance responses will not be easily overcome through diversification of effector profiles.

We chose to screen *P. sojae* resistant *G. soja* germplasm with core *P. sojae* effectors to identify new sources of *R* genes against *Phytophthora* root and stem rot disease. A core *P. sojae* effector is highly expressed in early *P. sojae* infection, conserved among the 4 most common *P. sojae* pathotypes, and essential for *P. sojae* virulence. To assess effector impact on virulence, Tyler et al. used transient gene silencing to suppress expression of candidate core *P. sojae* effectors. The silencing of core *P. sojae* effectors *Avh*16, *Avh*180, and *Avh*240 greatly reduced pathogen growth on the susceptible *G. max* cultivar Williams. We selected these 3 effectors as our most promising *P. sojae* core effectors. The silencing of core *P. sojae* effectors *Avh*53, *Avh*137, *Avh*23, *Avh*110, *Avh*488, and SNEL1 moderately decreased pathogen growth. We used these 9 core *P. sojae* effectors to probe for potential *R* genes in *P. sojae* resistant *G. soja* germplasm against core *P. sojae* effectors. Because these *P. sojae* effectors are monomorphic and important for virulence, we hypothesize that *P. sojae* will be unable to easily discard core effectors to evade *R* gene detection. For this reason, we predict that a *R* gene against a core *P. sojae* effector will provide durable resistance against *P. sojae* in the field. We hypothesize that *R* genes against core effector targets will provide broad spectrum resistance because these core effectors contain conserved sequences present among the most common field isolates of *P. sojae*.

Prior to effector-based screening of *G. soja* germplasm with our library of *P. sojae* core effector candidates we established the background of *Psg* in all accessions. This screen identified

three *G. soja* accessions: gs2763, gs730, and gs727 which contain resistance to *Psg* race 4. *Psg*, a bacterial pathogen, is the causal agent of bacterial blight on soybean [125]. *Psg* is most virulent in the northern most states and into parts of Canada [125]. By testing *Psg* resistant accessions with other pathotypes (races) of *Psg* whether this resistance is durable against all isolates of this pathogen. We can use segregating populations available in our germplasm collection to track resistance against both *Psg* and *P. sojae* using the assays developed in this study. It will be interesting to determine if there is a linkage between bacterial and oomycete resistance mechanisms.

Resistance responses against *Psg* in these three accessions excluded these accessions from effector-based screening. We compiled effector based screening data from the remaining 20 *G. soja* accessions with 10 effectors. We found putative *R* gene candidates against 8/10 core effector candidates. Effector responses for 6 core effectors were very specific (only one or two responding accessions per effector). We observed strong and clear resistance responses against our top candidate effectors: *Avh*16, *Avh*180, and *Avh*240. In some cases, we found a correlation between the effector response of a *P. sojae* resistant *G. soja* accession and geographic collection location. *Avh*53 provoked responses in 6 accessions, while *Avh*137 provoked resistance responses in 9 accessions. We confirmed that these HRs were effector specific by extensively screening *Avh*53 and *Avh*137 on non-responding *G. soja* accessions. Four *P. sojae* resistant Russian *G. soja* accessions responded with a HR to both core *P. sojae* effectors *Avh*53 and *Avh*137. From the 2 remaining *P. sojae* resistant Russian *G. soja* accessions, one accession responded to *Avh*53 and one accessions responded to *Avh*137. No other effector responses were observed in *P. sojae* resistant Russian *G. soja* accessions. This could indicate that *R* genes against *Avh*53 and *Avh*137 are under positive selective pressure in Russia. We found multiple *P.*

sojae resistant South Korean *G. soja* accessions which responded to *Avh*137 and 1 South Korean accession which responded to *Avh*53. One Japanese *G. soja* accession responded to *Avh*137 as well. Since, subgroups are genetically isolated from each other we hypothesize that evolution has either converged on these effector targets or that these accessions share *R* genes from ancestral origins.

We used the *Pseudomonas* effector screening system to analyze a segregating $F_{2:3}$ population, gs2292 (R) x Williams (S). Similar to the *G. soja* parental accession, $F_{2:3}$ seed required scarification prior to planting. We found that scarifying *G. soja* seeds and the $F_{2:3}$ seeds in 100% H_2SO_4 optimized seed germination and experimental throughput. Individuals in $F_{2:3}$ families shared morphological characteristics more similar to *G. max* cultivar Williams. We observed a 1:2:1 phenotypic ratio for the phenotype of response to the core *P. sojae* effector *Avh*240 with a HR. This suggests a classical dominance inheritance. All *P. sojae* resistant *G. soja* accessions which produced a HR against a core *P. sojae* effector were crossed with *G. max* cultivar Williams as part of our breeding program. We will use recombinant inbred lines to further evaluate and fine-map potential *R* genes. A limitation of our approach is applying this system in the *G. max* Williams background. Effectors which produce a strong HR will often produce background cell death in Williams. This makes scoring individuals within segregating populations more challenging. We hope to mitigate these limitations by further optimization of our system or by exploring other elite accessions. Since effector-based screening was not paired with pathogen infection assays in $F_{2:3}$ populations it is impossible to say for certain whether our identified effector response genes are truly responsible for pathogen resistance. The parental accession gs2292 is resistant to three accessions which overcome all known *Rps* resistance. Additionally, this accession responds to *Avh*240, one of our most promising core effectors, in

effector-based screens. These data taken together suggest that these techniques will complement each other in more advanced populations. We will analyze individuals within recombinant inbred populations using our trifoliate infection assay in combination with our effector-based screening assay to understand this interplay in future studies.

Effector-based screening is a new but powerful technique. We believe that this technique is an excellent complement to classic pathogen infection assays. These techniques can be used together to map resistance loci more accurately. Additionally populations containing multiple resistance loci can be more clearly separated. Some of the most successful examples of breeding for resistance have come from wild species. For example, the *R* gene *Pto* which confers resistance to *Pseudomonas syringae pathovar tomato* has been used to control speck disease for over 70 years [126]. Until recently, the only resistance against root-knot nematode in tomato was the *R* gene Mi-1[127]. Introgressed from the wild tomato species, this gene from *Lycopersicon peruvianum* is an excellent example of an effective resistance gene derived from a wild species. In potato, the *R* gene *Pi-ber* was derived from *Solanum berthaultii* and confers complete resistance against the *P. infestans* isolate US8 [128]. We built on work in *G. max* to develop an effector-based screening system for *G. sojae* (Chapter 2). We were able to utilize bacterial type III secretion to deliver individual effectors to the interior of *G. soja* unifoliates. After growth conditions were optimized, this system was seamlessly transitioned into *G. soja*, underscoring the potential of this system to be deployed across broad spectrum of crop plants. We used resources (germplasm and cultivars with specific *Rps* genes) available in *G. max* to develop a disease system that would be effective in both *G. max* and *G. soja* for any pathotype.

By targeting our effector screens to identify *R* genes against core *P. sojae* effectors, we can look for durable resistance in a unique way. Additionally, we designed a disease assay which

can be performed concurrently with effector response screens on the same individual plants, to facilitate linking effector responses with pathogen resistance. The introduction of these genes into cultivated soybean by traditional breeding allows for product introgression into all soy-based markets. We hope to map these genes to specific loci by examining phenotypes in segregating progeny. Mapping resistance genes using genetic markers is an effective and proven method [129]. We hope to use the unique information acquired from an intelligently designed effector-based screens and disease assays to predict *R* gene specificity and durability in a field setting [130].

Materials and Methods

Culture Preparation and Maintenance

Phytophthora sojae cultures of pathotypes pt1005, pt2004, and Race 7 were kindly provided by the Robertson Lab at Iowa State University [89]. Agar plugs were used to inoculate trifoliate leaves of susceptible Williams. Seven days post inoculation, visibly infected areas were cut and washed in 70% EtOH. Sterilized plant material was washed with diH_2O, dried, and plated on to PARP-V8 plates. Cultures were incubated in the dark at room temperature. Agar plugs containing *P. sojae* mycelium were taken from the edges of the growing colonies and used to start new V8 plates. *P. sojae* grows quickly on V8 media and fully colonized plates within two weeks. Pathogen material prepared in this fashion was used for infection assays. On average, *P. sojae* will colonize a PARP-V8 plate in 6-8 weeks. After 8 weeks, *P. sojae* pathotypes were re-isolated using the process outlined above, to maintain virulence.

Trifoliate Leaf Agar Plug Infection Assay

We used agar plugs from pathotypes pt1005, pt2004, and Race 7 to infect mature trifoliate leaves from our *G. soja* germplasm collection. Trifoliate leaves were detached and placed into Petri dishes containing filter paper saturated with water. A scalpel was used to wound trifoliate leaves. Wound size, shape, and depth are not important within reason; however the position and angle of the wound will sometime effect the direction of the disease lesion. Agar plugs were then placed over the wound and a drop of H_2O was added to the agar plug to hydrate the site of infection. We used a specialized tool, specifically a Large/Jumbo Double End Steel Amalgam Carrier ®Miltex Instrument Co. to rapidly generate consistent sized agar plugs. Plates were sealed with parafilm to prevent moisture loss and maintain humidity during infection. Sealed plates were stored under normal growing conditions until imaging. After 7-10 days, disease lesions on susceptible plants covered 80-100% of the leaf surface. While disease lesions are often present on resistant accessions, these lesions do not expand past the wound site.

Hypocotyl Inoculation Assay

We confirmed our results using standard hypocotyl inoculation assays [105]. We applied agar plugs to wounded hypocotyls of soil grown plants. After inoculation, lesions developed in resistant and susceptible accessions. Lesions did not expand outside of the site of inoculation in resistant germplasm. Lesions expanded rapidly in susceptible individuals making differences in susceptibility clear. We confirmed resistance and susceptibility phenotypes using this technique to validate our trifoliate screen.

Scarification

Seeds were scarified in 100% H_2SO_4, for 5 minutes. Seeds were then rinsed vigorously in H_2SO_4 and directly planted or dried for storage. As a high-throughput modification, accessions were scarified using a 98 well 1.5 mL centrifuge tube holder with holes bored through the wells (Figure 3.8). This allowed seed to be scarified in batch, while keeping accessions separate. Manual scarification using coarse sandpaper is effective; however germination rates and emergence times were improved with acid scarification.

Planting and Maintenance

For all screens, *G. max* was planted in Fafner P2 potting media. Fafner P2 potting media was hydrated with 2 L of water and Cal-Mag Fertilizer®. 2.5 inch pots were packed firmly with media. 5 seeds were sown per pot and covered with about 2-3 cm of loosely packed potting media. The top soil was treated with Marathon insecticide, put into flats and covered with clear plastic lids to maintain humidity during germination. After 24-36 h, lids were removed from the flats. Germination rates were between 80-95% for all *G. soja* accessions tested. *G. soja* were germinated and maintained under diurnal light (16 h light at 22 ^{0}C; 6 h dark at 20 ^{0}C). Light intensity was maintained between 250-300 µM for all experiments. Light intensity is critical for the production of consistent macroscopic HRs during screening. Flats were watered with 1.0 L of H_2O per flat every 36-48 hours or as needed. Before the end of the V2 stage of development, trifoliate leaves were pruned as described in the Results section.

Culture Preparation

Gateway clones of 10 RXLR core effectors (*Avh*16, *Avh*180, *Avh*240, *Avh*53, *Avh*137, *Avh*241, *Avh*488, SNEL1, *Avh*23, and *Avh*110) were generously provided by the Tyler Lab at

Oregon State University. The unstructured N terminus and secretion peptides of core RXLR effectors were removed during entry vector cloning in order to complement the design of the pEDV6 system. Bacterial cultures were prepared from single colonies and inoculated in 5 mL aliquots of KB media containing the appropriate antibiotic selection. The bacteria was pelleted as mentioned above and re-suspended in 10 mM $MgSO_4$. Single inoculums were prepared at ODs = 0.3-0.6 and pressure infiltrated into soybean unifoliates. Co-infiltration of EtHAN and *Psg* were done by mixing the two at ODs 0.6 and 0.3 respectively for a final OD = 0.9.

Infiltrations

Plants were infiltrated after 15-17 days (3 days after pruning the trifoliate leaves). Bacterial solutions were prepared 1 hour prior to infiltration. Needless syringes were used to pressure infiltrate attached unifoliate leaves. Each unifoliate received 4 infiltrations of 50-100 µL of bacterial solution. The identical process is performed on the adjacent unifoliate. Negative controls were performed on separate plants to avoid priming induced by effector recognition.

Scoring

Seven days post infiltration (DPI), unifoliate leaves were detached, imaged and, scored. A plant was scored positive if ≥6/8 infiltration spots produced a visual HR on both unifoliate leaves. Plants were scored negative if ≤2/8 infiltration spots produced a visible HR. Plants that fell between 3-5/8 were scored as ambiguous. Any data, scored as ambiguous, was discarded, and the experiment was repeated until the appropriate sample size was reached (Chapter 2). To calculate % HR, we used the equation, $\%\ HR = (\#\ of\ responding\ plants) \div (\#\ of\ infiltrated\ plants)$.

Delivery of P. sojae *Core Effectors to Resistant* G. soja *Germplasm*

In experiments with *Avh16*, *Avh180*, and *Avh240*, cultivars were screened with effectors individually in three biological replicates (n = 20 plants per replicate). Standard deviation was calculated between the three replicates. Statistical significance ($p<0.05$) was determined by a pairwise t-test against Harosoy.

Determination of R *Gene Inheritance in* $F_{2:3}$ *Populations*

Individuals from segregating $F_{2:3}$ families were screened with Avh240 as described above. Before effector screening, we determined the background that *Avh*240 produces in Williams. $F_{2:3}$ families were tested with an average sample size of $n\geq10$ individuals per family. We determined our range for homozygous dominant as ≥85 % HR. We determined our range for homozygous recessive as the background response of Avh240 on Williams ≤30 % HR. Families that fell within the two ranges are considered to be segregating. We use the Chi squared (χ^2) value to determine the probability at which the deviation is expected.

Figures and Tables

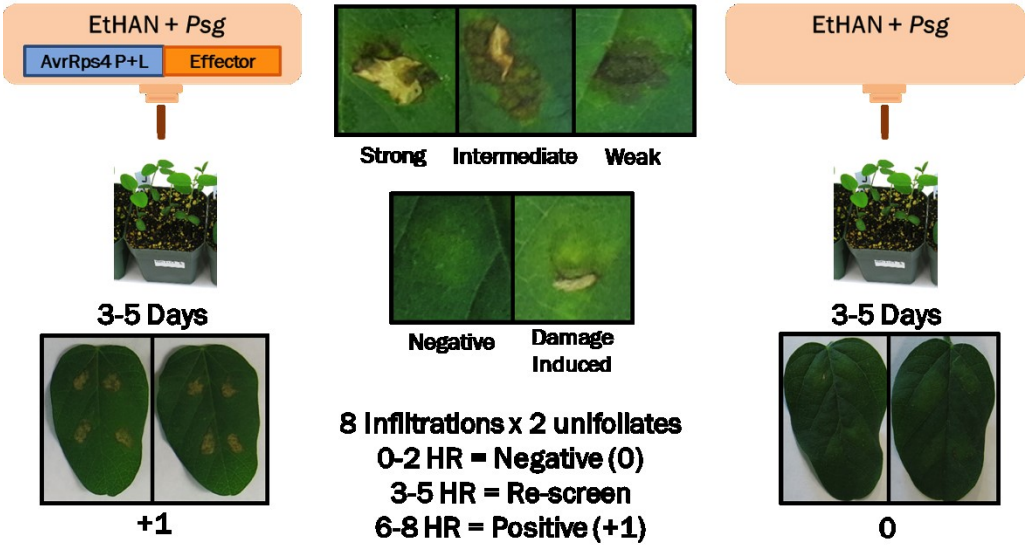

Figure 3.1 Overview of the procedure for screening *G. soja* accessions with core *P. sojae* RXLR effectors. *P. fluorescens* EtHAN was used to deliver *P. sojae* effector proteins to the interior of plant cell. The pEDV6 vector contains the Avr*Rps*4 promoter and leader sequence which were used to guide effector proteins through the Type III secretion system. We co-infiltrated EtHAN with *Psg* race 4 in a 2:1 ration to suppress PTI. This suppression creates a favorable environment for *P. fluorescens* to achieve high levels of growth, such that it delivers higher quantities of our desired effector and produces a more robust phenotype. Pressure infiltration was used to inoculate four areas per unifoliate leaf and we infiltrated both unifoliate leaves per plant. Plants were scored 3-5 DPI. If at least 6 out of 8 spots produced a visual HR, the plant was scored +1. If 0 out of 2 spots produced a visual HR, the plant was scored as 0, and if 3-5 spots produced a visual HR, the data point was discarded and the population was retested. An internal control of untransformed *P. fluor*escens co-infiltrated with *Psg* was used during screening.

Table 3.1 Accession Information for all tested *G. soja* germplasm is listed.

PI #	Accession ID	Origin
PI464935	gs2410	China: Jiangsu
PI549046	gs2761	China: Ningxia
PI549048	gs2763	China: Changping
PI464889A	gs727	China: Jilin
PI479746B	gs56	China Jilin
PI562538	gs2771	South Korea: Gyeon Gi Do
PI562539	gs2772	South Korea: Gyeon Gi Do
PI562542	gs725	South Korea: Gyeon Gi Do
PI407162	gs730	South Korea: Gyeon Gi Do
PI562544	gs2777	South Korea: Chung Ch'ong Nam Do
PI562547	gs2780	South Korea: Chung Ch'ong Nam Do
PI562549	gs2782	South Korea: Chung Ch'ong Nam Do
PI507582	gs2474	Japan: Aomori
PI507587	gs2479	Japan: Aomori
PI507597	gs2490	Japan: Nakajo
PI507621	gs2514	Japan: Nakajo
PI407076	gs2292	Japan: Unknown
PI507767	gs2601	Russia: Primorskaya Province
PI507788	gs2618	Russia: Primorskaya Province
PI507794	gs2623	Russia: Primorskaya Province
PI507814	gs714	Russia: Primorskaya Province
PI522215	gs719	Russia: Primorskaya Province
PI522216	gs720	Russia: Primorskaya Province

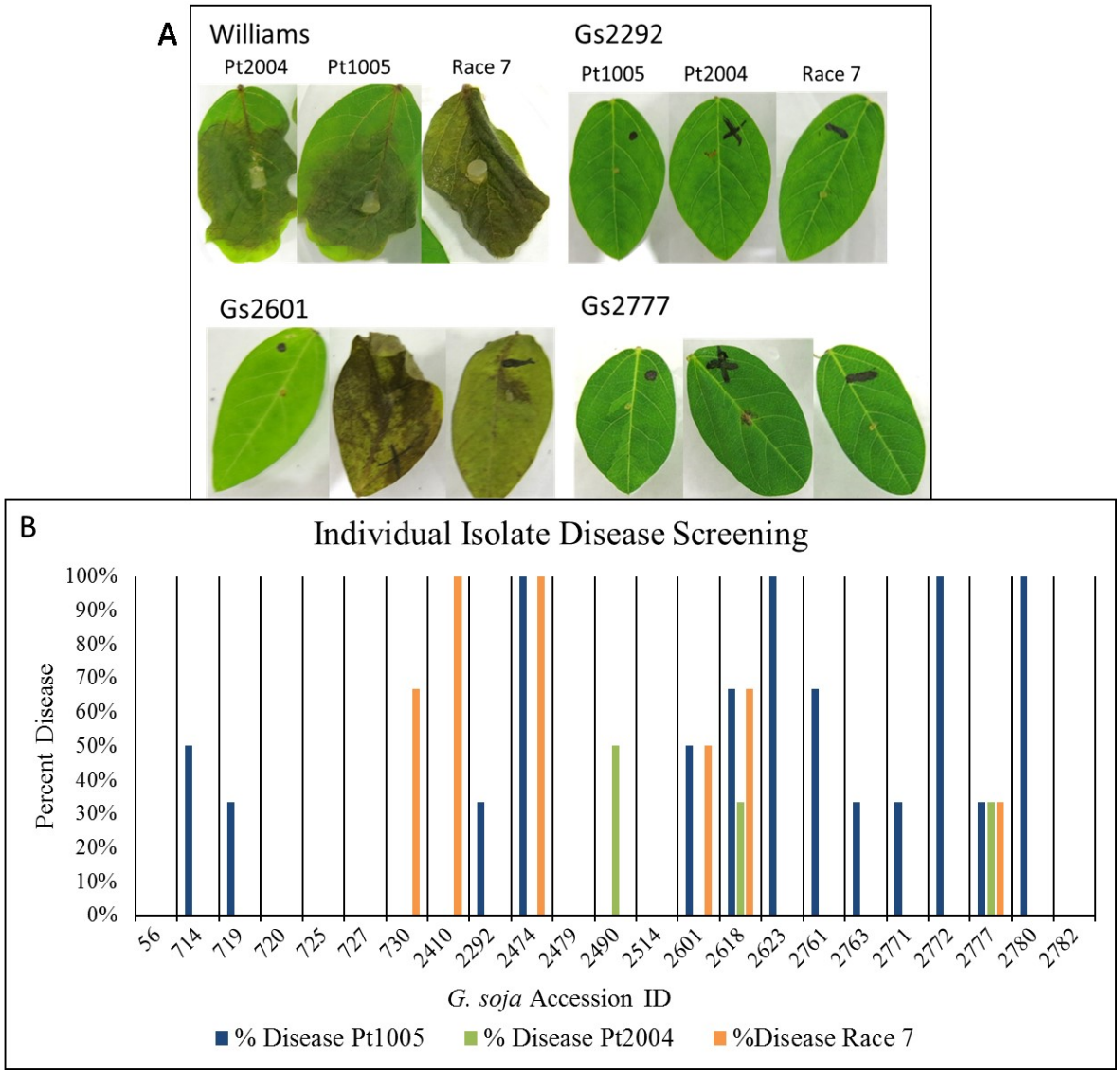

Figure 3.2 Disease screening of *G. soja* accessions with three common field isolates of *P. sojae*. Agar plugs containing mycelia were used to infect trifoliate leaves with isolates Pt2004 (X) Pt1005 (.) and PtRace7 (-). We found susceptible interactions among *G. soja* accessions; however most cultivars showed nearly complete resistance. On the X axis, *G. soja* germplasm is listed and on the Y axis, resistance or susceptibility was measured for n = 5 individuals in two biological replicates.

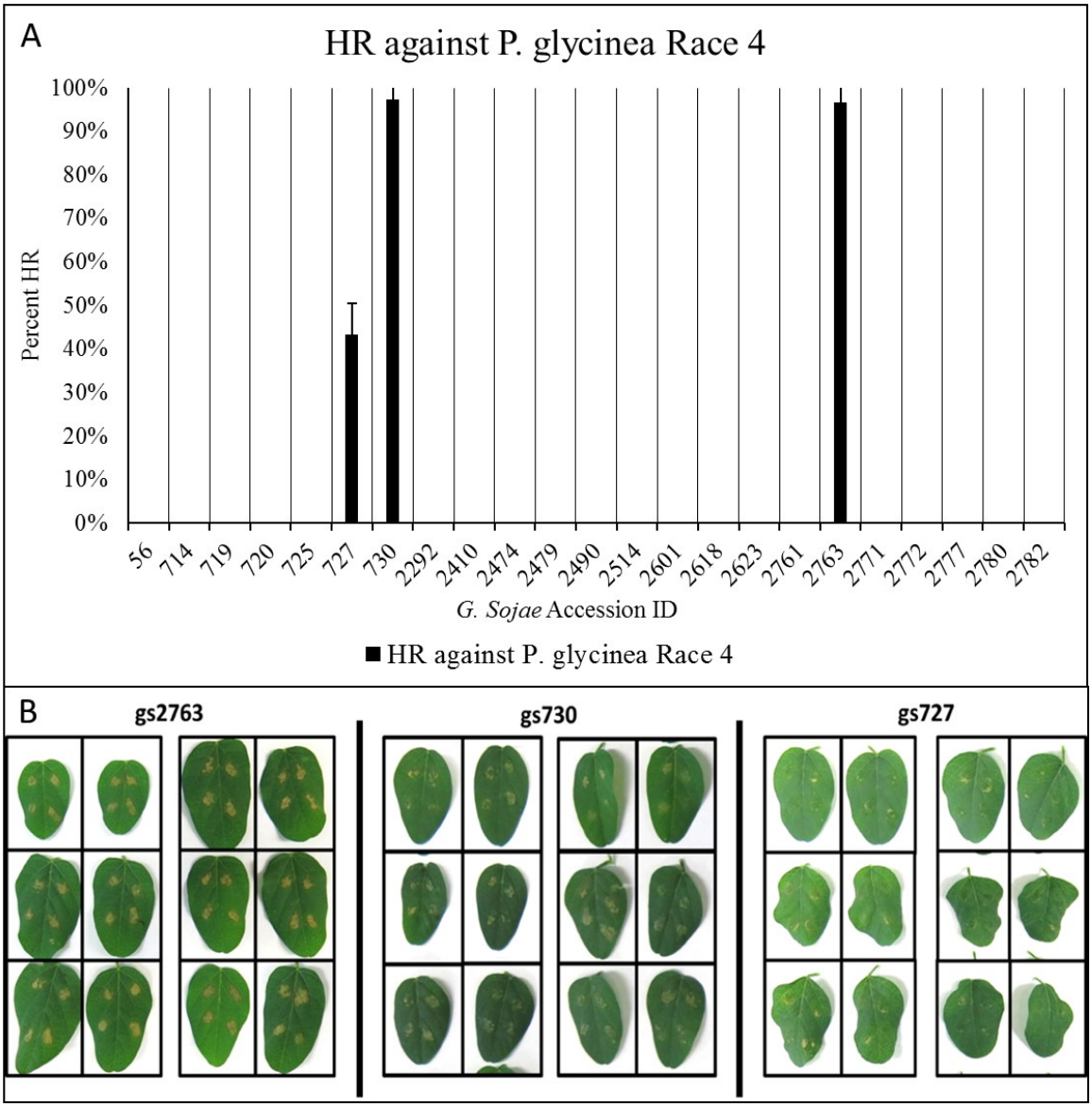

Figure 3.3 Gs2763, gs730, and gs727 are incompatible with *Psg* race 4. These *P. sojae* resistant *G. soja* accessions produced a faster, stronger HR when inoculated with *Psg* as opposed to when inoculated with a core *P. sojae* effector. A) The %HR in response to *Psg* was recorded over 3 biological replicates. B) The images were taken from 1 biological replicate where these accessions were infiltrated with *Psg*.

Table 3.2 Screening *G. soja* germplasm for a HR in response to *Psg* race 4. HRs against *Psg* race 4 were observed in *G. soja* accessions gs730, gs2763, and gs727.

G. soja **Line ID**	**% HR against *Psg* race 4**	**% Standard Deviation**
gs56	0%	0%
gs714	0%	0%
gs719	0%	0%
gs720	0%	0%
gs725	0%	0%
gs727	43%	7%
gs730	97%	4%
gs2292	0%	0%
gs2410	0%	0%
gs2474	0%	0%
gs2479	0%	0%
gs2490	0%	0%
gs2514	0%	0%
gs2601	0%	0%
gs2618	0%	0%
gs2623	0%	0%
gs2761	0%	0%
gs2763	97%	4%
gs2771	0%	0%
gs2772	0%	0%
gs2777	0%	0%
gs2780	0%	0%
gs2782	0%	0%

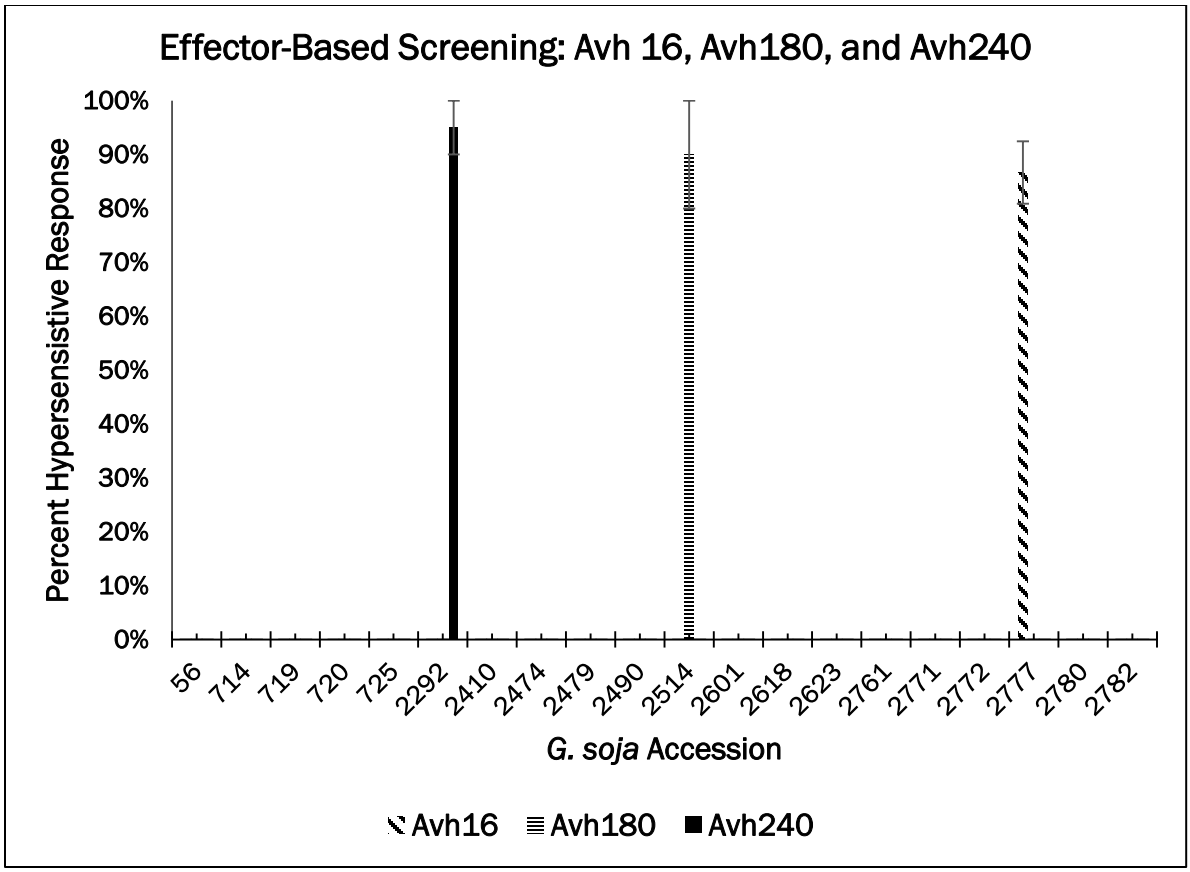

Figure 3.4 Gs2777, gs2514, and gs2292 produced HRs in response to *Avh*16, *Avh*180, and *Avh*240 respectively. On the X axis, *G. soja* accessions subjected to effector-based screening are listed. On the Y axis, percent hypersensitive response among individuals within accessions recorded. We confirmed the observed effector responses over 3 biological replicates to determine standard deviation (n≥60). The error bars represents the percent standard deviation between 3 biological replicates. Neither *P. fluorescens* nor *Psg* produced HRs individually or in combination in these accessions.

Table 3.3 Total *Avh*16, *Avh*180, and *Avh*240 effector-response in *G. soja* germplasm. Percent hypersensitive response and percent standard deviation is reported for the effectors *Avh*16, *Avh*180, and *Avh*240.

G. soja **Line ID**	***Avh*16 % HR**	***Avh*16 % StDev**	***Avh*180 % HR**	***Avh*180 % StDev**	***Avh*240 % HR**	***Avh*240 % StDev**
gs56	0%	0%	0%	0%	0%	0%
gs714	0%	0%	0%	0%	0%	0%
gs719	0%	0%	0%	0%	0%	0%
gs720	0%	0%	0%	0%	0%	0%
gs725	0%	0%	0%	0%	0%	0%
gs2292	0%	0%	0%	0%	95%	5%
gs2410	0%	0%	0%	0%	0%	0%
gs2474	0%	0%	0%	0%	0%	0%
gs2479	0%	0%	0%	0%	0%	0%
gs2490	0%	0%	0%	0%	0%	0%
gs2514	0%	0%	90%	10%	0%	0%
gs2601	0%	0%	0%	0%	0%	0%
gs2618	0%	0%	0%	0%	0%	0%
gs2623	0%	0%	0%	0%	0%	0%
gs2761	0%	0%	0%	0%	0%	0%
gs2771	0%	0%	0%	0%	0%	0%
gs2772	0%	0%	0%	0%	0%	0%
gs2777	87%	6%	0%	0%	0%	0%
gs2780	0%	0%	0%	0%	0%	0%
gs2782	0%	0%	0%	0%	0%	0%

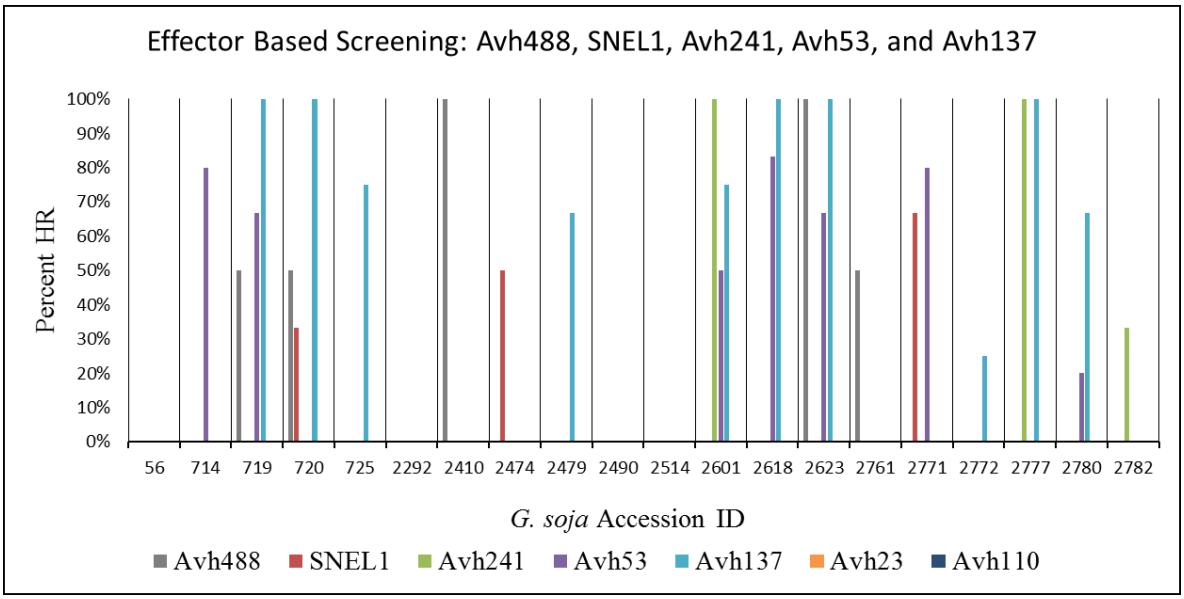

Figure 3.5 Cumulative effector based screening with *Avh*488, SNEL1, *Avh*241, *Avh*53, and *Avh*137. On the Y axis, percent hypersensitive response is reported for effectors screened individually on *G. soja* germplasm.

Table 3.4 A-G Effector-based screening data for *Avh*53*,* *Avh*137, *Avh*488, SNEL1, *Avh*241, *Avh*23, and *Avh*110. Response to a given effector (*Avh* HR) divided by total plants screened (Total *Avh*) gives percent hypersensitive response (*Avh* % HR).

A

G. soja **Line ID**	***Avh*53 HR**	**Total *Avh*53**	***Avh*53 % HR**
gs56	-	-	NT
gs714	4	5	80%
gs719	4	6	67%
gs720	0	3	0%
gs725	0	5	0%
gs2292	0	4	0%
gs2410	0	4	0%
gs2474	0	6	0%
gs2479	0	7	0%
gs2490	0	3	0%
gs2514	0	2	0%
gs2601	3	6	50%
gs2618	5	6	83%
gs2623	2	3	67%
gs2761	0	2	0%
gs2771	4	5	80%
gs2772	0	5	0%
gs2777	0	6	0%
gs2780	1	5	20%
gs2782	0	9	0%

B

G. soja **Line ID**	***Avh*137 HR**	**Total *Avh*137**	***Avh*137 % HR**
gs56	-	-	NT
gs714	0	2	0%
gs719	4	4	100%
gs720	2	2	100%
gs725	3	4	75%
gs2292	0	2	0%
gs2410	0	3	0%
gs2474	0	2	0%
gs2479	2	3	67%
gs2490	0	2	0%
gs2514	0	1	0%
gs2601	3	4	75%
gs2618	5	5	100%
gs2623	4	4	100%
gs2761	0	5	0%
gs2771	0	3	0%
gs2772	1	4	25%
gs2777	5	5	100%
gs2780	2	3	67%
gs2782	0	4	0%

C

G. soja Line ID	*Avh*488 HR	Total *Avh*488	*Avh*488 % HR
gs56	0	3	0%
gs714	0	2	0%
gs719	2	7	29%
gs720	1	5	20%
gs725	0	0	NT
gs2292	0	2	0%
gs2410	3	3	100%
gs2474	0	3	0%
gs2479	0	0	NT
gs2490	0	3	0%
gs2514	0	2	0%
gs2601	0	3	0%
gs2618	0	5	0%
gs2623	3	3	100%
gs2761	3	4	75%
gs2771	0	4	0%
gs2772	0	3	0%
gs2777	0	5	0%
gs2780	0	1	0%
gs2782	0	2	0%

D

G. soja Line ID	SNEL1 HR	Total SNEL1	SNEL1 % HR
gs56	0	3	0%
gs714	0	3	0%
gs719	0	6	0%
gs720	1	3	33%
gs725	0	0	NT
gs2292	0	1	0%
gs2410	1	5	20%
gs2474	0	3	0%
gs2479	0	0	NT
gs2490	0	1	0%
gs2514	0	1	0%
gs2601	0	0	NT
gs2618	0	5	0%
gs2623	0	0	NT
gs2761	0	5	0%
gs2771	0	2	0%
gs2772	0	2	0%
gs2777	0	4	0%
gs2780	0	1	0%
gs2782	3	3	100%

E **F**

G. soja Line ID	*Avh*241 HR	Total *Avh*241	*Avh*241 % HR	*G. soja* Line ID	*Avh*23 HR	Total *Avh*23	*Avh*23 % HR
gs56	0	6	0%	gs56	0	4	0%
gs714	4	4	100%	gs714	0	5	0%
gs719	1	8	13%	gs719	0	2	0%
gs720	0	2	0%	gs720	0	3	0%
gs725	0	3	0%	gs725	0	3	0%
gs2292	0	6	0%	gs2292	0	2	0%
gs2410	0	1	0%	gs2410	0	3	0%
gs2474	0	11	0%	gs2474	0	2	0%
gs2479	0	3	0%	gs2479	0	4	0%
gs2490	0	4	0%	gs2490	0	5	0%
gs2514	0	2	0%	gs2514	0	3	0%
gs2601	2	7	29%	gs2601	0	3	0%
gs2618	2	8	25%	gs2618	0	3	0%
gs2623	0	6	0%	gs2623	0	2	0%
gs2761	0	7	0%	gs2761	0	5	0%
gs2771	3	4	75%	gs2771	0	2	0%
gs2772	0	11	0%	gs2772	0	2	0%
gs2777	5	7	71%	gs2777	0	3	0%
gs2780	0	2	0%	gs2780	0	2	0%
gs2782	2	6	33%	gs2782	0	3	0%

G

G. soja Line ID	*Avh*110 HR	Total *Avh*110	*Avh*110 % HR
gs56	0	3	0%
gs714	0	3	0%
gs719	0	3	0%
gs720	0	4	0%
gs725	0	3	0%
gs2292	0	2	0%
gs2410	0	2	0%
gs2474	0	5	0%
gs2479	0	2	0%
gs2490	0	3	0%
gs2514	0	3	0%
gs2601	0	2	0%
gs2618	0	2	0%
gs2623	0	4	0%
gs2761	0	4	0%
gs2771	0	2	0%
gs2772	0	2	0%
gs2777	0	2	0%
gs2780	0	2	0%
gs2782	0	3	0%

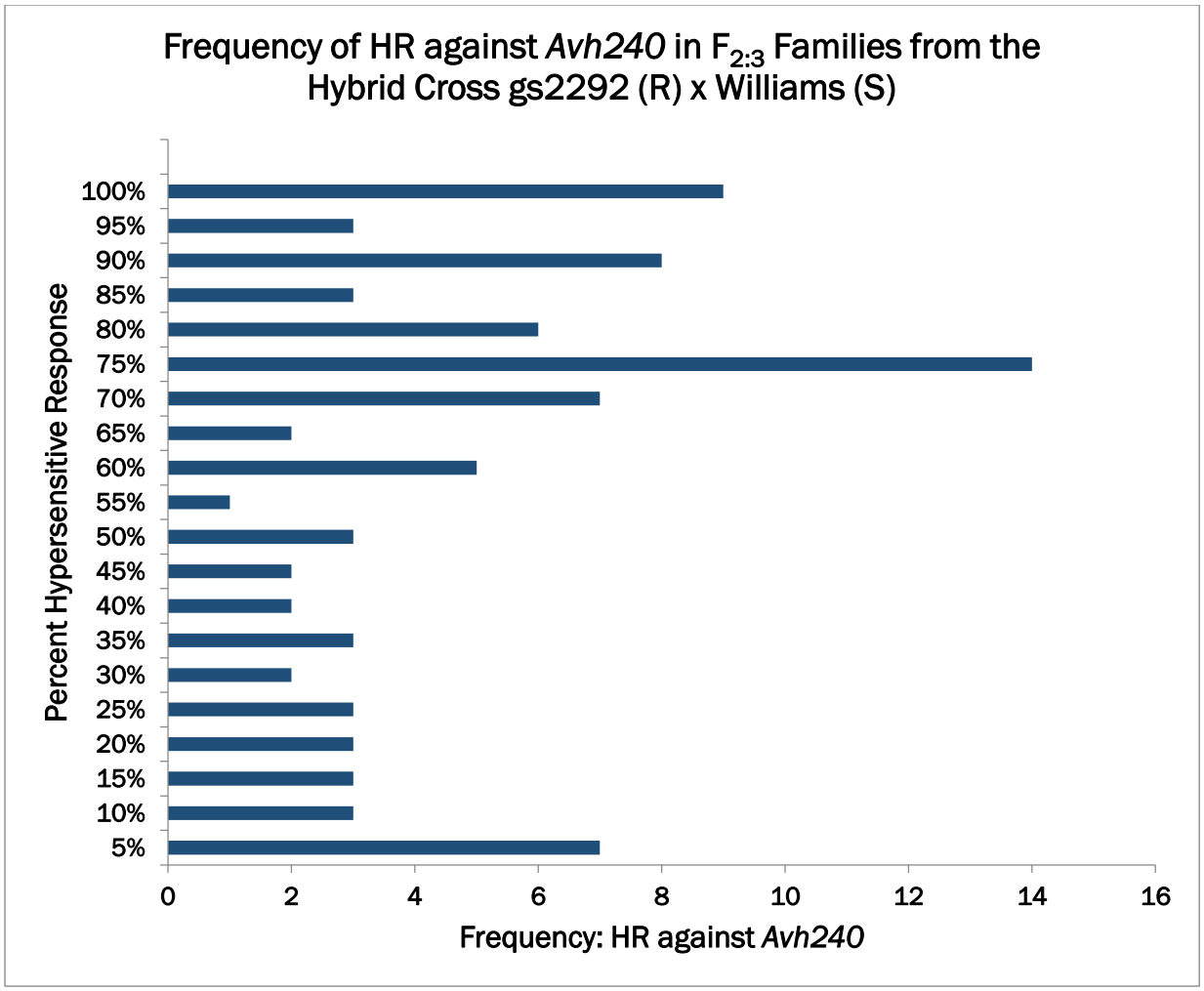

Figure 3.6 Histogram of effector-based screening on 88 $F_{2:3}$ hybrid families. The distribution of effector response in segregating populations suggests the presence of a single dominant *R* gene against *Avh*240.

A

Cross	# of $F_{2:3}$ Families			Expected Ratio	χ^2 value	Probability
	HgD	SEG	HgR			
gs2292 (R) X Williams (S)	21	48	20	1:2:1	0.230	>98%

B

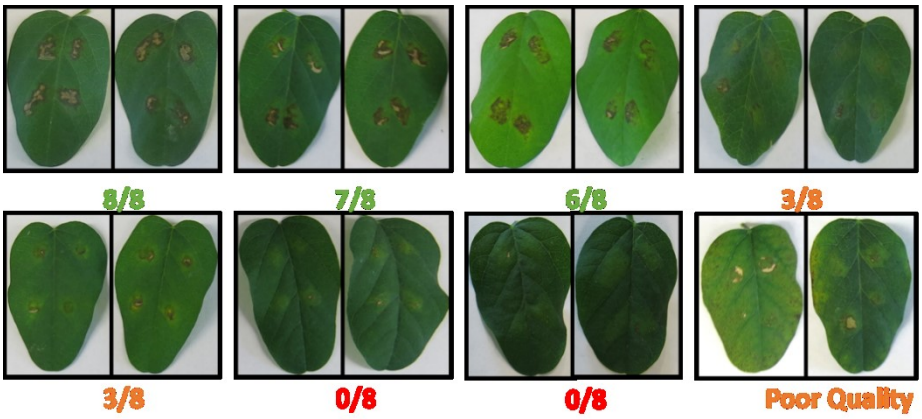

Figure 3.7 Segregating $F_{2:3}$ families were scored for response to *Avh*240. **a)** This table shows the distribution of families in response to the trait HR against *Avh*240. Families were separated into 3 groups homozygous dominant (HgD), homozygous recessive (HgR), and segregating (SEG). **b)** HR strength was variable in $F_{2:3}$ families. Individuals that produced HRs against *Avh*240 in ≥6/8 infiltrations were scored positive, whereas individuals which produced a HR in ≤2 infiltrations were scored negative. Individuals that produced HRs in 3-5/8 infiltrations were not included in scored data.

Table 3.5 Cumulative effector-based screening of wild soybean accessions. Shaded boxes indicate which *G. soja* accession responds to which effector. Percentages are included with standard deviation when possible.

Accession ID	*Avh*488	SNEL1	*Avh*241	*Avh*53	*Avh*137	*Avh*16	*Avh*180	*Avh*240	Subgroup
gs2410	100%								1
gs2761	75%								2
gs727									3
gs728									3
gs2771			75%	80%					4
gs2772									4
gs725					75%				4
gs2777			71%		100%	87% ± 6			4
gs2780					67%				4
gs2782		100%							4
gs2474									5
gs2479					67%				5
gs2490									5
gs2514							90% ± 10		5
gs2292								95% ± 5	5
gs2601				50%	75%				6
gs2618				83%	100%				6
gs2623				67%	100%				6
gs714			100%	80%					6
gs719				67%	100%				6
gs720					100%				6

Table 3.6 *Avh*240 effector-based screening data. - Cross gs2292 (R) x Williams (S). Replicate 1 *Avh*240 responding plants are labeled by the column header (R1P). Replicate 1 total plants are labeled by the column header (R1T). The remaining replicates were labeled by the above scheme. Responders (P) divided by total plants screened (T) gives percent hypersensitive response (%HR) for all biological replicates.

Cross	R1P	R2P	R3P	R4P	R5P	R1T	R2T	R3T	R4T	R5T	P	T	%HR
1	0	3	0	2	0	0	3	3	3	0	5	9	56%
2	0	1	0	0	0	0	3	1	1	2	1	7	14%
3	0	4	2	0	0	0	4	5	0	0	6	9	67%
4	0	0	0	0	0	0	0	5	2	3	0	10	0%
5	0	1	1	1	3	0	1	1	2	4	6	8	75%
6	0	3	2	2	3	0	4	3	4	4	10	15	67%
7	0	1	0	0	0	0	3	1	3	0	1	7	14%
8	0	0	1	1	0	0	0	1	1	2	2	4	50%
9	0	3	0	0	3	0	4	2	0	4	6	10	60%
11	0	1	2	0	0	0	3	5	1	0	3	9	33%
12	0	0	1	1	3	0	4	3	2	5	5	14	36%
13	0	0	0	0	0	0	2	2	0	5	0	9	0%
14	0	0	1	0	1	0	2	3	0	4	2	9	22%
15	0	4	3	3	3	0	4	5	5	4	13	18	72%
17	0	0	0	0	0	0	3	2	0	0	0	5	0%
18	0	2	3	3	0	0	4	3	4	0	8	11	73%
19	0	0	2	1	3	0	2	4	2	3	6	11	55%
20	0	0	1	4	3	0	2	1	4	4	8	11	73%
21	0	0	2	1	0	0	0	2	1	0	3	3	100%
22	0	3	1	4	0	0	3	2	5	0	8	10	80%
23	0	3	2	3	0	0	3	2	3	1	8	9	89%

24	0	0	0	2	3	0	0	1	4	3	5	8	63%
25	0	4	2	2	5	0	4	5	4	5	13	18	72%
26	0	5	3	4	2	0	5	3	4	3	14	15	93%
27	0	3	2	1	0	0	3	2	1	0	6	6	100%
28	0	0	5	4	5	0	0	5	4	5	14	14	100%
29	0	2	5	5	3	0	3	5	5	4	15	17	88%
30	0	3	1	0	2	0	3	2	0	3	6	8	75%
31	0	5	2	0	4	0	5	5	0	4	11	14	79%
32	0	4	2	0	0	0	4	4	0	2	6	10	60%
33	0	3	3	0	2	0	4	4	0	3	8	11	73%
34	0	2	1	0	0	0	2	5	0	0	3	7	43%
35	0	1	1	4	0	0	1	1	5	1	6	8	75%
36	0	4	2	1	3	0	4	4	1	3	10	12	83%
37	0	4	2	1	0	0	5	4	1	0	7	10	70%
39	0	4	1	0	3	0	4	2	2	3	8	11	73%
40	0	0	0	0	1	0	0	3	1	5	1	9	11%
41	0	0	2	1	0	0	4	4	1	2	3	11	27%
42	0	0	0	0	1	0	4	2	0	4	1	10	10%
44	0	0	0	0	0	0	2	3	0	3	0	8	0%
45	0	0	0	1	0	0	2	2	2	0	1	6	17%
46	0	2	3	4	0	0	4	4	4	1	9	13	69%
49	0	0	1	2	0	0	2	1	2	0	3	5	60%
51	2	0	2	0	0	4	2	4	0	3	4	13	31%
52	3	3	0	0	0	4	3	0	0	0	6	7	86%
53	2	3	3	0	3	3	3	3	1	3	11	13	85%
54	4	0	3	0	2	4	0	3	0	2	9	9	100%
55	4	4	5	0	4	4	4	5	0	4	17	17	100%
56	3	0	5	4	5	5	0	5	4	5	17	19	89%
57	0	2	0	0	0	1	2	1	1	0	2	5	40%

59	0	1	1	1	1	1	2	2	0	1	4	6	67%
60	3	1	2	0	2	4	2	3	0	4	8	13	62%
61	0	0	1	0	0	6	2	4	0	2	1	14	7%
63	2	0	0	0	2	4	1	1	0	2	4	8	50%
64	0	0	0	0	0	3	2	0	0	0	0	5	0%
65	0	0	1	0	2	3	4	4	1	5	3	17	18%
66	2	1	0	0	1	5	4	0	0	3	4	12	33%
67	0	1	2	0	1	3	1	2	0	1	4	7	57%
68	3	0	2	1	0	4	0	2	1	0	6	7	86%
70	4	1	1	0	0	5	1	1	0	1	6	8	75%
71	5	2	0	0	0	5	2	0	0	1	7	8	88%
72	2	0	0	0	0	4	2	4	0	3	2	13	15%
73	2	2	2	1	2	2	2	4	1	2	9	11	82%
74	4	5	3	1	2	4	5	5	3	3	15	20	75%
75	3	2	2	1	3	4	2	3	1	4	11	14	79%
76	2	0	1	0	2	3	4	2	0	2	5	11	45%
77	1	0	1	0	0	1	0	1	0	0	2	2	100%
78	1	0	0	0	1	5	6	5	3	5	2	24	8%
79	3	1	3	3	1	4	2	4	4	2	11	16	69%
80	1	0	0	0	0	2	1	0	0	1	1	4	25%
81	3	0	0	2	0	3	0	0	2	0	5	5	100%
82	4	3	4	1	1	5	4	4	3	3	13	19	68%
83	3	3	2	2	1	5	3	2	3	1	11	14	79%
85	3	2	3	1	1	3	2	3	1	1	10	10	100%
86	5	0	3	4	0	5	0	5	4	0	12	14	86%
87	5	4	4	4	2	5	4	4	5	2	19	20	95%
88	5	0	3	1	0	5	0	3	1	0	9	9	100%
89	2	1	0	0	1	4	2	0	0	3	4	9	44%
90	3	4	2	0	3	4	4	2	0	3	12	13	92%

91	5	1	0	1	0	5	2	0	1	0	7	8	88%
92	2	0	0	0	0	4	2	1	0	0	2	7	29%
93	4	1	2	0	3	5	3	3	0	3	10	14	71%
94	2	1	1	0	0	2	2	1	0	0	4	5	80%
95	2	2	1	0	0	4	2	1	0	0	5	7	71%
96	0	0	0	0	0	1	0	1	0	0	0	2	0%
97	0	1	0	1	0	2	2	1	3	0	2	8	25%
98	0	0	0	0	0	1	0	1	0	0	0	2	0%
99	4	2	0	3	3	5	3	1	3	4	12	16	75%
100	5	1	3	0	2	5	2	3	2	2	11	14	79%

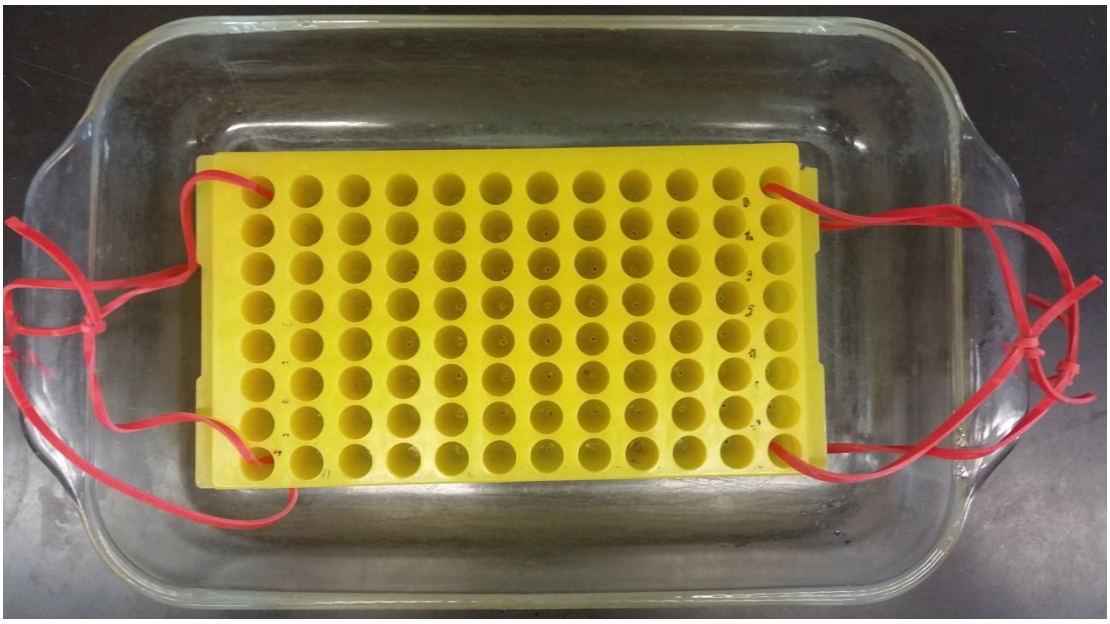

Figure 3.8 An apparatus for seed coat removal is shown in a photograph. Batch style acid scarification was used to remove the thick seed coats of *G. soja* seeds in a high throughput fashion. Small holes were bored through the bottom of a 1.5 mL micro-centrifuge tube holder for scarification in 100% H_2SO_4. After 5 minutes, the apparatus is carefully picked up and residual acid is drained back into the bath. Washes were performed in diH_2O to remove residual acid. The appropriate safety precautions are essential due the volatility of this strong acid. All material must be acid resistant and care must be taken to avoid splashing or dipping.

Chapter 4

Analysis of Publically Available Transcriptome Data Reveals Arabidopsis thaliana *Genes which Impact Susceptibility to* Hyaloperonospora arabidopsidis

Kevin E. Fedkenheuer[1], Haktan Suren[1], Elijah Myers[1], Kuan Yang[1], Michael G. Fedkenheuer[1], Ruth Grene[1], and John M. McDowell[1]

[1]Department of Plant Pathology, Physiology, and Weed Science, Virginia Polytechnic Institute, Blacksburg, VA

[*]for correspondence, johnmcd@vt.edu

Author Contributions: KF wrote and developed this manuscript with advice from JM and MF. JM and RG advised this project. EJ helped KF with initial data transformations. HS ran genes selected by KF through Ontologizer. KY ran genes selected by KF through BBC. MF aided KF in screening *A. thaliana* null mutants.

Abstract

The interaction between *Arabidopsis* and its natural pathogen *Hyaloperonospora arabidopsidis* (*Hpa*) comprises a useful pathosystem for identifying plant genes that contribute to plant resistance and susceptibility to oomycetes. Here, we describe an analysis of publically available transcriptome data to identify *Arabidopsis* genes that are differentially expressed in *Hpa*-susceptible plants compared to resistant plants. Such genes might comprise "susceptibility factors" that contribute to successful colonization, along with genes that regulate "basal resistance" that constrains the growth of virulent pathogens. Genes with expression specific to compatibility were sorted using a Bayesian algorithm. Bayesian biclustering generated five compatible specific gene clusters. We selected representative genes from each cluster which had not been linked to plant-oomycete interactions, and we challenged *Arabidopsis thaliana* null mutants with a virulent isolate of *Hpa*. The majority of null mutations produced statistically significant enhanced disease susceptibility (EDS) phenotypes when inoculated with *Hpa* isolate Emco5. We hypothesize that these genes are involved in the pattern-triggered immunity (PTI) response against *Hpa*. A null mutation in *At*Gcn5 provided full resistance against Emco5, suggesting that it functions as a susceptibility gene. In sum, this study demonstrates that an unbiased analysis of publically available transcript data from a plant-pathogen interaction provides a potentially valuable resource to identify novel genes and thereby fill gaps in understanding of plant-oomycete interactions.

Introduction

Oomycetes, commonly referred to as water molds, can cause disease on many plants [4]. The class Oomycota (oomycetes) reside in the kingdom Chromalveolata and belong to the phylum *Heterokontophyta* or *Stramenopila* [4, 6]. In the order *Leptomitales*, the families *Aphanomycetes*, *Pythiaceae*, *Albuginaceae*, and *Peronosporaceae* encompass most oomycete plant pathogens [7, 13, 14]. Downy mildew pathogens are a class of obligate plant parasites belong to the family *Peronosporaceae* [76]. Some downy mildews are extremely destructive, and downy mildew disease can cause significant damage to many crops, including lettuce, crucifers, grapes, and hops. In the last ten years, cucurbit downy mildew has evolved to become a devastating pathogen of cucumber and other cucurbits [131]. *Impatiens* downy mildew is threating the survival cultivated *impatiens* varieties [76], and sunflower downy mildew is evolving to evade sunflower *R* genes [132].

Morphologically similar to but evolutionarily distinct from true fungi, oomycetes are most closely related to brown algae and diatoms [7]. The *Peronosporaceae* share a common lineage with pathogens in the *Phytophthora* genus [76]. *Arabidopsis* downy mildew is caused by *Hyaloperonospora arabidopsidis*, which was previously referred to as *Peronospora parasitica* and *Hyaloperonospora parasitica* [133]. Like other downy mildew pathogens, *Hpa* is an obligate biotroph, which extracts nutrients only from living plant cells and cannot exist apart from its host. *Hpa* does not infect other crucifers and makes no significant agricultural impact [134]. *However, Hpa* is the only naturally occurring oomycete pathogens of the reference plant *Arabidopsis thaliana* (*A. thaliana*) [135].

The life cycle of *Hpa* is typical of other downy mildews. *Hpa* over-winters in the form of thick-walled oospores (sexual spores) which form inside infected organs and are deposited in the

soil after the plant dies and decays. In the spring, oospores germinate and infect *A. thaliana* roots using filamentous infection structures called hyphae [134-136]. *Hpa* utilizes a structure called the haustoria to interface with individual host cells. At the haustorial interface the pathogen draws nutrients and secretes effector proteins to subvert immunity. In a successful *Hpa* infection sporulation will occur 5-7 days post infection (DPI). After sporulation, the pathogen will reproduce sexually to produce oospores inside of the leaf. Asexual spores are produced from conidiophore and are dispersed naturally by wind and rain. As is the case with many downy mildew species, spores are most viable and virulent under wet conditions. After colonizing its host, *Hpa* produces sporangiophores emerge from *A. thaliana* leaves and produce asexual sporangia [134-136]. Sporangia detach from these structures, colonize leaves and propagate subsequent *Hpa* infections [134-136].

To better understand resistance against oomycetes, *Hpa* was adapted as a laboratory model in the 1990s [133]. Different *Arabidopsis* ecotypes display extensive natural variation for resistance and susceptibility to *Hpa*, and this has been exploited to genetically define 28 putative "RPP genes" that comprise *R* genes against various *Hpa* ecotypes [134]. Five of these *R* genes have been cloned and encode members of the nucleotide binding, leucine-rich repeat gene superfamily of innate immune surveillance proteins [134]. In 2010, Baxter et al. reported the genome sequence of the *Hpa* isolate Emoy2 which produced a 81.6 Mb genomic sequence [136]. This resource was necessary for advancement of the *Hpa* pathosystem. In later studies, *Hpa* isolate-specific effectors were identified and characterized [137, 138]. These genomic resources for *Hpa*, coupled with the experimental tools of *Arabidopsis*, provide a powerful pathosystem to understand resistance and susceptibility to downy mildew pathogens and oomycetes in general.

This study was designed to leverage publically available transcriptome data from *A. thaliana* during the process of infection with *Hpa*. The goal was to identify new genes which impact resistance and susceptibility to *Hpa*. We analyzed the *A. thaliana* transcriptome during infection with *Hpa* isolate Emwa1 using public data provided by Wang et al. [122]. The Emwa1 isolate is incompatible on Col-0 due to recognition by the NLR protein RPP4 [134]. This immune receptor recognizes the *Hpa* effector *Ha*Atr4 [122]. For comparison, Wang et al. produced a data set from a compatible interaction by infecting Emwa1 on an *rpp4* mutant the col-0 background [122]. This mutation is sufficient to render Col-0 highly susceptible to *Hpa* Emwa 1. The ability to analyze gene expression differences between compatibility and incompatibility mediated by a single gene allows us the ability to look at specific resistance and susceptibility mechanisms. In their initial analysis of this dataset, Wang et al. suggested that the major contributor to resistance was programmed cell death (PCD) [122]. More specifically, they suggested that the resistance response occurred around the 2 DPI and that the resistance response was repressed at the 4 and 6 DPI [122]. Interestingly, they found that CCA1 and the circadian clock may be used by the plant to "anticipate" pathogen infection during optimal environmental conditions before dawn [122]. *At*CCA1 is a well-characterized regulator of the circadian clock in *A. thaliana* which is manipulated by the pathogen to achieve susceptibility. Wang et al. found that *At*RPP4 expression was primed by circadian regulation to promote expression of defense genes at dawn [122]. However, other potentially interesting aspects of the transcriptomic data set were not analyzed in this study.

We used microarray data provided by Wang et al. to explore additional susceptibility mechanisms underlying RPP4 mediated immunity to the *Hpa* isolate Emwa1. We began by utilizing complementary data sets generated from compatible and incompatible interactions

between *Hpa/A. thaliana*. We looked at differences in gene expression between these two interactions to identify genes specific to susceptibility. We hypothesize that genes with susceptibility-specific expression may represent "susceptibility factors" that contribute to infection. Additionally, we hope to identify genes that regulate basal resistance. Although *Hpa* interactions have been well studied, genes involved in susceptibility and basal resistance to *Hpa* are poorly described. To fill the gaps in our understanding we used clustering and differential expression to identify new genes involved in susceptibility and resistance.

We used Bayesian Biclustering (BBC) to analyze gene patterns over pathogen infection. We used Ontologizer to annotate genes within clusters with susceptible specific expression. Based on these analyses, we selected 17 genes for reverse genetics. We ordered *A. thaliana* T-DNA insertional null mutants for these genes. We challenged knockout mutants with the *Hpa* isolate Emco5. We used Emco5 to understand how basal immunity was affected by the mutation. In most cases, susceptibility mutants identified by our analysis showed enhanced disease susceptibility. We hypothesize these genes are broadly involved PTI against *Hpa* because these susceptibility factors were not pathotype specific. Conversely, we observed full resistance when the epigenetic regulator *At*Gcn5 was knocked out. Since this host gene is required for virulence we consider *At*Gcn5 a susceptibility gene (*S* gene) against *Hpa*. None of the genes defined in this analysis had been previously associated with plant-oomycete interactions.

Results

Data normalization

Using the data from Wang et al., we analyzed expression profiles of *A. thaliana* genes over a time course of infection. Wang et al. collected infected tissue at 0.5, 2, 4, and 6 day time points to capture the entire course of a compatible pathogen infection. Expression data was captured using an Affymetrix microarray chip. The microarray chip used in this study contained 20,922 unique genes from *A. thaliana*. This represents nearly 85% of the total number of genes published for the *A. thaliana* genome [139]. In the first stage of our analysis, we normalized transcript abundance from each time point to the 0 DPI time point. This was done by dividing the 0.5, 2, 4, and 6 DPI time points by the 0 DPI. We then applied a $\log_2$ transformation to this ratio to normalize the data set. Dr. Wang kindly provided Q values from a mixed model ANOVA for each gene in the data set over the time points that were sampled. The Q value provides a statistical measure of gene expression change in the experiment. We applied a Q value cutoff of 0.05 (95% confidence) to produce a list of *A. thaliana* genes that showed statistically significant transcriptional regulation in response to an infection with *Hpa* Emwa1.

To visualize gene expression change and consistency together, we normalized the Q value using a $\log_{10}$ transformation. For easier visualization, $\log_{10}$ Q values were multiplied by -1. After these normalization steps, $\log_2$ expression values and $\log_{10}$ Q values followed a normal distribution. A cursory analysis of the data revealed that very few genes are significantly modulated at 2 DPI during a susceptible interaction (Figure 4.1). In contrast, gene movement is highest at this time point during a resistant interaction. This is interesting because there is much higher gene flux prior to this at the 0.5 DPI time point in *rpp4*Col-0 (Figure 4.1 b). We hypothesize that this reflects a possible stealth mechanism employed by the pathogen to subvert

immunity at the 2 DPI. Interestingly, we observed an overall increase in transcriptional repression during a compatible interaction (Figure 4.1).

GO Annotation using Ontologizer: Global Differences Between Resistance and Susceptibility to Hpa

To identify host genes that play a role in susceptibility to Emwa1, we compared annotations between transcriptomes from resistant and susceptible plants. This analysis was performed on genes with a Q value ≤ 0.05. A GO annotation was applied to genes that changed in each data set. The annotations are separated into 3 GO categories: Cellular Compartment (CC), Biological Process (BP), and Molecular Function (MF). The CC category provides the predicted location of the gene product. The BP category predicts which processes these genes are involved in, and the MF category suggest what function these genes have in the cell. In the CC category, we observed enrichment in resistant plants for genes encoding proteins that are localized to the ribosome or the chloroplast at the 0.5 DPI time point (Figure 4.2 a). At later time points, we observed enrichment for genes that are localized to the cell membrane (Figure 4.2 a). Thus, the CC enrichment at the 0.5 DPI is distinct from the 2, 4 and 6 DPI with respect to gene product localization (Figure 4.2 a). In the CC category for susceptible plants, there was no significant enrichment at the 0.5 DPI (Figure 4.2 b). At the 2 DPI we observed enrichment for proteins that are localized to the cell membrane, and at the 4 DPI we observed enrichment for genes that are localized to the chloroplast (Figure 4.2 b). At the 6 DPI, there is enrichment for genes which localize to the ribosome (Figure 4.2 b). In sum we observed enrichment for chloroplast- and ribosome-localized proteins at the early time points in resistance and at the late time points in susceptibility (Figure 4.2).

In the BP category for resistance, genes are enriched in nucleotide metabolism and photosynthesis at the 0.5 and 2 DPI (Figure 4.3 a). At 2 DPI, genes are enriched in response to SA and cell death which suggests that the resistance response against Emwa1 occurs at this time point, consistent with the timing of the onset of the hypersensitive response based on cytological assays (Figure 4.3 a). At the 4 and 6 DPI, there is enrichment in categories related to cell death (Figure 4.3 a). For susceptible plants, there is little enrichment at 0.5 DPI (Figure 4.3 b). At 2 DPI there is an enrichment for genes involved in response to SA and cell death (Figure 4.3 b). At 4 DPI, genes are enriched in categories related to protein folding and chlorophyll production (Figure 4.3 b). At the 6 DPI, we observe gene enrichment in translation, cellular transport, cell death, response to SA, and defense (Figure 4.3 b). In sum, when we compare resistance and susceptibility for the BP category, we note some significant differences (Figure 4.3). There is a lack of gene enrichment in photosynthesis and nucleotide metabolism at the early time point in compatibility (Figure 4.3). At the later time points, there are similarities between similarities and difference categories, but one major difference is gene enrichment in translation specific to compatibility at the 6 DPI (Figure 4.3).

In the MF category for resistance, genes are enriched at the 0.5 DPI for genes involved in iron binding, tetrapyrrole binding, ribosome structure, and H+ ion transport (Figure 4.4 a). The 2, 4, and 6 DPI time points are enriched for genes related to protein binding and transporter activity (Figure 4.4 a). For susceptibility, genes are enriched at 0.5 DPI for genes related to chitinase activity (Figure 4.4 b). At 2 DPI, there is gene enrichment for genes annotated for ATP transport, chitinase acitivty, and DNA binding (Figure 4.4 b). There is gene enrichment at 4 DPI for genes related to glutathione peroxidase activity and for protein binding (Figure 4.4 b). At 6 DPI, there is enrichment for genes encoding proteins which bind to the ribosome, nucleotides, and copper

and for genes involved in translation (Figure 4.4 b). There are many categories which are different between compatibility and incompatibility. We noted that the genes involved in chitinase activity were specific to the early time point in compatibility (Figure 4.4), and we again noted compatibility specific enrichment in genes related to translation at the late time points (Figure 4.4).

Co-expression clustering using Bayesian Biclustering

To identify host genes that might be manipulated by Emwa1 to enhance susceptibility, we compared gene expression between resistant and susceptible genotypes. We identified 408 genes that formed significant up- or down-regulated clusters when data was processed, using a 1.5 fold change cutoff to describe the maximum and minimum values of gene flux (0.584 normalized expression). We then used Bayesian Biclustering software to cluster genes by co-expression. This yielded five clusters with unique expression patterns in susceptible plants, compared to resistant plants (Figure 4.5). We picked highly expressed genes that had expression consistent with the average expression from clusters 1 and 3. We used sorting to organize these clusters by maximum/minimum expression to make graphical assessments of the most significant genes in each cluster. Clusters 1 and 3 were significantly different from R at the 0.5 DPI (Figure 4.5). From these clusters, we selected 17 genes that were related by annotation to GO categories which were enriched specific to compatibility. We observed substantial variability in gene expression within clusters (Figure 4.5). In a separate study, we are developing more efficient tools to cluster genes based on expression (M. Fedkenheuer, K. Fedkenheuer, J. McDowell, unpublished).

Using Salk Germplasm as a Resource for High-Throughput A. thaliana *Null Mutant Pathogenicity Assays*

We ordered T-DNA insertion mutants from the Salk Institute for 17 genes which change in expression specific to compatibility from susceptibility specific clusters 1 and 3 (Table 4.1). For 12 of the 17 genes we were able to order two null mutants for gene (Table 4.1). We assayed these null mutants with *Hpa* isolate Emco5 for enhanced disease resistance (EDR) or enhanced disease susceptibility (EDS) phenotypes compared to the parental accession Col-0 CS6000. To measure virulence, we spray-inoculated developing seedlings with 50,000 Emco5 spore/ml [134]. To assess the virulence phenotype, we increased humidity at the end of infection to promote sporulation. We counted the number of sporangiophore which appeared on cotyledons of developing *A. thaliana* seedlings at 7 DPI. Statistical significance was determined by a pairwise t-test against CS6000 and a p-value cutoff of 0.05. If fewer sporangiophores were present on a cotyledon on average compared to CS6000, a mutant was scored having an enhanced disease resistance (EDR) phenotype. If means were not statistically significant when compared to CS6000, it was scored as no change.

Many of our TDNA insertion mutants showed enhanced susceptibility when inoculated with the *Hpa* isolate Emco5 (Figure 4.7). In contrast to the majority of mutant phenotypes, disruption of the gene *At*Gcn5 resulted in full resistance (Figure 4.7). We utilized germplasm with a null mutation in the *At*Aba1 gene as a positive control for enhanced disease resistance among mutant accessions.

Discussion

We compared total gene expression between *Hpa* Emwa1 x *A. thaliana* ecotype Col-0 and *Hpa* Emwa1 x *rpp4*col-0 using data provided by Wang et al (2002) to identify new

Arabidopsis genes that are involved in the interaction with *Hpa*. Gene expression values were normalized to the 0 DPI time point using a log2 transformation. A Q value cutoff of 0.05 was applied to the data set to produce a list of genes with meaningful expression change over the time course infection. Interestingly, we noticed almost no significant gene flux at the 2 DPI in a compatible interaction. Since gene flux is highest in a resistant interaction during this time, we believe that the 2 DPI the focal point for resistance and susceptibility (Figure 4.1). In this case, we were able to use the resistant data set to determine that differential gene flux is highest at the 2 DPI. To further clarify this difference, we would need to increase sampling at early time points in infection.

To further compare compatibility and incompatibility, we annotated each data set using Ontologizer. The Ontologizer output was converted into a heatmap for easier visualization. In a heatmap comparison, we observed gene enrichment in genes which localize to the chloroplast and to the ribosome (Figure 4.2). Enrichment in these categories was at the 0.5 and 2 DPIs in the incompatible interaction and at the 4 and 6 DPIs in susceptible (Figure 4.2). When we examined the biological processes and molecular functions of these genes with a focus on susceptibility, we observed that genes involved in ribosome structure and translation were enriched at the 6 DPI (Figure 3, 4). We hypothesize that in the absence of RPP4, Emwa1 effectors are manipulating translation and chloroplastic processes (biosynthesis, signaling, and transport) to achieve susceptibility (Figure 4.2, Figure 4.3, Figure 4.4). A functional annotation of these categories is important to determine the host processes which are manipulated by the pathogen for compatibility. The CC annotation revealed that genes which are localized to the chloroplast and to the ribosome were differently expressed between compatibility and incompatibility (Figure 4.3). In the functional annotations provided by the BP and MF annotation, we observed an

enrichment in genes involved with protein translation. Since this change was specific to susceptibility, we hypothesize that *Hpa* modulates protein translation as a general susceptibility mechanism. (Figure 4.4, Figure 4.5).

To determine specific host genes which are manipulated by Emwa1 to produce susceptibility, we looked for genes with a 1.5 positive or negative fold change in S compared to R. We found 408 genes which we characterized as S specific genes. We used Bayesian biclustering to group these genes by co-expression (Figure 4.5). This produced 5 unique clusters (Figure 4.5). We examined null mutants from 2 of these clusters for a functional analysis. Within clusters, we observed a high degree of variability in gene expression (Figure 4.5). In the future, we hope to find a more refined method for clustering genes based on expression patterns. The process by which candidate susceptibility genes were selected is described in Figure 4.7.

We ordered 17 null mutants from SALK which we produced T3 seed for (Table 4.1). The T4 plants were inoculated with Emco5 spores and virulence was assessed. We used Emco5 to assay broad resistance and susceptibility mechanism rather than pathotype specific mechanisms. The majority of null mutants produced an enhanced disease susceptibility phenotype when challenged with Emco5 (Figure 4.7). We believe that these genes are involved in a PTI like response against *Hpa*.

The strongest and most consistent EDS phenotypes were produced on col-0 null mutants for nine-cis-epoxycarotenoid dioxygenase (NCED) 4, expansin-like B3 precursor (EXLB3), DNAJ heat shock protein (AT5G23240), and genomes uncoupled 5 (GUN5). These genes are expressed or repressed early and are specific to a compatible Emwa1 interaction. A test with compatible isolate Emco5 informs us of generic gene function during an *Hpa* attack.

Many NCEDs have been characterized and have been proposed to catalyze the rate limiting step in ABA synthesis [140]. No functional information is available that describes NCED4. Expansins are non-enzymatic proteins found around the plant cell wall which impact growth and development [141]. Unfortunately, EXLB3 and expansin-like genes are not well characterized in *A. thaliana*. AT5G23240 is an uncharacterized gene that is annotated as a heat shock protein [142]. This gene is transcriptionally associated to OSMATE1 and OSMATE2 expression [142]. These genes have a negative impact on *A. thaliana* resistance against *Pseudomonas syringae* DC3000 (*Pst* DC3000) [142].

Interestingly, GUN5 encodes the ChlH subunit of Mg-chelatase [143]. This gene is suggested to play a role in plastid-to-nucleus signal transduction [143]. Mochizuki et al. observed that changes in the tetrapyrrole biosynthetic pathway suppressed transcription of nuclear genes which localize to plastids [143]. GUN5 function is implicated in this signaling pathway [143]. At the 0.5 DPI, we noticed GO enrichment for genes targeted the chloroplast. GUN5 is likely involved directly or indirectly with this process early in a *Hpa* infection. We predict that these genes are involved in PTI responses against *Hpa*.

Our strongest *S* gene candidate *At*Gcn5 was susceptible to *Hpa* Emco5 in a Col-0 knockout. *At*Gcn5 is a non-repressible histone acetyltransferase which controls developmental processes through regulation of transcription [144, 145]. Since *At*Gcn5 is annotated as a general repressor of transcription it is likely that *Hpa* targets this gene to broadly influence transcription. High levels of gene flux related to transcription were observed in both resistant and susceptible specific gene clusters. Since Bayesian Biclustering was incomplete, we were not able to assess percent annotation representation among clusters. Bayesian Biclustering did reveal that this gene shared an expression profile with CCA1. This cluster was repressed early in a compatible

interaction but unchanged during incompatibility. It is possible that the pathogen targets transcription hubs early in infection to modulate the processes as a whole. By general transcriptional repression perception and signaling could be manipulated to influence downstream expression on a global scale.

S genes can be utilized in cultivated crops for resistance. *At*Gcn5 has homologs in crop plants and could be knocked out to provide resistance to other oomycete diseases if they share the same susceptibility mechanism. Mutants can then be tested for resistance against field isolates. Downy mildews are obligate biotrophs which make them hard to work with and characterize. Our approach takes advantage of host transcript differences between compatible and incompatible interactions to identify host factors which are manipulated by the pathogen. Despite our extensive analysis, we characterized a small portion of very significant genes. We want to build on the framework developed in this study to draw conclusions about resistance and susceptibility mechanisms from increasingly available RNA sequencing and microarray data. A recent study by Jones et al. characterized another series of compatible and incompatible *Hpa* interactions. We hope to develop a clustering algorithm to overcome the incomplete and inaccurate results produced by Bayesian Biclustering. In order to draw more concrete conclusions about the *Hpa/A. thaliana* pathosystem more accurate and complete infection profiles must be generated. Techniques to compare differential data sets will be critical to extract usable information from the array of transcript profiling experiments being made publicly available.

Materials and Methods

Data Location

The raw data is available online at NCBI's Gene Expression Omnibus and are accessible through GEO Series accession number GSE22274. This data is backed up on a lab external hard drive. Q values, obtained from a mixed model ANOVA, were sent electronically by Dr. Wang via email and are saved on a lab external hard drive.

Gene Expression Normalization using log_2

We normalized each time point to the 0 DPI time point by dividing microarray values at the 0.5, 2, 4, and 6 DPI time points by microarray values at the 0 DPI time point. This gave a ratio for each time point with respect to the 0 DPI time point. Wang et al. only included a water mock at the 0 DPI time point. We did a log_2 transformation of this value to normalize gene expression values. We used the excel formula =LOG(Ratio,2) and applied it to the data set to get log_2 normalized values.

Volcano Plot Construction

Wang et al. performed a mixed model ANOVA on the transcriptome data from the incompatible and compatible interactions. This provided us with a Q value. Using the Q value, we can look at only consistent and reliable gene movement. On the y-axis we plotted log_{10} (Qvalue)*-1. The log_{10} transformation was applied to the Q values by using the excel formula = LOG (Qvalue,10)*-1. This formula was applied to all data sets for volcano plot formation. On the x-axis, we plotted log_2 expression values. For all following analyses, we only used genes which met a Q value cutoff of 0.05 or 95% confidence which is represented by the thick black line.

GO Annotation using Ontologizer

We applied a GO Annotation to the incompatible and compatible data sets using the program Ontologizer. We visually compared the CC, BP, and MF annotations for similarities and differences between incompatibility and compatibility

Co-expression Clustering using Bayesian Biclustering

We used the Bayesian Biclustering algorithm to group 408 S specific genes by coexpression. We attempted to cluster a larger number of genes and returned too many clusters to analyze. It is imperative to use normalized expression values for this analysis. We attempted to cluster genes based on fold change expression values which was unsuccessful. The Log_2 values for the 408 S specific genes were run through Bayesian Biclustering software and clustered into 5 unique gene expression clusters.

Susceptibility Specific Gene Selection

We selected genes from clusters 1 and 3 which represent S specific factors with high up or downregulation respectively during early infection. We chose genes in these clusters which are not known to have EDS or EDR phenotypes against *Hpa*. As a positive control for an EDR phenotype, we chose to order a null mutant for the ABA1 gene which is known to produce an EDR phenotype against *Hpa*. All ordered genes are in the col-0, CS6000 background.

Plant Growth for Seed Collection

T2 *A. thaliana* null mutants from SALK, CS6000, WS, and eds1-1 were planted in 2 inch pots. Before planting, a nutrient solution was prepared by adding 1 TSP of Miracle Grow © to 2 L of water. In a bin 2L of the mixed nutrient solution was added to 3-4 kg of soil. Plants were grown at 22 degrees C under long day (16h light/8h dark, light intensity = 250uM) conditions for 1 week. Four seedlings per line were transferred to 4inch pots for seed harvesting. When plants

began bolting, we wrapped them in wax paper to prevent seed contamination. Young plants required once per week. Plants that were bolting and forming siliques required water once every 2 days. Plants were watered until siliques were produced. After a significant amount of siliques were formed, we stopped watering the plants. Plants were left to dry for 3 weeks. After 3 weeks, seed was collected for each planted line.

Plant Growth for Pathogenicity Assays

Plants were potted according to the methods in "Plant Growth for Seed Collection" in 2 inch pots. These plants were grown at short day conditions (8h light/16h dark, light intensity = 180uM). Five days prior to infection, seedlings were thinned out such that no cotyledons were overlapping.

Propagation of Hpa *isolate Emco5*

Emco5 infected and sporulating WS plant material was stored at -80 degrees C for the long term storage of *Hpa*. To use Emco5, we first removed a 1.5ml tube of infected material from the -80 degree freezer and let it thaw on ice for 30 minutes. 1 mL of sterile dH2O was added to the tube. The tube was gently vortexed 3 times with 10 second rests at a vortex power setting of 5/10. Plant material was removed using a small spatula. The remaining solution was then filtered through a folded piece of cheese cloth. The filtered solution was then sprayed onto WS and *eds1-1* plants. After 6 DPI, lids and plants were sprayed with water (spray bottle using eyewash water). Lids were taped to increase humidity in the container. At 7 DPI, lids were removed and new spores were collected from infected WS and *eds1-1*. Spores were collected by adding water to sporulating material, vortexing, removing plant material, and filtering out plant material by the above protocol. After the first passage, sporulation may be weak on WS and

spores taken from infected eds1-1 can be used for the second passage. When Emco5 produced a consistently robust infection on WS two weeks in a row, we started using it for virulence assays.

Pathogenicity Assay with Emco5

To investigate if any of these null mutations confer broad spectrum host EDR or EDS phenotypes in response to *Hpa*, we inoculated 11 day old *A. thaliana* seedlings with *Hpa*. *A. thaliana* seedlings were planted in 2 inch pots and thinned one day before inoculation to improve consistency of sporangiophore counting. Seedlings were sprayed with 500ul to 1 ml of solution. Pots were rotated during spray inoculation. This virulence assay was performed in 3 biological replicates. Since the *Hpa* isolate Emco5 is compatible on CS6000, we assessed Emco5 virulence on the null mutants compared to Emco5 virulence on CS6000. For pathogen assays, we prepared a solution of 50,000 Emco5 spores/ml in sterile dH_2O. Conidiophore were harvested from infected WS plants. Within 5 minutes of spore solution preparation, we sprayed ≥500ul of spore solution on each pot. Pots were sprayed from all angles by rotating the pot during spraying. A generic compressed air sprayer was used to deliver the spore solution to plant leaves. At 6 DPI before the start of the dark cycle, lids and plants were sprayed with a light film of water (spray bottle using water from the eyewash). Lids were loosely taped to prevent humidity loss. At 7DPI, the lids were removed and sporulation was observed. We counted the number of conidiophore per line with an average sample size of 25 seedlings or 50 cotyledons per line. Sporangiophores were counted under a dissecting scope at 100X magnification. A top and bottom light provides the optimal lighting conditions for sporangiophores counts on *A. thaliana* cotyledons.

Figures and Tables

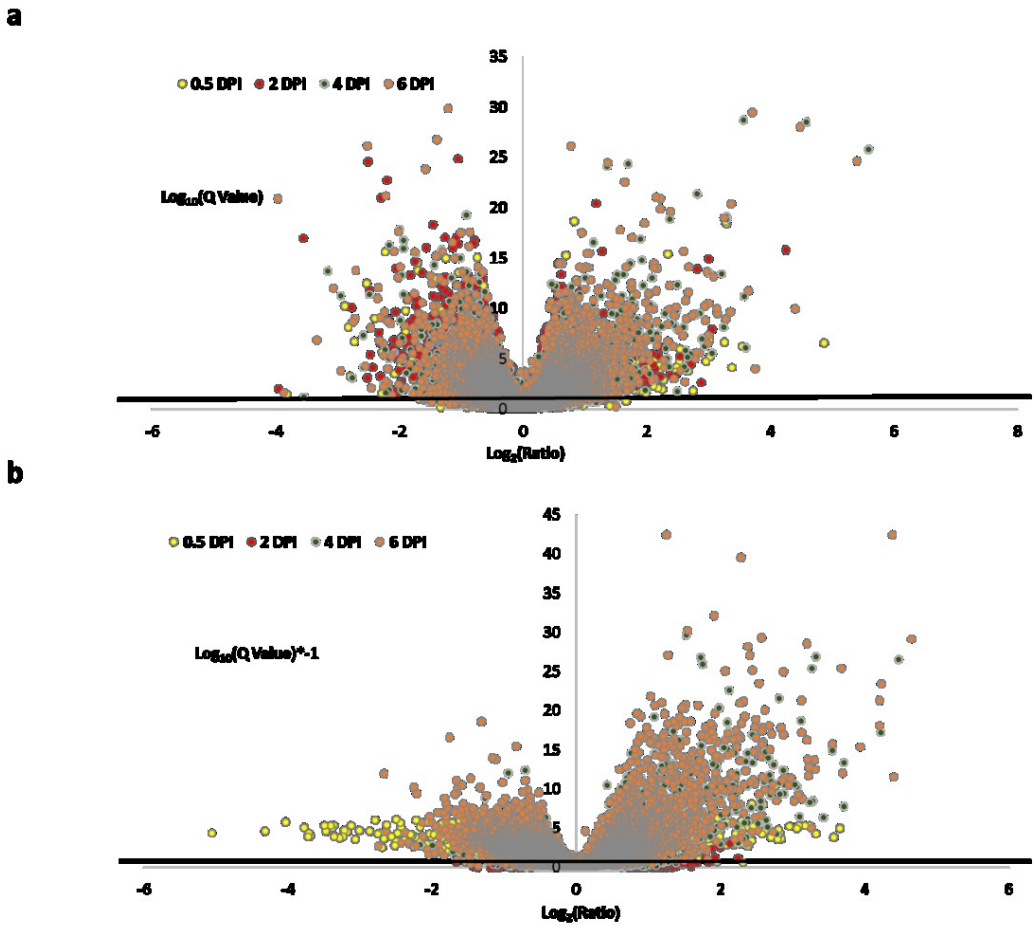

Figure 4.1 Volcano plot showing a normalized distribution. **a)** incompatible *Hpa* interaction and **b)** compatible *Hpa* interaction. The 2 DPI (red) shows reduced gene expression at a Q value cutoff of 0.05. We observed a lack of gene repression in compatibility compared with incompatibility.

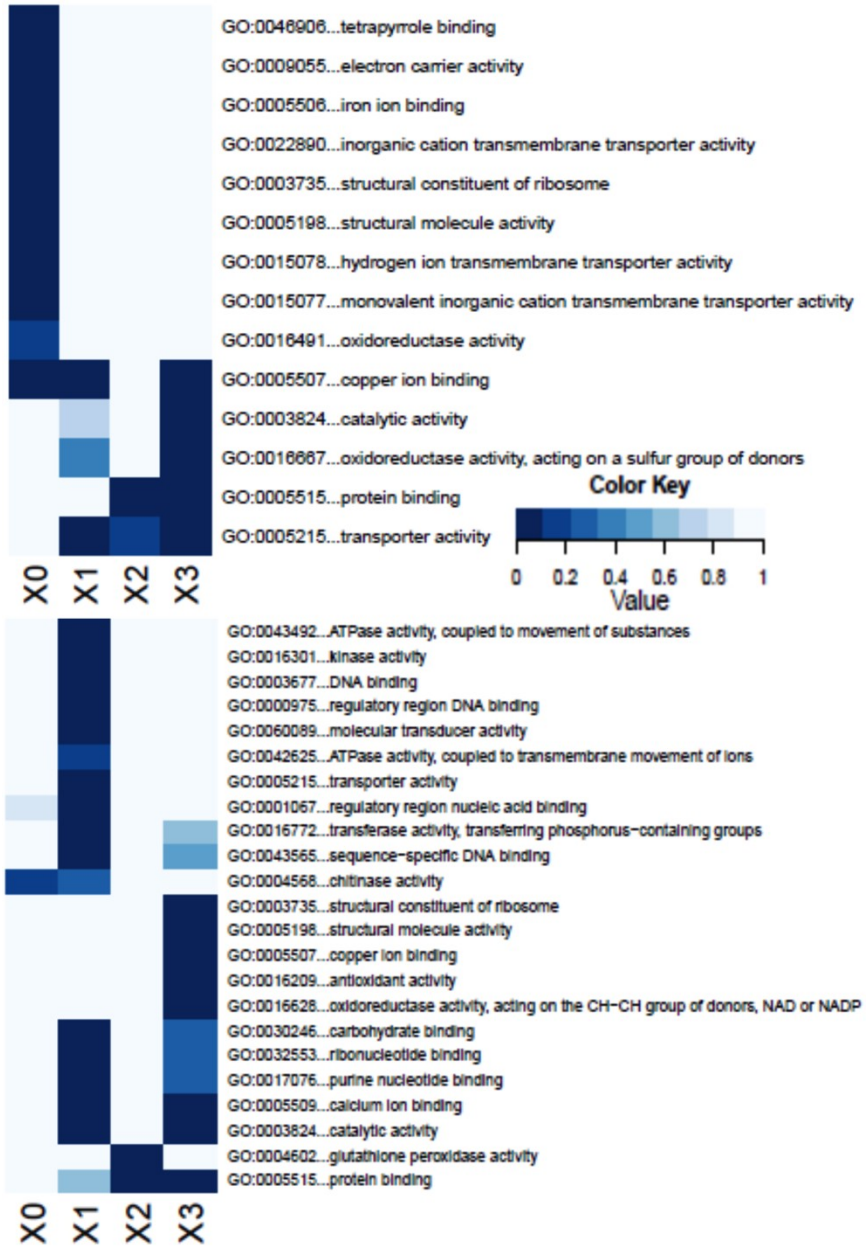

Figure 4.2 Gene ontology using cellular compartment (CC) analysis. Genes which met a Q-value cutoff of 0.05 in a. incompatible and b. compatible *Hpa* infections were annotated using Ontologizer. The Ontologizer output for CC was reformatted as a heatmap. The darker color indicates higher statistical significance. The 0.5 DPI, 2 DPI, 4 DPI, and 6 DPI are labeled as X0, X1, X2, and X3 respectively.

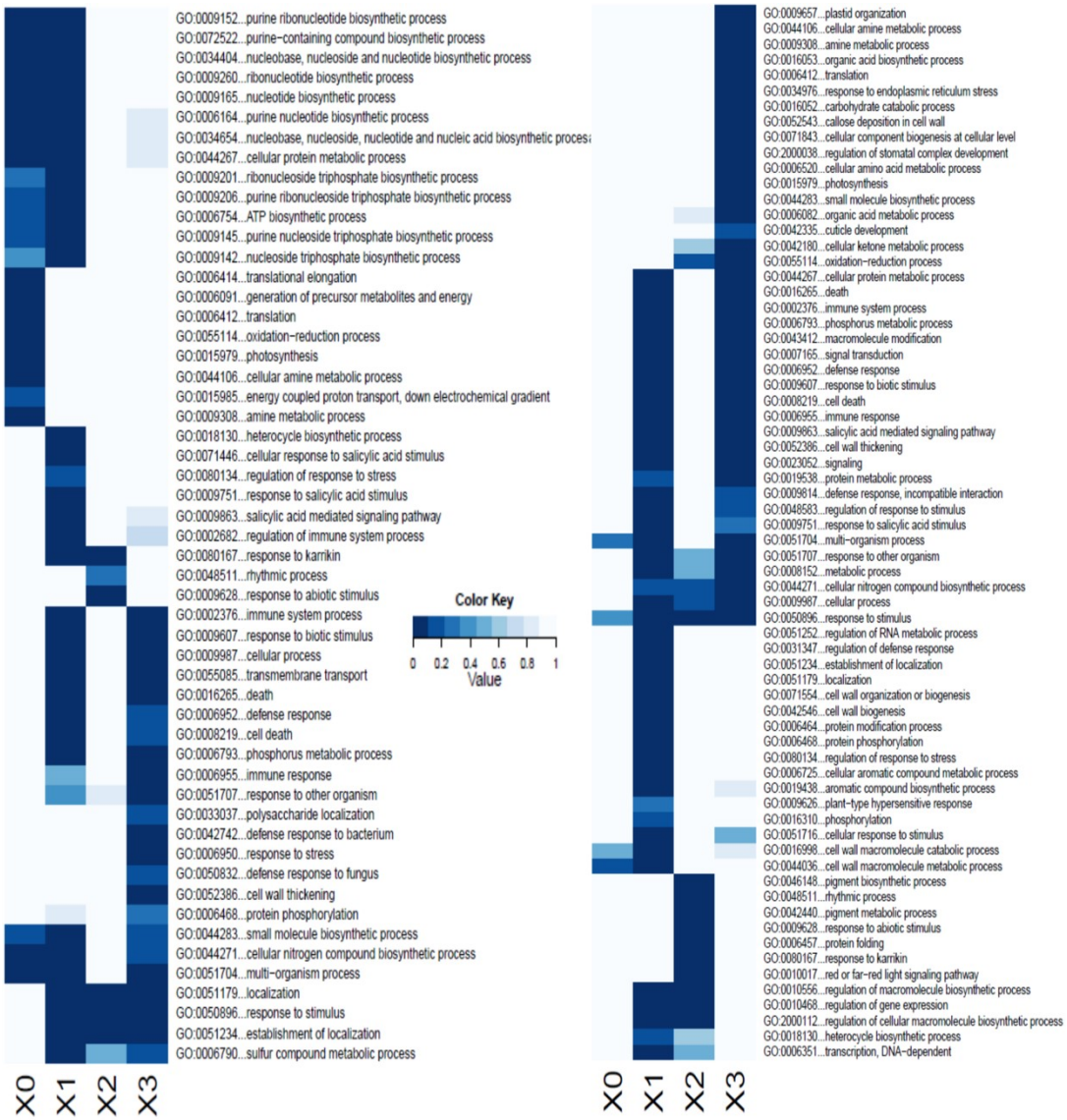

Figure 4.3 Gene ontology using biological process (BP) analysis. Genes which met a Q-value cutoff of 0.05 in a. incompatible and b. compatible *Hpa* infections were annotated using Ontologizer. The Ontologizer output for BP was reformatted as a heatmap. The darker color indicates higher statistical significance. The 0.5 DPI, 2 DPI, 4 DPI, and 6 DPI are labeled as X0, X1, X2, and X3 respectively

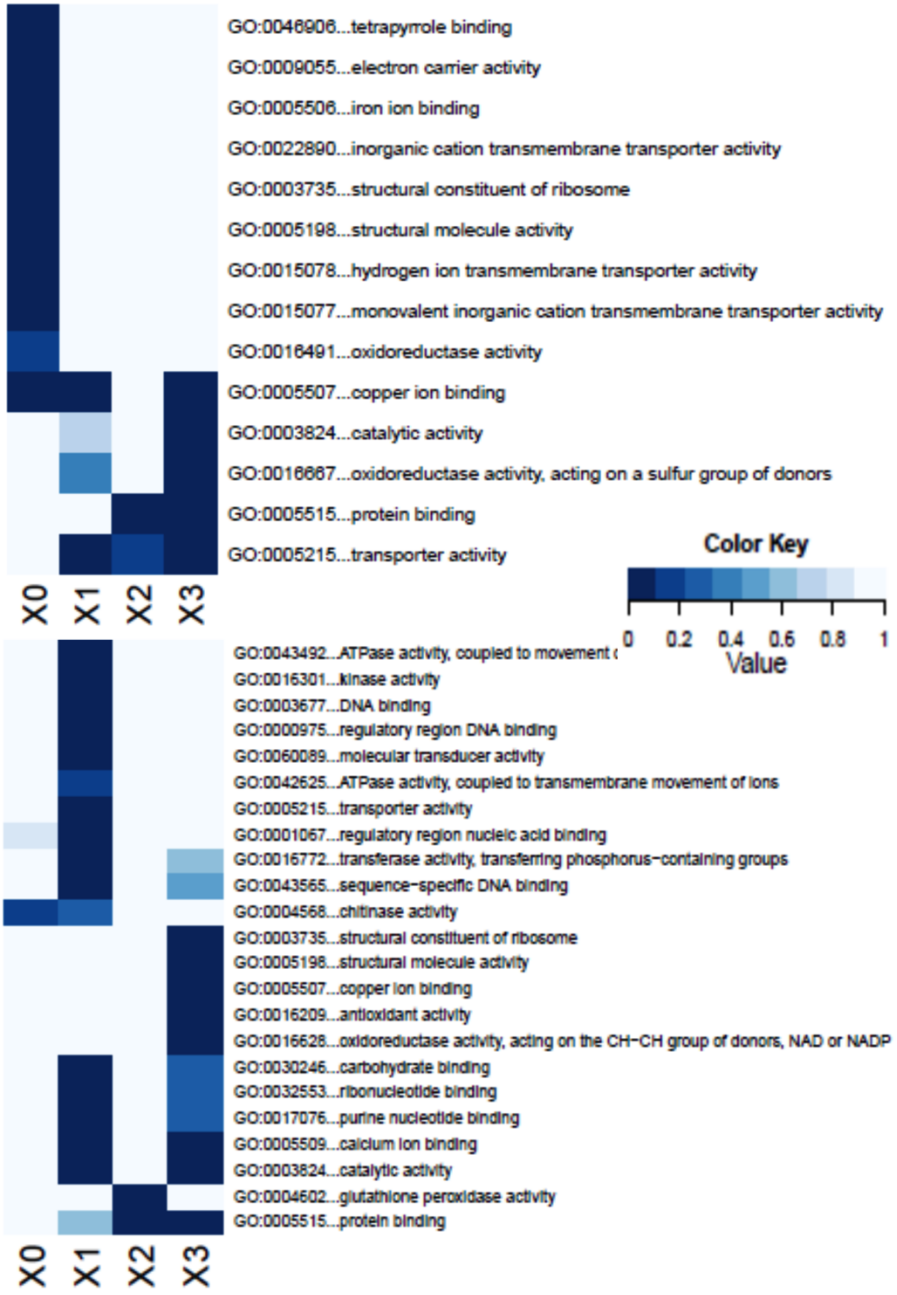

Figure 4.4 Gene ontology using molecular function (MF) analysis. Genes which met a Q-value cutoff of 0.05 in a. incompatible and b. compatible *Hpa* infections were annotated using Ontologizer. The Ontologizer output for MF was reformatted as a heatmap. The darker color indicates higher statistical significance. The 0.5 DPI, 2 DPI, 4 DPI, and 6 DPI are labeled as X0, X1, X2, and X3 respectively.

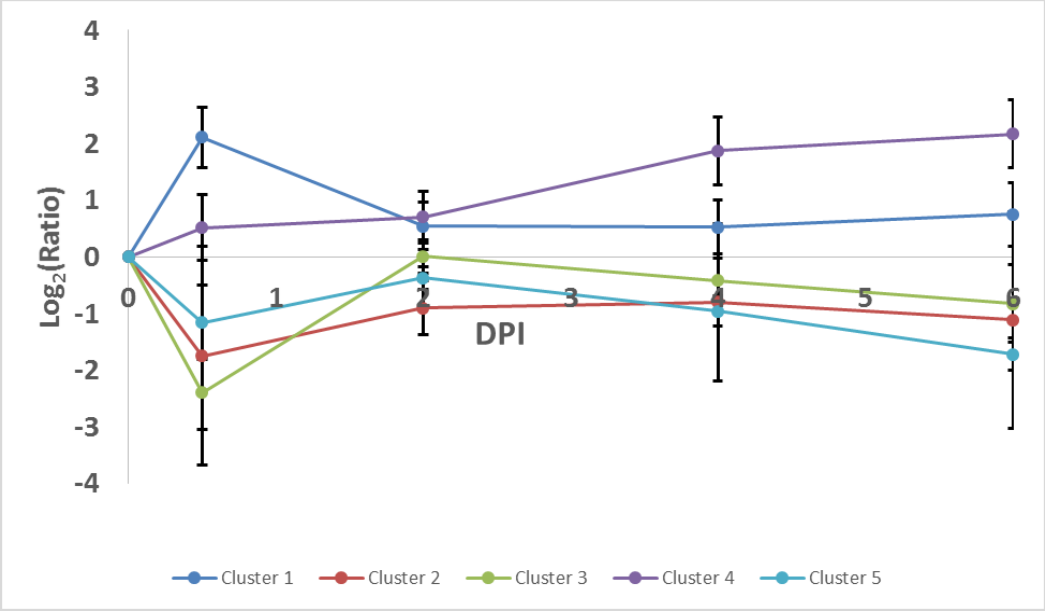

Figure 4.5 Major susceptibility clusters during *Hpa* Infection. 408 genes with an expression profile which was specific to the compatible interaction were analyzed with Bayesian Biclustering for co-expression. We observed 5 gene clusters with unique expression patterns. We chose genes from clusters 1 and 3 for a virulence assessment.

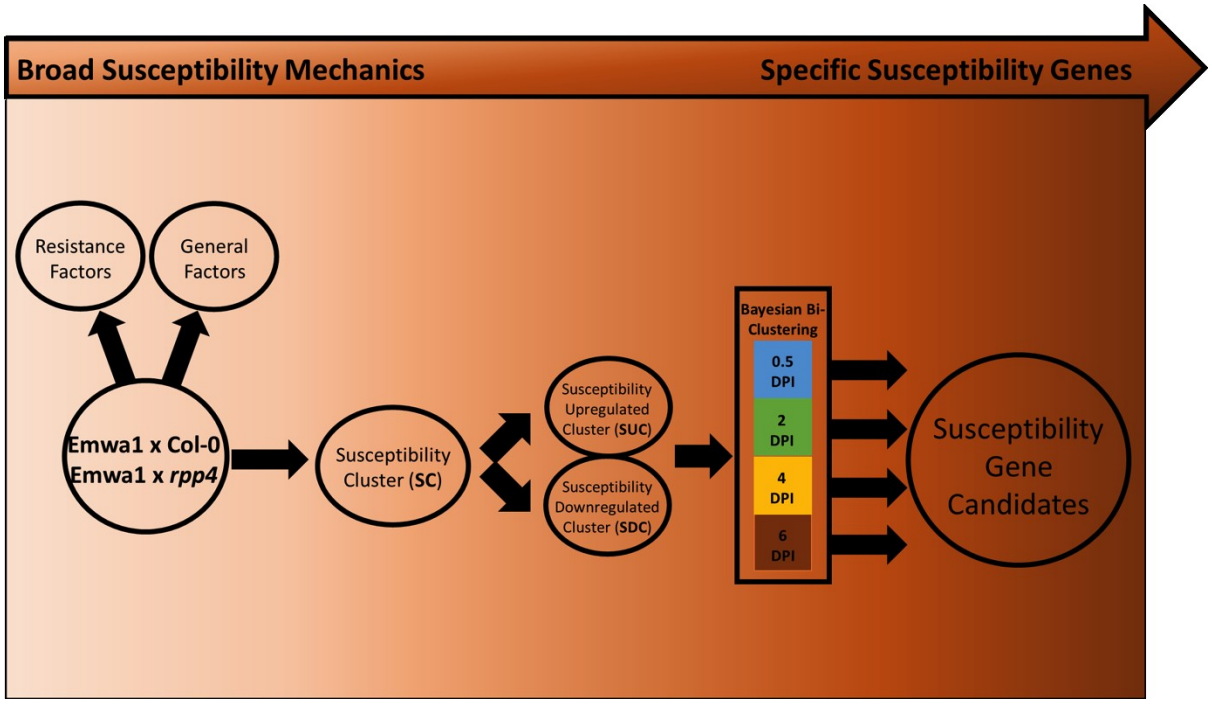

Figure 4.6 A schematic of the bioinformatic approaches used to identify gene candidates involved in susceptibility. In some analyses we compared resistance and susceptibility factors; however clustering of resistance factors was very incomplete. Genes with significant but conserved expression among both data sets were considered general disease factors.

Table 4.1 *A. thaliana* null mutants involved in susceptibility were innoculated with *Hpa* Emco5. *A. thaliana* null mutants were ordered from the Salk Institue Genomic Analysis Laboratory. When available, we selected two null mutants for each of these genes.

Gene ID	Location	LINE #1	LINE #2
AT4G19170	**cluster 3**	**SALK_109403C**	**SALK_097984C**
AT5G67030	**cluster 3**	**CS25407**	**SALK_027326C**
AT4G12980	**cluster 3**	**SALK_013527C**	**SALK_066533C**
AT3G20810	**cluster 1**	**CS67787**	
AT5G23240	**cluster 1**	**SALK_144377C**	**SALK_008678C**
AT4G32280	**cluster 3**	**SALK_091933C**	**SALK_152235C**
AT2G33830	**cluster 1**	**SALK_098437C**	
AT2G19450	**cluster 1**	**SALK_039456C**	
AT4G19410	**cluster 1**	**SALK_085171C**	**SALK_091346C**
AT5G13630	**cluster 3**	**SALK_133118C**	**SALK_152096C**
AT5G64840	**cluster 3**	**SALK_149585C**	
AT5G03350	**cluster 4**	**SALK_036814C**	**SALK_074760C**
AT5G18470	**cluster 4**	**CS860018**	**SALK_019318C**
AT2G26440	**cluster 4**	**CS25083**	**SALK_058895C**
AT2G18660	**cluster 4**	**SALK_000951C**	
AT1G43910	**cluster 4**	**SALK_136570C**	
AT2G21320	**cluster 5**	**SALK_061956C**	
AT4G17460	**cluster 5**	**SALK_006022C**	**SALK_059835C**
AT5G23750	**cluster 5**	**SALK_007458C**	**SALK_062367C**

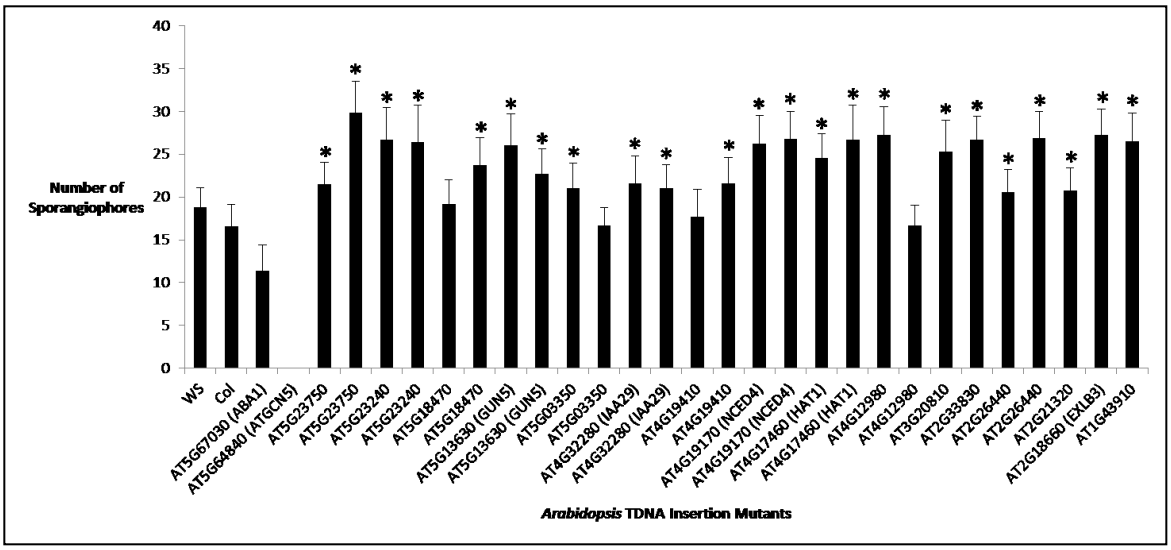

Figure 4.7 *A. thaliana* null mutants for candidate susceptibility genes were infected with *Hpa* isolate Emco5. Virulence of this isolate on *A. thaliana* null mutants was assessed in the col-0 background for 17 S specific genes. These genes were identified using a differential gene expression between resistance and susceptible data sets. Virulence was measured by counting the number of conidiophores on the cotyledon leaves at 7 DPI. This figure was produced from 3 biological replicates.

Chapter 5

Concluding Remarks

Kevin E. Fedkenheuer

Department of Plant Pathology, Physiology, and Weed Science, Virginia Polytechnic Institute, Blacksburg, VA

Summary

As the population expands, plant scientists are expected to satisfy global food concerns. Plant diseases negatively impact crop plants and ornamentals. Oomycete and fungal diseases are an increasing risk to food security [5]. By planting in monoculture, we select for plastic organisms which can rapidly evolve [5]. *Phytophthora sojae*, the causal agent of *Phytophthora* root and stem rot disease, is a destructive pathogen on soybean which causes yield suppression around 1% per year [31]. We detailed the recent advancements in the study of *Phytophthora* root and stem rot disease in Chapter 1.

To better manage *Phytophthora* root and stem rot disease, we probed soybean germplasm for potential new resistance (*R*) genes against core *P. sojae* effectors. We developed a system to deliver *P. sojae* effectors into soybean using *Pseudomonas fluorescens* Type III secretion. If an effector is recognized by a *R* gene, a avirulence (*Avr*) activity is observed, typically producing a hypersensitive response or HR. Known *Avr/R* interactions were used to validate this approach. We delivered core *P. sojae* effectors into *P. sojae* resistant soybean germplasm. We assessed the *Avr* phenotypes in segregating $F_{2:3}$ populations. Two $F_{2:3}$ crosses, accession 32 (gm32) x Williams and gm326 x Williams, were analyzed. In all cases, we observed a phenotypic ratio which suggests dominant inheritance. Additional *P. sojae* core effectors revealed additional effector response genes. Our ultimate goal is to provide growers with durable resistance against *Phytophthora* root and stem rot disease on soybean. This work is described in Chapter 2.

We adapted *Pseudomonas* effector delivery to screen for potential *P. sojae R* genes in wild soybean. We screened 24 *P. sojae*-resistant *Glycine soja* accessions with individual RXLR effectors. We observed *G. soja* accessions which responded to core *P. sojae* effectors with a HR. We assessed the effector response phenotype in $F_{2:3}$ progeny from a cross of accession 2292 (gs)

x Williams to the effector *Avh240*. The phenotypic ratio suggests that gs2292 contains one dominant *R* gene against the core *P. sojae* effector *Avh*240. The wild soybean screening is presented in Chapter 3.

We analyzed transcript for Col-0 (Incompatible) and for *rpp4*Col-0 (Compatible) during time-course infections with *Hyaloperonospora arabidopsidis* (*Hpa*) isolate Emwa1. We noticed compatibility specific gene ontology (GO) enrichment in genes related to translation and ribosome structure in late infection. We sorted genes specific to compatibility and applied Bayesian Biclustering. This produced five unique compatibility gene clusters. We selected representative genes from each cluster and prepped *A. thaliana* null mutants for each gene. Most null mutations produced enhanced disease susceptibility (EDS) phenotypes when challenged with *Hpa*. A null mutation in *At*Gcn5 provided full resistance against *Hpa* Emco5. The translation potential of this susceptibility (*S*) gene should be evaluated. To expand on this analysis, we created a temporal clustering algorithm to better differentiate genes involved in resistance and susceptibility. Chapter 4 will be combined with the bioinformatic section in Michael Fedkenheuer's dissertation for publication.

References

1. Kevin E Fedkenheuer, M.G.F., and John M McDowell, *A Role for Oomycete Biology in Development of Disease Resistant Soybean*, in *Educational Webcasts*. 2015: The Plant Management Network.

2. Serge Savary, A.F., Jean-Noel Aubertot, and Clayton Hollier, *Crop Losses Due to Disease and their Implications for Global Food Production Losses and Food Security.* Food Security, 2012. **4**(4): p. 519 - 537.

3. Strange, R.N. and P.R. Scott, *Plant disease: a threat to global food security.* Annu Rev Phytopathol, 2005. **43**: p. 83-116.

4. Virginia Heffer Link1, M.L.P., and Kenneth B. Johnson, *Oomycetes.* The Plant Health Instructor, 2002 (Updated 2012).

5. Bebber, D.P. and S.J. Gurr, *Crop-destroying fungal and oomycete pathogens challenge food security.* Fungal Genet Biol, 2015. **74**: p. 62-4.

6. Palm, A.Y.R.a.M.E., *Why are Phytophthora and other Oomycota not true Fungi?* The Plant Health Instructor, 2006.

7. Tyler, B.M., *Entering and breaking: virulence effector proteins of oomycete plant pathogens.* Cell Microbiol, 2009. **11**(1): p. 13-20.

8. Haverkort, A.J., et al., *Societal Costs of Late Blight in Potato and Prospects of Durable Resistance Through Cisgenic Modification.* Potato Research, 2008. **51**(1): p. 47-57.

9. Parke, J.L., and S. Lucas, *Sudden oak death and ramorum blight.* The Plant Health Instructor, 2008.

10. Kamoun, S., *Molecular genetics of pathogenic oomycetes.* Eukaryot Cell, 2003. **2**(2): p. 191-9.

11. James, T.Y., et al., *A molecular phylogeny of the flagellated fungi (Chytridiomycota) and description of a new phylum (Blastocladiomycota).* Mycologia, 2006. **98**(6): p. 860-71.

12. Fry, W.E.a.G., N., *Introduction to Oomycetes.* The Plant Health Instructor, 2010.

13. M. C. Lerclerc, J.G., and M. Deville, *Taxonomic and phylogenetic analysis of Saprolegniaceae (Oomycetes) inferred from LSU rDNA and ITS sequence comparisons.* Antonie van Leeuwenhoek, 2000. **77**(4): p. 369 - 377.

14. Cooke, D.E., et al., *A molecular phylogeny of Phytophthora and related oomycetes.* Fungal Genet Biol, 2000. **30**(1): p. 17-32.

15. Kang, S., et al., *The promise and pitfalls of sequence-based identification of plant-pathogenic fungi and oomycetes.* Phytopathology, 2010. **100**(8): p. 732-7.

16. White, T.J., Bruns, T., Lee, S., and Taylor J. W., *Amplification and direct sequencing of fungal ribosomal RNA genes for phylogenetics.*, in *PCR Protocols: A Guide to Methods and Applications*. 1990, Academic Press Inc.: New York. p. 315 - 322.

17. Robideau, G.P., et al., *DNA barcoding of oomycetes with cytochrome c oxidase subunit I and internal transcribed spacer.* Mol Ecol Resour, 2011. **11**(6): p. 1002-11.

18. Lab, V. *Conserved primer sequences for PCR amplification and sequencing from nuclear ribosomal RNA*. 2014; Available from: http://biology.duke.edu/fungi/mycolab/primers.html.

19. Kim, M.Y., et al., *Tracing soybean domestication history: From nucleotide to genome.* Breed Sci, 2012. **61**(5): p. 445-52.

20. Kim, M.Y., et al., *Whole-genome sequencing and intensive analysis of the undomesticated soybean (Glycine soja Sieb. and Zucc.) genome.* Proc Natl Acad Sci U S A, 2010. **107**(51): p. 22032-7.

21. Roy, K.W., R.E. Baird, and T.S. Abney, *A review of soybean (Glycine max) seed, pod, and flower mycofloras in North America, with methods and a key for identification of selected fungi.* Mycopathologia, 2001. **150**(1): p. 15-27.

22. Dalgaarg, R., Schmidt, J., Halberg, N., Christensen, P., Thrane, M., Pengue, W. , *LCA of Soybean Meal.* Int J LCA, 2008. **13**(3): p. 240 - 254.

23. www.soystats.com, *U. S. Crop Area Planted*. 2014, American Soybean Association.

24. Oosterveer, P., *Global Governance of Food Prodution and Consumption: Issues and Challenges*. 2007, Business and Economics: Edward Elgar Publishing.

25. Grushkin, D., *Threat to global GM soybean access as patent nears expiry.* Nat Biotechnol, 2013. **31**(1): p. 10-1.

26. Hildebrand, A.A., *A Root and Stalk Rot of Soybeans cause by Phytophthora megasperma Drechsler var. sojae var. nov.* Canadian Journal of Botany, 1959. **37**(5): p. 927-957.

27. Helga Forster, B.M.T., and Michael D. Coffey, *Phytophthora sojae Races Have Arisen by Clonal Evolution and by Rare Outcrosses.* Molecular Plant-Microbe Interactions, 1994. **7**(6): p. 780 - 791.

28. Schmitthenner, A.F., *Phytophthora Rot of Soybean.* Plant Health Progress, 2000.

29. Johnson, J.P.J.a.H.W., *Lupine, a new host for Phytophthora megasperma var. sojae.* Phytopathology, 1969. **59**: p. 504 - 507.

30. Buttner, D. and S.Y. He, *Type III protein secretion in plant pathogenic bacteria.* Plant Physiol, 2009. **150**(4): p. 1656-64.

31. Wrather, A., Shannon, G., Balardin, R., Carregal, L., Escobar, R., Gupta, G. K., Ma, Z., Morel, W., Ploper, D., and Tenuta, A., *Effects of Disease on Soybean Yield in the Top Eight Producing Countries in 2006.* Plant Management Network, 2010.

32. Kamoun, S., et al., *The Top 10 oomycete pathogens in molecular plant pathology.* Mol Plant Pathol, 2015. **16**(4): p. 413-34.

33. Tyler, B.M., *Phytophthora sojae: root rot pathogen of soybean and model oomycete.* Mol Plant Pathol, 2007. **8**(1): p. 1-8.

34. Dorrance, A.E., D. Mills, A.E. Robertson, M.A. Draper, L. Giesler, and A.Tenuta, *Phytophthora root and stem rot of soybean.* The Plant Health Instructor, 2007.

35. Morris, P.F., E. Bone, and B.M. Tyler, *Chemotropic and contact responses of phytophthora sojae hyphae to soybean isoflavonoids and artificial substrates.* Plant Physiol, 1998. **117**(4): p. 1171-8.

36. Pieterse, C.M., et al., *Networking by small-molecule hormones in plant immunity.* Nat Chem Biol, 2009. **5**(5): p. 308-16.

37. Tsuda, K. and F. Katagiri, *Comparing signaling mechanisms engaged in pattern-triggered and effector-triggered immunity.* Curr Opin Plant Biol, 2010. **13**(4): p. 459-65.

38. Hein, I., et al., *The zig-zag-zig in oomycete-plant interactions.* Mol Plant Pathol, 2009. **10**(4): p. 547-62.

39. Jones, J.D. and J.L. Dangl, *The plant immune system.* Nature, 2006. **444**(7117): p. 323-9.

40. Sharp, J.K., B. Valent, and P. Albersheim, *Purification and partial characterization of a beta-glucan fragment that elicits phytoalexin accumulation in soybean.* J Biol Chem, 1984. **259**(18): p. 11312-20.

41. Umemoto, N., et al., *The structure and function of a soybean beta-glucan-elicitor-binding protein.* Proc Natl Acad Sci U S A, 1997. **94**(3): p. 1029-34.

42. Nurnberger, T., et al., *High affinity binding of a fungal oligopeptide elicitor to parsley plasma membranes triggers multiple defense responses.* Cell, 1994. **78**(3): p. 449-60.

43. Brunner, F., et al., *Pep-13, a plant defense-inducing pathogen-associated pattern from Phytophthora transglutaminases.* EMBO J, 2002. **21**(24): p. 6681-8.

44. Jiang, R.H., et al., *RXLR effector reservoir in two Phytophthora species is dominated by a single rapidly evolving superfamily with more than 700 members.* Proc Natl Acad Sci U S A, 2008. **105**(12): p. 4874-9.

45. Govers, F. and K. Bouwmeester, *Effector trafficking: RXLR-dEER as extra gear for delivery into plant cells.* Plant Cell, 2008. **20**(7): p. 1728-30.

46. Anderson, R.G., et al., *Recent Progress in RXLR Effector Research.* Mol Plant Microbe Interact, 2015. **28**(10): p. 1063-72.

47. Wang, Q., et al., *Transcriptional programming and functional interactions within the Phytophthora sojae RXLR effector repertoire.* Plant Cell, 2011. **23**(6): p. 2064-86.

48. Torto, T.A., et al., *EST mining and functional expression assays identify extracellular effector proteins from the plant pathogen Phytophthora.* Genome Res, 2003. **13**(7): p. 1675-85.

49. Schornack, S., et al., *Ancient class of translocated oomycete effectors targets the host nucleus.* Proc Natl Acad Sci U S A, 2010. **107**(40): p. 17421-6.

50. Haas, B.J., et al., *Genome sequence and analysis of the Irish potato famine pathogen Phytophthora infestans.* Nature, 2009. **461**(7262): p. 393-8.

51. Stam, R., Jupe, J., Howden, A., Morris J., Boevink P., Hedley, P., Huitema, E., *Identification and Characterisation CRN Effectors in Phytophthora capsici Shows Modularity and Functional Diversity.* PLoS One, 2013.

52. Liu, T., et al., *Two host cytoplasmic effectors are required for pathogenesis of Phytophthora sojae by suppression of host defenses.* Plant Physiol, 2011. **155**(1): p. 490-501.

53. Rajput, N.A., et al., *Phytophthora sojae effector PsCRN70 suppresses plant defenses in Nicotiana benthamiana.* PLoS One, 2014. **9**(5): p. e98114.

54. Wawra, S., et al., *Secretion, delivery and function of oomycete effector proteins.* Curr Opin Microbiol, 2012. **15**(6): p. 685-91.

55. Whisson, S.C., et al., *A translocation signal for delivery of oomycete effector proteins into host plant cells.* Nature, 2007. **450**(7166): p. 115-8.

56. Dou, D., et al., *RXLR-mediated entry of Phytophthora sojae effector Avr1b into soybean cells does not require pathogen-encoded machinery.* Plant Cell, 2008. **20**(7): p. 1930-47.

57. Dou, D., et al., *Conserved C-terminal motifs required for avirulence and suppression of cell death by Phytophthora sojae effector Avr1b.* Plant Cell, 2008. **20**(4): p. 1118-33.

58. Kale, S.D., et al., *External lipid PI3P mediates entry of eukaryotic pathogen effectors into plant and animal host cells.* Cell, 2010. **142**(2): p. 284-95.

59. Yaeno, T., et al., *Phosphatidylinositol monophosphate-binding interface in the oomycete RXLR effector AVR3a is required for its stability in host cells to modulate plant immunity.* Proc Natl Acad Sci U S A, 2011. **108**(35): p. 14682-7.

60. Wawra, S., et al., *Avirulence protein 3a (AVR3a) from the potato pathogen Phytophthora infestans forms homodimers through its predicted translocation region and does not specifically bind phospholipids.* J Biol Chem, 2012. **287**(45): p. 38101-9.

61. Gizen, B.M.T.a.M., *The Phytophthora sojae Genome Sequence: Foundation for a Revolution*, in *GENOMICS OF PLANT-ASSOCIATED FUNGI AND OOMYCETES: DICOT PATHOGENS*, R.A.D.A.L.-P.C. Kole, Editor. 2014, Springer.

62. A. F. Schmitthenner, A.F.H., and R. G. Bhat, *Phytophthora sojae races in Ohio over a 10-year interval.* Plant Disease, 1994. **78**(3): p. 269 - 276.

63. Burnham, K.D., et al., *Rps8, A New Locus in Soybean for Resistance to Phytophthora sojae Salaries and research support provided by State and Federal Funds appropriated to the Ohio Agricultural Research and Development Center, The Ohio State University. This research project was supported by Ohio's Soybean Producers' check-off dollars through the Ohio Soybean Council.* Crop Science, 2003. **43**.

64. Ortega, M.A. and A.E. Dorrance, *Microsporogenesis of Rps8/rps8 heterozygous soybean lines.* Euphytica, 2011. **181**(1): p. 77-88.

65. Lin, F., et al., *Molecular mapping of two genes conferring resistance to Phytophthora sojae in a soybean landrace PI 567139B.* Theor Appl Genet, 2013. **126**(8): p. 2177-85.

66. Song, T., et al., *Two RxLR avirulence genes in Phytophthora sojae determine soybean Rps1k-mediated disease resistance.* Mol Plant Microbe Interact, 2013. **26**(7): p. 711-20.

67. Vleeshouwers, V.G., et al., *Effector genomics accelerates discovery and functional profiling of potato disease resistance and phytophthora infestans avirulence genes.* PLoS One, 2008. **3**(8): p. e2875.

68. Vleeshouwers, V., Oliver, R, *Effectors as Tools in Disease Resistance Breeding Against Biotrophic, Hemibiotrophic, and Necrotrophic Plant Pathogens.* Molecular Plant-Microbe Interactions, 2014. **27**(3): p. 196-206.

69. Kevin E Fedkenheuer, M.G.F., Colin L. Davis, Joel L. Shuman, Nick A. Dietz, Brett M. Tyler, M. A. Saghai Maroof, and John M. McDowell, *Effector-Directed Screens for New Disease Resistance Genes against the Soybean Root and Stem Rot Pathogen Phytophthora sojae.* New Phytologist (Pending), 2016.

70. Staskawicz, B.J., D. Dahlbeck, and N.T. Keen, *Cloned avirulence gene of Pseudomonas syringae pv. glycinea determines race-specific incompatibility on Glycine max (L.) Merr.* Proc Natl Acad Sci U S A, 1984. **81**(19): p. 6024-8.

71. Staskawicz, B., et al., *Molecular characterization of cloned avirulence genes from race 0 and race 1 of Pseudomonas syringae pv. glycinea.* J Bacteriol, 1987. **169**(12): p. 5789-94.

72. Keen, N.T. and R.I. Buzzell, *New disease resistance genes in soybean against Pseudomonas syringae pv glycinea: evidence that one of them interacts with a bacterial elicitor.* Theor Appl Genet, 1991. **81**(1): p. 133-8.

73. Michael G. Fedkenheuer, K.E.F., Colin L. Davis, Brett M. Tyler, M. A. Saghai-Maroof, and John M. McDowell, *Development of an Effector-Based Screening System to Identify Novel R Genes in a Wild Relative of Cultivated Soybean.* MPMI (Pending), 2016.

74. Program, S.E.a.R., *Tillage Practices.* Iowa State Extension, 2006.

75. Dr. George S. Smith, D.D.P., Ms. Lynnae Jess, Dr. Michael Schmidt, Dr. Terry Niblack, Dr. Craig R. Grau, Dr. Anne E. Dorrance, Dr. Glen L. Hartman, Dr. Reid Frederick, *Soybean Pest Management Strategic Plan.* USDA and United Soybean Board, 2002.

76. Kamoun, K.L.a.S., *Oomycete Genetics and Genomics: Diversity, Interactions and Research Tools*. Science. 2009: John Wiley & Sons. 406.

77. Rojas, A., Miles, D. T., Coffey D. M., Chilvers M., Martin, N. F.,, *Development of diagnostic assays for rapid detection of Phytophthora spp. causing soybean root rot.* Phytopathology, 2014. **Poster Session**.

78. Yang, X.B., Ruff, R. L., Meng, X. Q., and Workneh, F., *Races of Phytophthora sojae in Iowa.* Plant Disease, 1996. **80**(12): p. 1418 - 1420.

79. Leitz, R.A., *Races of Phytophthora sojae on soybean in Illinois.* The American Phytopathological Society, 2000. **84**(4): p. 487.

80. Kaitany, R.C., L.P. Hart, and G.R. Safir, *Virulence Composition of Phytophthora sojae in Michigan.* Plant Disease, 2001. **85**(10): p. 1103-1106.

81. Wrather, J.A. and S.R. Koenning, *Estimates of disease effects on soybean yields in the United States 2003 to 2005.* J Nematol, 2006. **38**(2): p. 173-80.

82. Catanzariti, A.M., P.N. Dodds, and J.G. Ellis, *Avirulence proteins from haustoria-forming pathogens.* FEMS Microbiol Lett, 2007. **269**(2): p. 181-8.

83. Mao, Y. and B.M. Tyler, *The Phytophthora sojae genome contains tandem repeat sequences which vary from strain to strain.* Fungal Genet Biol, 1996. **20**(1): p. 43-51.

84. Qutob, D., et al., *Copy number variation and transcriptional polymorphisms of Phytophthora sojae RXLR effector genes Avr1a and Avr3a.* PLoS One, 2009. **4**(4): p. e5066.

85. Dong, S., et al., *Sequence variants of the Phytophthora sojae RXLR effector Avr3a/5 are differentially recognized by Rps3a and Rps5 in soybean.* PLoS One, 2011. **6**(7): p. e20172.

86. Anderson, R.G., et al., *Homologous RXLR effectors from Hyaloperonospora arabidopsidis and Phytophthora sojae suppress immunity in distantly related plants.* Plant J, 2012. **72**(6): p. 882-93.

87. Tyler, B.M., and Gizen, M.J., *Genomics of Plant-Associated Fungi and Oomycetes: Dicot Pathogens*

The Phytophthora sojae genome sequence: foundation for a revolution

ed. R.A. Dean, Lichens-Park, A. and Kole, C. Vol. 7. 2014: Springer.

88. Schmitthenner, A.F., *Problems and progress in control of Phytophthora root rot of soybean.* Plant Disease, 1985. **69**(4): p. 362-368.

89. Matthiesen, R.L., et al., *A Method for Combining Isolates of Phytophthora sojae to Screen for Novel Sources of Resistance to Phytophthora Stem and Root Rot in Soybean.* Plant Disease, 2016: p. PDIS-08-15-0916-RE.

90. Wise, H., Anderson, R., McDowell, M. J., Wang Y., Tyler, M. B., *Identifying core P. sojae effectors.* Unpublished Communication, 2016.

91. Fabro, G., et al., *Multiple candidate effectors from the oomycete pathogen Hyaloperonospora arabidopsidis suppress host plant immunity.* PLoS Pathog, 2011. **7**(11): p. e1002348.

92. Lindeberg, M., S. Cunnac, and A. Collmer, *Pseudomonas syringae type III effector repertoires: last words in endless arguments.* Trends Microbiol, 2012. **20**(4): p. 199-208.

93. Thomas, W.J., et al., *Recombineering and stable integration of the Pseudomonas syringae pv. syringae 61 hrp/hrc cluster into the genome of the soil bacterium Pseudomonas fluorescens Pf0-1.* Plant J, 2009. **60**(5): p. 919-28.

94. Keen, N.T., Ersek, T., Long, M., Bruegger, B., Hoi, M., *Inhibition of the hypersensitive reaction of soybean to incompatible Pseudomonas spp. by blasticidin streptomycin or elevated temperature.* Physiological Plant Pathology, 1981. **18**: p. 325-337.

95. Hartman, G., Sinclair, J., Rupe, J., *Compedium of Soybean Diseses*. Fourth Edition, ed. G. Hartman, Sinclair, J., Rupe, J. 1999, St. Paul, Minnesota: APS Press.

96. Schmutz, J., et al., *Genome sequence of the palaeopolyploid soybean.* Nature, 2010. **463**(7278): p. 178-183.

97. Zhu, Y.L., et al., *Single-Nucleotide Polymorphisms in Soybean.* Genetics, 2003. **163**(3): p. 1123-1134.

98. Kale, S.D. and B.M. Tyler, *Assaying Effector Function in Planta Using Double-Barreled Particle Bombardment*, in *Plant Immunity: Methods and Protocols*, M.J. McDowell, Editor. 2011, Humana Press: Totowa, NJ. p. 153-172.

99. Dou, D., et al., *Different domains of Phytophthora sojae effector Avr4/6 are recognized by soybean resistance genes Rps4 and Rps6.* Mol Plant Microbe Interact, 2010. **23**(4): p. 425-35.

100. Hulbert, C.Y.a.S., *Prospects for functional analysis of effectors from cereal rust fungi.* Euphytica, 2011(179): p. 57-67.

101. Upadhyaya, N.M., et al., *A bacterial type III secretion assay for delivery of fungal effector proteins into wheat.* Mol Plant Microbe Interact, 2014. **27**(3): p. 255-64.

102. USDA/FAS, *Oilseeds: World Markets and Trade*, U.S.D.o.A.a.F.A. Service, Editor. 2016.

103. USDA, *World Agricultural Supply and Demand Estimates.* 2016.

104. Shannon, A.W.a.G., *Effect of Diseases on Soybean Yield in the Top Eight Producing Countries in 2006.* Plant Management Network (PMN), 2010.

105. Dorrance, A.E., D. Mills, A.E. Robertson, M.A. Draper, L. Giesler, and A.Tenuta, *Phytopthora root and stem rot of soybean.* The Plant Health Instructor, 2012.

106. Kale, S.D. and B.M. Tyler, *Entry of oomycete and fungal effectors into plant and animal host cells.* Cell Microbiol, 2011. **13**(12): p. 1839-48.

107. Win, J., et al., *Sequence divergent RXLR effectors share a structural fold conserved across plant pathogenic oomycete species.* PLoS Pathog, 2012. **8**(1): p. e1002400.

108. Bozkurt, T.O., et al., *Oomycetes, effectors, and all that jazz.* Curr Opin Plant Biol, 2012. **15**(4): p. 483-92.

109. Zhang, J., et al., *Effector-triggered and pathogen-associated molecular pattern-triggered immunity differentially contribute to basal resistance to Pseudomonas syringae.* Mol Plant Microbe Interact, 2010. **23**(7): p. 940-8.

110. Tyler, B.M., and Gizen, M.J., *Genomics of Plant-Associated Fungi and Oomycetes: Dicot Pathogens*. The Phytophthora sojae genome sequence: foundation for a revolution ed. R.A. Dean, Lichens-Park, A. and Kole, C. Vol. 7. 2014: Springer.

111. Raffaele, S. and S. Kamoun, *Genome evolution in filamentous plant pathogens: why bigger can be better.* Nat Rev Microbiol, 2012. **10**(6): p. 417-30.

112. Li, X., et al., *Physiological and proteomics analyses reveal the mechanism of Eichhornia crassipes tolerance to high-concentration cadmium stress compared with Pistia stratiotes.* PLoS One, 2015. **10**(4): p. e0124304.

113. Gijzen, M., C. Ishmael, and S.D. Shrestha, *Epigenetic control of effectors in plant pathogens.* Front Plant Sci, 2014. **5**: p. 638.

114. Dorrance, A.E., et al., *Pathotype Diversity of Phytophthora sojae in Eleven States in the United States.* Plant Disease, 2016: p. PDIS-08-15-0879-RE.

115. Sherman-Broyles, S., et al., *The wild side of a major crop: soybean's perennial cousins from Down Under.* Am J Bot, 2014. **101**(10): p. 1651-65.

116. Ross, H. and C.A. Huijsman, *[On the resistance of species of Solanum (Tuberarium) against the European Races of the potato nematode (Heterodera rostochiensis Woll.)].* Theor Appl Genet, 1969. **39**(3): p. 113-22.

117. Wen, Z., et al., *Genetic diversity and peculiarity of annual wild soybean (G. soja Sieb. et Zucc.) from various eco-regions in China.* Theor Appl Genet, 2009. **119**(2): p. 371-81.

118. Joshi, T., et al., *Genomic differences between cultivated soybean, G. max and its wild relative G. soja.* BMC Genomics, 2013. **14 Suppl 1**: p. S5.

119. Winter, S.M., et al., *QTL associated with horizontal resistance to soybean cyst nematode in Glycine soja PI464925B.* Theor Appl Genet, 2007. **114**(3): p. 461-72.

120. Ilut, D.C., et al., *Identification of haplotypes at the Rsv4 genomic region in soybean associated with durable resistance to soybean mosaic virus.* Theor Appl Genet, 2015.

121. Oh, S.K., H. Kim, and D. Choi, *Rpi-blb2-mediated late blight resistance in Nicotiana benthamiana requires SGT1 and salicylic acid-mediated signaling but not RAR1 or HSP90.* FEBS Lett, 2014. **588**(7): p. 1109-15.

122. Wang, W., et al., *Timing of plant immune responses by a central circadian regulator.* Nature, 2011. **470**(7332): p. 110-4.

123. Tyler and McDowell, *Identification of Core Effectors in P. sojae.* Unpublished_Manuscript.

124. American Soybean Association, S. *U. S. Crop Area Planted*. 2015.

125. Gnanamanickam, S.S. and E.W.B. Ward, *Bacterial blight of soybeans: a new race of Pseudomonas syringae pv. glycinea and variations in systemic symptoms.* Canadian Journal of Plant Pathology, 1982. **4**(1): p. 73-78.

126. Pedley, K.F. and G.B. Martin, *Molecular basis of Pto-mediated resistance to bacterial speck disease in tomato.* Annu Rev Phytopathol, 2003. **41**: p. 215-43.

127. Yaghoobi, J., J.L. Yates, and V.M. Williamson, *Fine mapping of the nematode resistance gene Mi-3 in Solanum peruvianum and construction of a S. lycopersicum DNA contig spanning the locus.* Mol Genet Genomics, 2005. **274**(1): p. 60-9.

128. Rauscher, G., et al., *Quantitative resistance to late blight from Solanum berthaultii cosegregates with R(Pi-ber): insights in stability through isolates and environment.* Theor Appl Genet, 2010. **121**(8): p. 1553-67.

129. Maughan, P.J., et al., *Amplified fragment length polymorphism (AFLP) in soybean: species diversity, inheritance, and near-isogenic line analysis.* Theor Appl Genet, 1996. **93**(3): p. 392-401.

130. Liu, B., et al., *Candidate defense genes as predictors of quantitative blast resistance in rice.* Mol Plant Microbe Interact, 2004. **17**(10): p. 1146-52.

131. Cohen, Y., et al., *Resurgence of Pseudoperonospora cubensis: The Causal Agent of Cucurbit Downy Mildew.* Phytopathology, 2015. **105**(7): p. 998-1012.

132. Gascuel, Q., et al., *The sunflower downy mildew pathogen Plasmopara halstedii.* Mol Plant Pathol, 2015. **16**(2): p. 109-22.

133. Koch, E. and A. Slusarenko, *Arabidopsis is susceptible to infection by a downy mildew fungus.* Plant Cell, 1990. **2**(5): p. 437-45.

134. Slusarenko, A.J. and N.L. Schlaich, *Downy mildew of Arabidopsis thaliana caused by Hyaloperonospora parasitica (formerly Peronospora parasitica).* Mol Plant Pathol, 2003. **4**(3): p. 159-70.

135. Coates, M.E. and J.L. Beynon, *Hyaloperonospora Arabidopsidis as a pathogen model.* Annu Rev Phytopathol, 2010. **48**: p. 329-45.

136. Baxter, L., et al., *Signatures of adaptation to obligate biotrophy in the Hyaloperonospora arabidopsidis genome.* Science, 2010. **330**(6010): p. 1549-51.

137. Cabral, A., et al., *Identification of Hyaloperonospora arabidopsidis transcript sequences expressed during infection reveals isolate-specific effectors.* PLoS One, 2011. **6**(5): p. e19328.

138. Asai, S., et al., *Expression profiling during arabidopsis/downy mildew interaction reveals a highly-expressed effector that attenuates responses to salicylic acid.* PLoS Pathog, 2014. **10**(10): p. e1004443.

139. Bevan, M. and S. Walsh, *The Arabidopsis genome: a foundation for plant research.* Genome Res, 2005. **15**(12): p. 1632-42.

140. Schwartz, S.H., X. Qin, and J.A. Zeevaart, *Elucidation of the indirect pathway of abscisic acid biosynthesis by mutants, genes, and enzymes.* Plant Physiol, 2003. **131**(4): p. 1591-601.

141. Irshad, M., et al., *A new picture of cell wall protein dynamics in elongating cells of Arabidopsis thaliana: Confirmed actors and newcomers.* BMC Plant Biology, 2008. **8**(1): p. 1-16.

142. Tiwari, M., et al., *Expression of OsMATE1 and OsMATE2 alters development, stress responses and pathogen susceptibility in Arabidopsis.* Sci Rep, 2014. **4**: p. 3964.

143. Mochizuki, N., et al., *Arabidopsis genomes uncoupled 5 (GUN5) mutant reveals the involvement of Mg-chelatase H subunit in plastid-to-nucleus signal transduction.* Proc Natl Acad Sci U S A, 2001. **98**(4): p. 2053-8.

144. Bertrand, C., et al., *Arabidopsis histone acetyltransferase AtGCN5 regulates the floral meristem activity through the WUSCHEL/AGAMOUS pathway.* J Biol Chem, 2003. **278**(30): p. 28246-51.

145. Servet, C., N. Conde e Silva, and D.X. Zhou, *Histone acetyltransferase AtGCN5/HAG1 is a versatile regulator of developmental and inducible gene expression in Arabidopsis.* Mol Plant, 2010. **3**(4): p. 670-7.

Appendix A

Recent Progress in RXLR Effector Research

Ryan G. Anderson, Devdutta Deb, Kevin Fedkenheuer, and John M. McDowell*

Department of Plant Pathology, Physiology, and Weed Science

Virginia Tech

Blacksburg, VA, USA 24061-0390

*for correspondence: johnmcd@vt.edu, 540-231-2388

Introduction

Much attention has been recently focused on oomycete RXLR effectors that are secreted to the interior of plant cells [147]. This area of study was launched in 2005 by a seminal paper that identified the RXLR motif based on its conservation in divergent oomycete avirulence proteins [148]. This was followed by evidence that the RXLR motif mediates entry of effectors into host cells [55, 56]. At the same time, the RXLR motif played a central role in bioinformatic screens for candidate effector genes from three *Phytophthora* genomes [50, 149]. Several RXLR effectors were shown to suppress plant immunity [150-154], the first plant targets of RXLR proteins were identified [155, 156], and phospholipids were implicated as host membrane receptors for RXLR proteins [58], albeit with controversy. These and other aspects of RXLR effector biology have been discussed in several excellent reviews [54, 107, 157-162]. Our intent is to integrate the initial insights into RXLR biology with recent studies. We discuss evolution, structure, and function, and include references to key review papers that provide more detail about specific aspects of RXLR effector biology. We do not discuss mechanisms of RXLR host cell entry or translational aspects of RXLR biology in detail, because these subjects have been covered in recent issues of *MPMI* and elsewhere [163-167].

Comparative genomics suggests that RXLR genes play a major role in virulence only for *Phytophthora* and downy mildew species

The first genome-wide inventories of RXLR genes were conducted in *P. sojae*, *P. ramorum*, and *P. infestans* [44, 50, 149]). Since then, the collection of oomycete

genomes has expanded dramatically. For example, 20 oomycete genomes now reside within Fungi DB (www.fungiDB.org). These genomes collectively encompass a wide range of taxonomy and lifestyle diversity within the oomycetes, ranging from the downy mildew and white rust pathogens that represent independent evolutions of obligate biotrophy, to *Pythium* species that are canonical broad host-range necrotrophs (Fig. 1).

Analyses of these genomes have revealed proliferation of RXLR genes in *Phytophthora* species and downy mildew pathogens, which together comprise a major pathogenic lineage within the oomycetes (Fig. 1, [168, 169]). Initial estimates of the size of the RXLR family in this lineage ranged from over 500 in *Phytophthora infestans* to approximately 130 in the *Arabidopsis* downy mildew pathogen *Hyaloperonospora arabidopsidis* (reviewed in [170]). However, evidence is accumulating to support the existence of RXLR variants [56, 58, 139, 171-173]. These observations suggest that the downy mildew and *Phytophthora* species might possess even larger complements of RXLR (or “RXLR-like”) effectors than initially predicted from conservative bioinformatic criteria.

In marked contrast to the *Phytophthora*/downy mildew lineage, other oomycete lineages appear to contain few or no RxLR genes. RXLR genes are absent from necrotrophs such as *Pythium* and the animal pathogens in the *Saprolegnia* genus [174-178]. The biotrophic white blister pathogens in the *Albugo* genus contain only a small number of putative RXLR genes, none of which have been functionally validated [179, 180]. Different classes of effectors are predominant in these lineages, including the CHXC class in *Albugo* and the broadly distributed Crinkler and YxSL[RK] superfamilies [170, 174, 175, 179, 180]. Thus, it appears that RXLR proteins are not important for

virulence in all pathogenic oomycetes; rather, they have undergone a dramatic expansion in the *Phytophthora*/downy mildew lineage. This proliferation has been postulated as a key innovation during evolution of biotrophy in the ancestor of *Phytophthora* and downy mildews (reviewed in [170, 181, 182]).

Gene-for-gene resistance in oomycetes is based largely on recognition of RXLR proteins

Gene-for-gene resistance (also termed effector-triggered immunity, or ETI) is a critically important component of plant innate immunity and an important tool for management of crop diseases, including those caused by *Albugo*, *Phytophthora* and downy mildew pathogens. A large sample of Avr genes have now been molecularly cloned (Table 1); almost every one of these genes encodes a protein with a canonical RXLR motif. The only exception, *H. arabidopsidis* Atr5, contains an EER motif which could be functionally equivalent to a canonical RXLR motif [171]. The near-ubiquity of the RXLR motif in oomycete Avr proteins is quite striking, and indeed provided the basis for its identification [148]. Despite the current controversy over the molecular function of the RXLR domain [163-167], the prevalence of RXLR in Avr proteins leaves no doubt that this motif is critically important.

Another generality for oomycete gene-for-gene resistance is that the corresponding *R* genes encode nucleotide-binding, leucine rich repeat (NLR) proteins (Table 1). Most of these proteins contain a coiled-coil domain at the N-terminus. How are these immune surveillance proteins activated by RXLR effectors? The activation of RPP1 by Atr1 from involves direct physical interaction with a high degree of allelic specificity [148, 183]. In a contrasting case, the R2 NLR protein appears to recognize a

complex comprised of the Avr2 RXLR protein and its putative target BSL2 [184]. Interestingly, a non-recognized form of Avr2 can bind to BSL2 but is not capable of engagement of with R2, suggesting that additional aspects of this interaction remain to be defined.

A couple of RXLR-NLR interactions exhibit interesting subcellular dynamics. The R1 and AvrR1 proteins localize to the nucleus and cytoplasm, and both proteins must be present in the nucleus to activate immunity [185]. This example follows others from bacterial and fungal effectors in which nuclear localization of the NLR is an important aspect of function. However, not all immune receptors operate within the nucleus. The NLR R3a resides in the nucleus and cytoplasm in its resting state, but is relocalized to endosomal vesicles in the presence of the recognized form of Avr3a, which exhibits the same relocalization [186]. This relocalization is necessary for activation of resistance and does not occur in the presence of a non-recognized form of Avr3a.

These examples presage the mechanistic complexity that likely underlies activation of ETI by RXLR proteins, and highlight the need for more experimental focus on this area that is understudied for oomycete effectors, compared to bacteria and fungi. The potential applied payoff lies in the prospect for engineering receptors with enhanced recognition [187]. Even with our relatively limited current understanding, promising initial steps towards this goal have been reported [188].

Oomycetes can defeat gene-for-gene resistance through a variety of mechanisms

Gene-for-gene resistance to oomycetes is often broken under field conditions [189], implying that RXLR genes are highly mutable. Moreover, RXLR genes have been

recently postulated as key factors in host range and non-host resistance [190-193]. Thus, there is substantial interest in the genomic mechanisms that underpin RXLR gene evolution.

To begin with, the proliferation of RXLR genes in *Phytophthora* and downy mildew genomes suggests potential for functional redundancy. This could allow pathogens to discard deleterious RXLR genes (i.e., Avr genes) without a substantial fitness penalty. Interestingly, RXLR genes are predominantly located in genomic regions that contain relatively few genes and a high frequency of transposons and other repetitive elements. Contrastingly, housekeeping genes are located in gene-dense, repeat-sparse regions [50, 190]. This bipartite organization suggests a “two-speed genome”, in which genes that support core functions reside in stable, slow-evolving regions of the genome, while effector genes are located in fast-evolving regions of the genome to facilitate co-evolution with the host (reviewed in [112]). Accordingly, genome-level comparisons of RXLR genes has provided evidence for diversifying selection, presence/absence polymorphisms and gene copy number variation, intra-genic recombination, and gene conversion (reviewed in [170] and recently exemplified by [192, 194, 195]).

These DNA-level changes can defeat gene-for-gene resistance by deleting the Avr gene or altering the structure of the encoded protein so that it is not perceived by the host surveillance system. The potential complexity of these dynamics was illustrated by a study of the *AvrBlb2* gene family in worldwide populations of *P. infestans* [196]. This survey identified four variants, one of which is not recognized by the R gene *Blb2* that is currently being deployed for control of potato late blight [197]. Interestingly,

pathogen populations maintained all four variants, likely because they are functionally diversified to provide differential fitness in different host environments.

Gene-for-gene resistance can also be defeated by expression-level polymorphisms in which the protein coding sequence is intact but the gene is not transcribed (e.g., [198, 199] and Table 1). In principle, this can be caused by DNA mutations that affect gene regulatory sequences. Moreover, recent studies suggest that variation in RXLR gene expression can be generated by epigenetic mechanisms (reviewed in [200, 201]). Silenced epialleles of Avr genes from *P. sojae* and *P. infestans* have now been documented (Table 1); the most striking study demonstrated heritable silencing of the *P. sojae* Avr3a gene [202]. The mechanisms responsible for establishment, propagation, and release of silencing remain to be defined, but likely involve small RNAs and/or histone methylation. Interestingly, the repeat- and effector-rich regions of the *P. infestans* genome are enriched for regulators of epigenetic processes [112]. The proximity of RXLR genes to transposable elements suggests a scenario in which epigenetic control of transposition might be co-opted to provide for global silencing of RXLR effector genes that could be reversed under conditions of environmental stress or jumps to a new host, to provide a much higher evolutionary potential than could be achieved via mutation alone [200, 201, 203].

Yet another strategy for defeating gene-for-gene resistance was suggested by analysis of the IPI-O effector, in which an allele for virulence interferes with detection of the avirulence allele by competitively binding the recognition domain on the cognate NB-LRR surveillance protein [204]. Altogether, these examples demonstrate that *Phytophthora* and downy mildew pathogens are truly artists of escape from gene-for-

gene resistance (Table 1). The varied mechanisms through which effector/avr genes are rendered non-functional will complicate strategies to detect resistance-breaking alleles in the field; it will be particularly challenging to develop facile assays for genes that are transcriptionally silenced.

Structure of RXLR effector proteins reveals core motifs and a structural foundation for adaptability

Previous mutational studies have demonstrated that the RXLR domain does not contribute to the virulence function (e.g., [150]). Rather, the virulence function is provided by the C-terminal "effector domain" [157]. Unfortunately, biochemical functions for C-terminal regions have proven difficult to predict from primary sequence because the majority of RXLR effectors share little or no similarity with previously characterized proteins. This mirrors the situation with bacterial effectors. For this reason, 3D structures of RXLR effector proteins have been eagerly anticipated in the hope of functional insights similar to those enabled by knowledge of the structure of bacterial effectors (e.g., [205]).

Several RXLR effector structures have now been solved by x-ray crystallography or NMR (reviewed in [206]). These structures do not contain the N-terminal RXLR domain, which is predicted to form a disordered structure. Rather, the structures were resolved from recombinant proteins in which the RXLR region was deleted. These structures highlight tertiary motifs in the C-terminal effector domain that mediate effector activity and recognition by host surveillance proteins. For example, the *H. arabidopsidis*

avirulence effector ATR1 consists of two, all helical domains with a unique, tandemly-duplicated 5-helicase motif [207]. ATR1 is recognized by the *Arabidopsis* NB-LRR protein RPP1 [148, 208]. Key residues involved in the recognition of ATR1 by two different RPP1 alleles were positioned on different surface-exposed regions. This suggests that different alleles of RPP1 can recognize distinct surface regions of ATR1. Similarly, solution of the ATR13 structure by NMR revealed two patches of surface-exposed polymorphism [209, 210]. Mutation experiments demonstrated that only one of these patches mediates recognition by the RPP13 resistance protein. No similarities to other proteins were found, but the structure did reveal a nucleolar localization signal that is an insertion/deletion polymorphism in the ATR13 sequence from different *H. arabidopsidis* isolates.

Structures have been solved for *Phytophthora capsici* Avr3a11, a homologue of *P. infestans* Avr3a and *P. sojae* Avr1b, and *Phytophthora infestans* PexRD2 [211]. These proteins share less than 20% primary sequence identity; thus it is surprising that 37 out of the 64 residues from the monomeric PexRD2 structure align with the Avr3a11 monomeric structure. Importantly, both proteins share a core α-helical fold called the WY domain, corresponding to motifs that had been previously identified in *Phytophthora* RXLR proteins based on primary sequence [44, 154]. Both structures reveal functionally important, polymorphic residues on the surface of the helix. Boutemy et al. predicted that this core fold is present in ~44% of *Phytophthora* RXLR effectors and ~26% of the *H. arabidopsidis* RXLR effectors. Many RXLR proteins contain repeats of the WY domain. Copy number variation in the WY domains has been documented for RXLR genes in *P. ramorum* [195]. Based on variability observed within WY-containing regions,

it is likely that the WY domain is an evolvable platform that can support polymorphism in surface residues, repeat copy number variation, insertions with and between repeats, and oligomerization. Interestingly, the WY domain appears to be restricted to the *Phytophthora*/downy mildew lineage [206], suggesting that this fold was a key innovation during evolution of RXLR effectors in this lineage.

Functional genomic studies suggest that a large proportion of RXLR proteins can suppress host immunity

The discovery of hundreds of potential RXLR proteins in *Phytophthora* genomes prompts the obvious questions of "What are their functions, and why so many?" Important first steps towards addressing these questions at genomic scale have been taken by high-throughput studies in which effectors were transiently expressed inside plant cells. For example, Wang et al. (2011) assayed 169 RXLR effectors from the soybean pathogen *Phytophthora sojae*, using *Agrobacterium*-mediated transient expression in *Nicotiana benthamiana*. These genes were tested for their ability to suppress cell death elicited by the mammalian cell death elicitor Bax, the oomycete elicitor INF1, or avirulence effectors from *P. sojae*. The majority of *P. sojae* RXLR effectors could suppress immune responses in this system, suggesting that a major function of the RXLR secretome is to sabotage plant immunity.

Another insight from the Wang et al. study is that the timing of RXLR gene expression could play an important role in oomycete virulence. Transcript profiling of *P. sojae* effector genes provided evidence for coordination, in which effectors expressed

early in infection predominantly suppress ETI, while effectors expressed later in infection suppress PTI [212]. This implies complex transcriptional programming to maximize virulence potential. Expression profiling in combination with analysis of allelic diversity suggests that a small number of highly expressed, polymorphic effectors may make the largest contributions to *P. sojae* virulence while other, less abundantly expressed effectors may be dispensable. Additionally, the avirulence activities of some RXLR effectors can be suppressed by other RXLR effectors [212]. This points to a strategy in which early-expressed effectors could act as “bodyguards” to conceal essential effectors that possess avirulence activity but are indispensable for virulence.

Similar to the Wang et al. study, Fabro and colleagues’ functional analysis of RXLR genes from *Hyaloperonospora arabidopsidis* revealed substantial capacity to suppress plant immunity [91]. Because *Agrobacterium*-mediated transient assays do not work efficiently in *Arabidopsis* [213], this study exploited *Pseudomonas syringae* as a surrogate pathogen to deliver RXLR proteins to *Arabidopsis* [91]. The screening system was based on an “effector detector vector” in which RXLR genes are fused to an N-terminal leader that guides the effector through the type III secretion system [151]. The screen also used strains of *Pseudomonas* constitutively expressing a luciferase reporter gene (*Pst*-LUX) for facile quantification of bacterial growth *in planta*. This system was used to test 64 predicted *H. arabidopsidis* RXLR effector genes, by assaying for enhancement or reduction of growth in 12 different *Arabidopsis* accessions (ecotypes). 70% of the tested effectors enhanced *Pst*-LUX growth on multiple *Arabidopsis* ecotypes. This effect is likely attributable to the suppression of PTI, because the majority of effectors that increased bacterial growth also suppressed the accumulation

of callose. Notably, few of the effectors were able to enhance *Pst*-LUX growth in all 12 screened *Arabidopsis* ecotypes, suggesting that their host targets may have diverged among *Arabidopsis* accessions. Expression of a subset of the *H. arabidopsidis* RXLR effectors in stably transformed plants recapitulated the results obtained via the *Pst*-LUX system. Only 22% of tested effectors could suppress PTI in turnip, a close relative of *Arabidopsis* but a non-host for *H. arabidopsidis*, further suggesting that most of the effectors are optimized for their host targets.

Other screening methods have been employed to yield additional interesting results. Perhaps the simplest was to screen bioinformatically for “core” RXLR genes that are conserved between downy mildew pathogens and *Phytophthora* species. Only a handful were found [137]. Comparative functional analysis of one pair of homologous effectors from *H. arabidopsidis* and *P. sojae* revealed that both effectors can suppress ETI and/or PTI in soybean, *N. benthamiana*, and *Arabidopsis* [86]. It will be of interest to determine whether conserved effectors target homologous proteins in these divergent hosts.

Transgenic plants overexpressing effector genes have been critically important for understanding the functions of bacterial effectors [214]. This approach was used to delineate virulence contributions of *H. arabidopsidis* RXLR genes [215]. A creative alternative was devised by Badel et al., in which mixed pools of bacteria with different *H. arabidopsidis* RXLR effectors were inoculated into *Arabidopsis* leaves, and the relative success of each strain was measured three days later by high throughput sequencing or capillary electrophoresis. This “effector competition assay” provided an estimate of the contribution of each effector to virulence [216]. Data from both of these studies support

the concept that RXLR effectors make quantitative contributions by acting at multiple levels in the immune network.

Additional creative approaches were used in medium-throughput screens for effectors that target specific plant pathways. One screen was for RXLR proteins that suppress responses to the bacterial PAMP flg22 [217]. In this system, *P. infestans* RXLR effector genes were transiently transfected into tomato protoplasts containing a flg22-responsive promoter fused to the luciferase reporter. This screen revealed RXLR effectors that suppress PTI at different steps in the signaling hierarchy. Interestingly, several effectors suppressed PTI in both tomato and *Arabidopsis* [217]. A similar screen utilized stably transformed plants overexpressing RXLR genes to screen specifically for effectors that interfere with SA-responsive gene induction. Nine RXLR genes from *H. arabidopsidis* were screened for suppression of SA-inducible *PR-1* transcription and one (HaRxL62) demonstrated this capacity [139].

Another important question concerns the subcellular localization of effectors *in planta*. [218] examined subcellular localization of 49 *H. arabidopsidis* RXLR-GFP fusions, expressed from stably transformed *Arabidopsis*. The majority of effectors targeted either the nucleus or host membranes. Some cellular components were not targeted, including the mitochondria or chloroplast, and little correlation was found between predicted subcellular localization and observed localization. Allelic polymorphisms in localization were identified for several effectors. Importantly, relocalization during *H. arabidopsidis* infections of stably transformed GFP-effector fusions was also observed. For example, HaRxL17 displays a unique subcellular address at the host tonoplast and is the first oomycete effector known to associate with

this compartment (Figure 2). During *H. arabidopsidis* infection, GFP-HaRxL17 fusions re-localized to the haustoria. This study highlights the utility of live cell imaging of infected tissue for understanding RXLR effector function.

Interactome studies reveal protein complexes convergently targeted by oomycetes, fungi, and bacteria

High-throughput strategies have also been used to identify candidate protein targets of RXLR effectors. A landmark report described a large-scale yeast two-hybrid screen for targets of 99 RXLR effector proteins from *H. arabidopsidis* and 53 Type III effectors from *Pseudomonas syringae* [219]. These effectors were screened against a library comprising three classes of *Arabidopsis* immune proteins: N-terminal regions from NB-LRR surveillance proteins, cytoplasmic domains from LRR-receptor line kinases, and known defense proteins. Additionally, the effectors were screened against ~8000 *Arabidopsis* proteins that comprised version 1 of the *Arabidopsis* interactome described in a companion study (AI-1, [220]). Finally, the immune proteins were tested for interaction with each other and with the AI-1 set.

The interactions from this screen were combined with literature-curated interactions to generate a network that predicts interaction of 165 plant proteins with 53 RXLR effectors and 30 Type III effectors [219]. This network supports a key prediction of the guard model, which states that independently evolved plant pathogens will have common defense-related host targets: 18 plant proteins interacted with effectors from

both pathogens; loss of function mutants in 15/17 of these displayed altered immunity, suggesting that they are *bona fide* target proteins.

A subsequent publication extended the evidence for convergent targeting to the fungal, obligate biotrophic fungal pathogen *Golovinomyces orontii* [221]. 63 effector proteins were screened against 12,000 *Arabidopsis* proteins. These data were integrated with the interactions documented by Mukhtar et al. to provide the first plant-pathogen interactome (PPIN-2) encompassing bacterial, fungal, and oomycete pathogens. Nine *Arabidopsis* proteins interacted with effectors from all three pathogens, and another 23 interacted with effectors from two pathogens. Loss-of-function mutants in 123 candidate target genes were tested with all three pathogens, including 3 different isolates of *H. arabidopsidis*. Interestingly, the three *H. arabidopsidis* isolates interacted differentially with a number of mutants, including opposite phenotypes for several (i.e., enhanced disease resistance vs. enhanced disease susceptibility). This suggests intra-specific polymorphism in the effectors and their targets.

The results of the interaction survey, combined with simulation studies, suggest general properties of effectors. Effectors from all three pathogens collectively converge onto a set of proteins that likely comprise points of vulnerability in the immune network. Effectors preferentially target highly connected proteins, perturbation of which is more likely to destabilize the associated network. Finally, a substantial proportion of effector targets also interact with NB-LRR proteins, suggestive of guarding. Some targets interact with many effectors, suggesting that they are under massive attack (e.g., the AtTCP14 protein interacts with 29 effectors), and some effectors interact with several plant proteins, suggesting that these saboteurs have multiple targets. This dataset

represents a treasure trove for future studies and presages the complexity of host cell manipulation by RXLR proteins. This complexity is further underscored by mechanistic analysis of RXLR proteins that are summarized in the following section.

RXLR effectors target a diverse array of pathways within the host cell

As mentioned above, very few oomycete effector sequences possess recognizable motifs or domains. One exception is *P. sojae* Avr3b, which contains a Nudix motif with ADP-ribose/NADH pyrophosphorylase activity [222]. Avr3b is essential for full *P. sojae* virulence in susceptible soybean. When expressed as a transgene, Avr3b enhances host susceptibility to two other oomycete pathogens. Mutations in the Avr3b Nudix motif established the importance of ADP-ribose/NADH pyrophosphorylase activity and suggested a link to suppression of reactive oxygen species (ROS, Figure 2). However, ADP-ribose/NADH pyrophosphorylase activity is not necessary for recognition by the cognate R protein. The exact link between immune suppression and the Nudix motif remains to be elucidated, but might involve reduction of NADH levels and/or recycling nucleosides from ADP-ribose, consequently reducing the accumulation of ROS.

Another RXLR effector with a recognizable functional motif is IPI-O from *P. infestans*. The motif, RGD, is associated with integrins, a class of membrane spanning receptors that mediate cell adhesion. RGD motifs are also found in proteins that bind to and antagonize integrins, and RGD peptides are known to disrupt adhesions between the plasma membranes and walls of plant cells. Accordingly, IPI-O was shown to disrupt

these adhesions, in part by targeting the *Arabidopsis* lectin receptor kinase LecRK-I.9 [155, 223]. Genetic experiments revealed the importance of LecRK-1.9 for resistance of *Arabidopsis* to *Phytophthora brassicae* [223]. These studies underscore the importance of the plasma membrane-cell wall continuum in immunity, and reinforce the notion that the pathogen-plant plasma membrane interface is an active battleground. Interestingly, LecRK-I.9 was recently demonstrated to be the receptor for extracellular ATP [224], and it will be interesting to follow up on this connection in the context of plant-oomycete interactions.

Avrblb2 from *P. infestans* is a second effector that operates spatially at the plant-pathogen interface. Live cell imaging was used to demonstrate that Avrblb2 relocalizes from the plant plasma membrane in uninfected plant cells to the haustorial interface in infected cells [225] (Figure 2). A proteomic screen for Avrblb2 host targets revealed the secreted papain-like cysteine protease C14, which is present in diverse plant species. The relevance of this interaction was verified by experiments demonstrating that Avrblb2 interferes with secretion of C14 to the apoplast. How Avrblb2 specifically inhibits C14 secretion remains to be described. Interestingly, C14 is also targeted by two unrelated non-RXLR apoplastic oomycete effectors [226] suggesting that the C14 is an important target for *P. infestans*.

A different mode of spatial interference was recently revealed for the *P. infestans* effector Pi03192 [227]. This effector interacts with two NAC transcription factors that positively regulate immune responses to *P. infestans* culture filtrate and are genetically necessary for basal resistance to *P. infestans* in *N. benthamiana*. Both proteins relocalize from the ER to the nucleus following treatment with culture filtrate.

Importantly, Pi03192 interferes with this relocalization; the mechanism is yet to be determined.

The *P. infestans* RXLR effector Avr3a alters the localization and proteasome-mediated turnover of the plant immune regulator, CMPG1 [156]. This link to the proteasome mirrors bacterial effectors that manipulate the stability of their targets. A recent study linked CMPG1 with perception of pathogen signals at the plasma membrane; resistance mediated by cytoplasmic NB-LRR proteins does not require CMPG1 [228]. A structure/function study of Avr3a identified a positively charged patch of amino acids in the C-terminal domain that mediates binding to phosphatidylinositol monophosphates (PIPs), in particular, phosphatidylinositol 3-phosphate (PI3P) [229]. The ability of Avr3a to bind PIPs is not necessary for recognition by the cognate resistance protein R3a, but is necessary for Avr3a virulence functions, including suppression of immune responses and stabilization of CMPG1. The mechanistic link between PIP binding and virulence functions remains unresolved. The most likely scenario is that Avr3a interacts with PIPs to target vesicular CMPG1 and to relocalize CMPG1 to the nucleus, thereby altering signaling cascades that originate at the plasma membrane (Figure 2).

MAP kinase pathways are important components of the immune network and are extensively targeted by bacterial pathogens [230]. A two-hybrid screen revealed that *P. infestans* PexRD2 (see above) directly interacts with MAPKKK epsilon. This study elegantly leveraged the PexRD2 structure to identify key residues mediating the interaction. Interestingly, PexRD2 related-proteins do not target MAPKKK epsilon, thus providing a case study of how effector target specificity can evolve. It will be of great

interest to better understand the mechanistic consequences of this interaction: which pathways are altered and does the alteration result from direct manipulation of the putative target? As the authors note, it is conceivable that MAPKKK epsilon could phosphorylate PexRD2 and thereby act as the effector's "accomplice", rather than its target *per se* (see [231] for discussion of this concept).

Qiao and colleagues searched for RXLR effectors that suppress host RNA silencing [232]. This screen identified two such effectors, PSR1 and PSR2, and set the stage for a better understanding of how RNA silencing mediates immunity to oomycetes [233]. Interestingly, these effectors are conserved in the *Phytophthora* genus and can suppress RNA silencing in two distantly related species [234]. A target of PSR1, called PINP1, was recently identified as a aspartate-glutamate-alanine-histidine-box RNA helicase domain protein [235]. This protein is likely involved in regulation of small RNA accumulation as a component of the Dicer complex, and is necessary for plant development and regulation of immunity. Importantly, this protein had not been previously associated with RNAi.

Another possible example of RXLR-mediated interference with host post-transcriptional regulation was provided by *P. infestans* RXLR effector Pi04089. This protein interacts with a putative RNA binding protein from potato (StKRBP1) that contains a K-homology domain [236]. The molecular function of StKRBP1 remains to be determined, but it was clearly validated as an important factor contributing to successful infection by *P. infestans*. As with PNP1, the function of StKRBP1 had not been investigated prior to its identification as a pathogen-targeted protein; thus, the examples of PNP1 and StKRBP1 underscore how effectors can lead to important but

understudied host regulatory proteins and pathways [231]. This is a major rationale to continue with mechanistic studies of RXLR proteins in diverse pathosystems.

Hormone signaling pathways are a major target of RXLR effectors

Multiple lines of evidence have indicated that manipulation of plant hormone signaling is a major strategy of oomycete pathogens, including genetic experiments, transcriptome profiles, and overrepresentation of hormone-associated proteins in PPIN. Now, several effectors have been linked with hormone responses. Two of these, HaRxL62 and HaRxL44 from *H. arabidopsidis*, manipulate host responsiveness to the hormone salicylic acid (SA), which is a key positive regulator of immunity. HaRxL62 was identified in the screen for suppression of SA-responsive gene described above [139]; its target remains to be identified. In the case of HaRxL44, a target was identified in PPIN-1 and a sophisticated mechanism has been revealed: This effector targets a specific subunit of the Mediator transcription complex. The MED19a protein is engaged by HaRxL44 and this results in proteasome-dependent degradation. Importantly, loss of MED19a activates jasmonic acid (JA)-responsive gene expression that, in turn, suppresses SA-responsive gene expression. Thus, it appears that *H. arabidopsidis* can exploit JA-SA antagonism in a manner similar to but distinct from *P. syringae*, which activates the JA signaling sector with the JA mimic coronatine and two different Type III effectors [237-239].

RXLR proteins have also been linked to brassinosteroid (BR) and auxin responses. The tentative link to BR occurs via the aforementioned *P. infestans* Avr2

protein, which interacts with BLS2 proteins from solanaceous species [184]. BLS2 proteins are related to the *Arabidopsis* BR response regulator BSU1. The Avr2-BLS2 interaction is important for recognition mediated by the R2 immune surveillance protein [184], but its significance for *P. infestans* virulence has not been established. A link to auxin responses was provided by analysis of Penetration-Specific Effector 1 (PSE1) from *Phytophthora parasitica* [240]. Like many effectors, PSE1 suppresses immune responses and enhances susceptibility. However, this effector also causes auxin-related phenotypes when overexpressed in *Arabidopsis* and reduces auxin concentrations in roots infected by *P. parasitica*. Notably, auxin efflux proteins were mislocalized in PSE1-overexpressing plants, suggesting that the effector perturbs auxin responses by interfering with transport. In this way, there is commonality between oomycete, bacterial [241], and nematode effectors [242] in terms of auxin perturbation.

Conclusions

We hope to have conveyed that exciting advances in understanding of RXLR effector biology have been reported in recent years. Challenging but important questions will provide foci in the longer term: What is the complete set of operative targets of RXLR effectors in a host plant, and how does the composition of this set vary between pathosystems? Do RXLR effectors perform sophisticated molecular functions that mimic plant proteins, or might some simply bind to plant protein complexes and thereby disrupt function? How are RXLR effector gene expression and protein secretion regulated, and how does this impact virulence? How many RXLR effectors are essential for virulence by stringent genetic criteria, and how does the set of essential effectors

vary amongst pathogens? Do RXLR effectors cooperate with each other or other types of effectors, and if so, is it possible to identify emergent properties resulting from effector cooperation? Can we develop a systems-level understanding of effector manipulations of the host [243]. Answers to each of these questions will inform the ultimate goal of oomycete research, which is to develop new tools to support durable, low-input control of oomycete diseases.

ACKNOWLEDGEMENTS

We thank Boris Vinatzer and Sheng Yang He for comments on the manuscript. Support was provided by the NSF (IOS-0744875 and IOS-1353366) and the USDA-NIFA (2009-03008 and 2011-68004).

Appendix A: References

1. Hogenhout, S.A., et al., *Emerging concepts in effector biology of plant-associated organisms.* Mol Plant Microbe Interact, 2009. **22**(2): p. 115-22.
2. Rehmany, A.P., et al., *Differential recognition of highly divergent downy mildew avirulence gene alleles by RPP1 resistance genes from two Arabidopsis lines.* Plant Cell, 2005. **17**(6): p. 1839-50.
3. Whisson, S.C., et al., *A translocation signal for delivery of oomycete effector proteins into host plant cells.* Nature, 2007. **450**(7166): p. 115-8.
4. Dou, D., et al., *RXLR-mediated entry of Phytophthora sojae effector Avr1b into soybean cells does not require pathogen-encoded machinery.* Plant Cell, 2008. **20**(7): p. 1930-47.
5. Tyler, B.M., et al., *Phytophthora genome sequences uncover evolutionary origins and mechanisms of pathogenesis.* Science, 2006. **313**(5791): p. 1261-6.
6. Haas, B.J., et al., *Genome sequence and analysis of the Irish potato famine pathogen Phytophthora infestans.* Nature, 2009. **461**(7262): p. 393-8.
7. Bos, J.I.B., et al., *The C-terminal half of Phytophthora infestans RXLR effector AVR3a is sufficient to trigger R3a-mediated hypersensitivity and suppress INF1-induced cell death in Nicotiana benthamiana.* Plant Journal, 2006. **48**(2): p. 165-176.
8. Sohn, K.H., et al., *The downy mildew effector proteins ATR1 and ATR13 promote disease susceptibility in Arabidopsis thaliana.* Plant Cell, 2007. **19**(12): p. 4077-90.
9. Oh, S.K., et al., *In planta expression screens of Phytophthora infestans RXLR effectors reveal diverse phenotypes, including activation of the Solanum bulbocastanum disease resistance protein Rpi-blb2.* Plant Cell, 2009. **21**(9): p. 2928-47.
10. Kelley, B.S., et al., *A secreted effector protein (SNE1) from Phytophthora infestans is a broadly acting suppressor of programmed cell death.* Plant J, 2010. **62**(3): p. 357-66.
11. Dou, D., et al., *Conserved C-terminal motifs required for avirulence and suppression of cell death by Phytophthora sojae effector Avr1b.* Plant Cell, 2008. **20**(4): p. 1118-33.
12. Senchou, V., et al., *High affinity recognition of a Phytophthora protein by Arabidopsis via an RGD motif.* Cellular and Molecular Life Sciences, 2004. **61**(4): p. 502-509.
13. Bos, J.I., et al., *Phytophthora infestans effector AVR3a is essential for virulence and manipulates plant immunity by stabilizing host E3 ligase CMPG1.* Proc Natl Acad Sci U S A, 2010. **107**(21): p. 9909-14.
14. Kale, S.D., et al., *External lipid PI3P mediates entry of eukaryotic pathogen effectors into plant and animal host cells.* Cell, 2010. **142**(2): p. 284-95.
15. Schornack, S., et al., *Ten things to know about oomycete effectors.* Mol Plant Pathol, 2009. **10**(6): p. 795-803.
16. Birch, P.R., et al., *Towards understanding the virulence functions of RXLR effectors of the oomycete plant pathogen Phytophthora infestans.* J Exp Bot, 2009. **60**(4): p. 1133-40.

17. Stassen, J.H. and G. Van den Ackerveken, *How do oomycete effectors interfere with plant life?* Curr Opin Plant Biol, 2011. **14**(4): p. 407-14.
18. de Jonge, R., M.D. Bolton, and B.P.H.J. Thomma, *How filamentous pathogens co-opt plants: the ins and outs of fungal effectors.* Current Opinion in Plant Biology, 2011. **14**(4): p. 400-406.
19. Koeck, M., A.R. Hardham, and P.N. Dodds, *The role of effectors of biotrophic and hemibiotrophic fungi in infection.* Cell Microbiol, 2011. **13**: p. 1849–1857.
20. Kale, S.D. and B.M. Tyler, *Entry of oomycete and fungal effectors into plant and animal host cells.* Cell Microbiol, 2011. **13**(12): p. 1839-48.
21. Wawra, S., et al., *Secretion, delivery and function of oomycete effector proteins.* Curr Opin Microbiol, 2012. **15**(6): p. 685-91.
22. Pais, M., et al., *From pathogen genomes to host plant processes: the power of plant parasitic oomycetes.* Genome Biol, 2013. **14**(6): p. 211.
23. Petre, B. and S. Kamoun, *How do filamentous pathogens deliver effector proteins into plant cells?* PLoS Biol, 2014. **12**(2): p. e1001801.
24. Wawra, S., et al., *In vitro translocation experiments with RxLR-reporter fusion proteins of Avr1b from Phytophthora sojae and AVR3a from Phytophthora infestans fail to demonstrate specific autonomous uptake in plant and animal cells.* Mol Plant Microbe Interact, 2013. **26**(5): p. 528-36.
25. Tyler, B.M., et al., *Microbe-independent entry of oomycete RxLR effectors and fungal RxLR-like effectors into plant and animal cells is specific and reproducible.* Mol Plant Microbe Interact, 2013. **26**(6): p. 611-6.
26. Vleeshouwers, V.G. and R.P. Oliver, *Effectors as tools in disease resistance breeding against biotrophic, hemibiotrophic, and necrotrophic plant pathogens.* Mol Plant Microbe Interact, 2014. **27**(3): p. 196-206.
27. Du, J. and V.G. Vleeshouwers, *The do's and don'ts of effectoromics.* Methods Mol Biol, 2014. **1127**: p. 257-68.
28. Jiang, R.H., et al., *RXLR effector reservoir in two Phytophthora species is dominated by a single rapidly evolving superfamily with more than 700 members.* Proc Natl Acad Sci U S A, 2008. **105**(12): p. 4874-9.
29. Thines, M., *Phylogeny and evolution of plant pathogenic oomycetes,Äîa global overview.* European Journal of Plant Pathology, 2014: p. 1-17.
30. Thines, M. and S. Kamoun, *Oomycete-plant coevolution: recent advances and future prospects.* Curr Opin Plant Biol, 2010. **13**: p. 427-433.
31. Jiang, R.H. and B.M. Tyler, *Mechanisms and evolution of virulence in oomycetes.* Annu Rev Phytopathol, 2012. **50**: p. 295-318.
32. Bailey, K., et al., *Molecular cloning of ATR5(Emoy2) from Hyaloperonospora arabidopsidis, an avirulence determinant that triggers RPP5-mediated defense in Arabidopsis.* Mol Plant Microbe Interact, 2011. **24**(7): p. 827-38.
33. Tian, M., et al., *454 Genome sequencing of Pseudoperonospora cubensis reveals effector proteins with a QXLR translocation motif.* Mol Plant Microbe Interact, 2011. **24**(5): p. 543-53.
34. Stassen, J.H., et al., *Specific in planta recognition of two GKLR proteins of the downy mildew Bremia lactucae revealed in a large effector screen in lettuce.* Mol Plant Microbe Interact, 2013. **26**(11): p. 1259-70.

35. Asai, S., et al., *Expression profiling during arabidopsis/downy mildew interaction reveals a highly-expressed effector that attenuates responses to salicylic acid.* PLoS Pathog, 2014. **10**(10): p. e1004443.
36. Adhikari, B.N., et al., *Comparative genomics reveals insight into virulence strategies of plant pathogenic oomycetes.* PLoS One, 2013. **8**(10): p. e75072.
37. Levesque, C.A., et al., *Genome sequence of the necrotrophic plant pathogen Pythium ultimum reveals original pathogenicity mechanisms and effector repertoire.* Genome Biol, 2010. **11**(7): p. R73.
38. Krajaejun, T., et al., *Transcriptome analysis reveals pathogenicity and evolutionary history of the pathogenic oomycete Pythium insidiosum.* Fungal Biol, 2014. **118**(7): p. 640-53.
39. Krajaejun, T., et al., *Expressed sequence tags reveal genetic diversity and putative virulence factors of the pathogenic oomycete Pythium insidiosum.* Fungal Biol, 2011. **115**(7): p. 683-96.
40. Jiang, R.H., et al., *Distinctive expansion of potential virulence genes in the genome of the oomycete fish pathogen Saprolegnia parasitica.* PLoS Genet, 2013. **9**(6): p. e1003272.
41. Kemen, E., et al., *Gene Gain and Loss during Evolution of Obligate Parasitism in the White Rust Pathogen of <italic>Arabidopsis thaliana</italic>.* PLoS Biol, 2011. **9**(7): p. e1001094.
42. Links, M., et al., *De novo sequence assembly of Albugo candida reveals a small genome relative to other biotrophic oomycetes.* BMC Genomics, 2011. **12**(1): p. 503.
43. Kemen, E. and J.D. Jones, *Obligate biotroph parasitism: can we link genomes to lifestyles?* Trends Plant Sci, 2012. **17**(8): p. 448-57.
44. McDowell, J.M., *Genomes of obligate plant pathogens reveal adaptations for obligate parasitism.* Proc Natl Acad Sci U S A, 2011. **108**(22): p. 8921-2.
45. Steinbrenner, A.D., S. Goritschnig, and B.J. Staskawicz, *Recognition and activation domains contribute to allele-specific responses of an Arabidopsis NLR receptor to an oomycete effector protein.* PLoS Pathog, 2015. **11**(2): p. e1004665.
46. Saunders, D.G., et al., *Host protein BSL1 associates with Phytophthora infestans RXLR effector AVR2 and the Solanum demissum Immune receptor R2 to mediate disease resistance.* Plant Cell, 2012. **24**(8): p. 3420-34.
47. Du, Y., et al., *Immune activation mediated by the late blight resistance protein R1 requires nuclear localization of R1 and the effector AVR1.* New Phytol, 2015.
48. Engelhardt, S., et al., *Relocalization of Late Blight Resistance Protein R3a to Endosomal Compartments Is Associated with Effector Recognition and Required for the Immune Response.* The Plant Cell, 2012. **24**(12): p. 5142-5158.
49. Dangl, J.L., D.M. Horvath, and B.J. Staskawicz, *Pivoting the plant immune system from dissection to deployment.* Science, 2013. **341**(6147): p. 746-51.
50. Segretin, M.E., et al., *Single amino acid mutations in the potato immune receptor R3a expand response to Phytophthora effectors.* Mol Plant Microbe Interact, 2014. **27**(7): p. 624-37.
51. Fry, W., *Phytophthora infestans: the plant (and R gene) destroyer.* Molecular Plant Pathology, 2008. **9**(3): p. 385-402.

52. Raffaele, S., et al., *Genome evolution following host jumps in the Irish potato famine pathogen lineage.* Science, 2010. **330**(6010): p. 1540-3.
53. Lee, H.A., et al., *Multiple recognition of RXLR effectors is associated with nonhost resistance of pepper against Phytophthora infestans.* New Phytol, 2014. **203**(3): p. 926-38.
54. Cooke, D.E., et al., *Genome analyses of an aggressive and invasive lineage of the irish potato famine pathogen.* PLoS Pathog, 2012. **8**(10): p. e1002940.
55. Vega-Arreguin, J.C., et al., *Recognition of an Avr3a homologue plays a major role in mediating nonhost resistance to Phytophthora capsici in Nicotiana species.* Mol Plant Microbe Interact, 2014. **27**(8): p. 770-80.
56. Raffaele, S. and S. Kamoun, *Genome evolution in filamentous plant pathogens: why bigger can be better.* Nat Rev Microbiol, 2012. **10**(6): p. 417-30.
57. Na, R., et al., *Genome re-sequencing and functional analysis places the Phytophthora sojae avirulence genes Avr1c and Avr1a in a tandem repeat at a single locus.* PLoS One, 2014. **9**(2): p. e89738.
58. Goss, E.M., C.M. Press, and N.J. Grunwald, *Evolution of RXLR-class effectors in the oomycete plant pathogen Phytophthora ramorum.* PLoS One, 2013. **8**(11): p. e79347.
59. Oliva, R.F., et al., *A recent expansion of the RXLR effector gene Avrblb2 is maintained in global populations of Phytophthora infestans indicating different contributions to virulence.* Mol Plant Microbe Interact, 2015.
60. Vleeshouwers, V.G., et al., *Understanding and exploiting late blight resistance in the age of effectors.* Annu Rev Phytopathol, 2011. **49**: p. 507-31.
61. Cui, L., et al., *Analysis of polymorphism and transcription of the effector gene Avr1b in Phytophthora sojae isolates from China virulent to Rps1b.* Molecular Plant Pathology, 2012. **13**(2): p. 114-122.
62. Gilroy, E.M., et al., *Presence/absence, differential expression and sequence polymorphisms between PiAVR2 and PiAVR2-like in Phytophthora infestans determine virulence on R2 plants.* New Phytol, 2011. **191**(3): p. 763-76.
63. Kasuga, T. and M. Gijzen, *Epigenetics and the evolution of virulence.* Trends Microbiol, 2013. **21**(11): p. 575-82.
64. Gijzen, M., C. Ishmael, and S.D. Shrestha, *Epigenetic control of effectors in plant pathogens.* Frontiers in Plant Science, 2014. **5**.
65. Qutob, D., B.P. Chapman, and M. Gijzen, *Transgenerational gene silencing causes gain of virulence in a plant pathogen.* Nat Commun, 2013. **4**: p. 1349.
66. Whisson, S., et al., *Can silencing of transposons contribute to variation in effector gene expression in Phytophthora infestans?* Mob Genet Elements, 2012. **2**(2): p. 110-114.
67. Chen, Y., Z. Liu, and D.A. Halterman, *Molecular determinants of resistance activation and suppression by Phytophthora infestans effector IPI-O.* PLoS Pathog, 2012. **8**(3): p. e1002595.
68. Janjusevic, R., et al., *A bacterial inhibitor of host programmed cell death defenses is an E3 ubiquitin ligase.* Science, 2006. **311**(5758): p. 222-6.
69. Win, J., et al., *Sequence divergent RXLR effectors share a structural fold conserved across plant pathogenic oomycete species.* PLoS Pathogens, 2012. **IN PRESS**.

70. Chou, S., et al., *Hyaloperonospora arabidopsidis ATR1 effector is a repeat protein with distributed recognition surfaces.* Proc Natl Acad Sci U S A, 2011. **108**(32): p. 13323-8.
71. Krasileva, K.V., D. Dahlbeck, and B.J. Staskawicz, *Activation of an Arabidopsis Resistance Protein Is Specified by the in Planta Association of Its Leucine-Rich Repeat Domain with the Cognate Oomycete Effector.* The Plant Cell Online, 2010. **22**(7): p. 2444-2458.
72. Allen, R.L., et al., *Host-parasite coevolutionary conflict between Arabidopsis and downy mildew.* Science, 2004. **306**(5703): p. 1957-1960.
73. Leonelli, L., et al., *Structural Elucidation and Functional Characterization of the Hyaloperonospora arabidopsidis Effector Protein ATR13.* PLoS Pathogens, 2011. **In press**.
74. Boutemy, L.S., et al., *Structures of Phytophthora RXLR effector proteins: a conserved but adaptable fold underpins functional diversity.* Journal of Biological Chemistry, 2011. **286**: p. 35834-35842.
75. Wang, Y.C., et al., *Transcriptional Programming and Functional Interactions within the Phytophthora sojae RXLR Effector Repertoire.* Plant Cell, 2011. **23**: p. 2064-2086.
76. Fabro, G., et al., *Multiple candidate effectors from the oomycete pathogen Hyaloperonospora arabidopsidis suppress host plant immunity.* PLoS Pathog, 2011. **7**(11): p. e1002348.
77. Wroblewski, T., A. Tomczak, and R. Michelmore, *Optimization of Agrobacterium-mediated transient assays of gene expression in lettuce, tomato and Arabidopsis.* Plant Biotechnology Journal, 2005. **3**(2): p. 259-273.
78. Baxter, L., et al., *Signatures of adaptation to obligate biotrophy in the Hyaloperonospora arabidopsidis genome.* Science, 2010. **330**(6010): p. 1549-51.
79. Anderson, R.G., et al., *Homologous RXLR effectors from Hyaloperonospora arabidopsidis and Phytophthora sojae suppress immunity in distantly related plants.* Plant J, 2012. **72**(6): p. 882-93.
80. Munkvold, K.R. and G.B. Martin, *Advances in experimental methods for the elucidation of Pseudomonas syringae effector function with a focus on AvrPtoB.* Mol Plant Pathol, 2009. **10**(6): p. 777-93.
81. Pel, M.J., et al., *Functional Analysis of Hyaloperonospora arabidopsidis RXLR Effectors.* PLoS One, 2014. **9**(11): p. e110624.
82. Badel, J.L., et al., *In planta effector competition assays detect Hyaloperonospora arabidopsidis effectors that contribute to virulence and localize to different plant subcellular compartments.* Mol Plant Microbe Interact, 2013. **26**(7): p. 745-57.
83. Zheng, X., et al., *Functionally redundant RXLR effectors from Phytophthora infestans act at different steps to suppress early flg22-triggered immunity.* PLoS Pathog, 2014. **10**(4): p. e1004057.
84. Caillaud, M.-C., et al., *Subcellular Localization of the Hpa RxLR Effector Repertoire Identifies the Extrahaustorial Membrane-Localized HaRxL17 that Confers Enhanced Plant Susceptibility.* The Plant Journal, 2011.
85. Mukhtar, M.S., et al., *Independently evolved virulence effectors converge onto hubs in a plant immune system network.* Science, 2011. **333**(6042): p. 596-601.

86. Arabidopsis Interactome Mapping, C., *Evidence for Network Evolution in an Arabidopsis Interactome Map.* Science, 2011. **333**(6042): p. 601-607.
87. Wessling, R., et al., *Convergent targeting of a common host protein-network by pathogen effectors from three kingdoms of life.* Cell Host Microbe, 2014. **16**(3): p. 364-75.
88. Dong, S., et al., *Phytophthora sojae Avirulence Effector Avr3b is a Secreted NADH and ADP-ribose Pyrophosphorylase that Modulates Plant Immunity.* PLoS Pathog, 2011. **7**(11): p. e1002353.
89. Bouwmeester, K., et al., *The Lectin Receptor Kinase LecRK-I.9 Is a Novel Phytophthora Resistance Component and a Potential Host Target for a RXLR Effector.* PLoS Pathogens, 2011. **7**(3): p. e1001327.
90. Choi, J., et al., *Identification of a plant receptor for extracellular ATP.* Science, 2014. **343**(6168): p. 290-4.
91. Bozkurt, T.O., et al., *Phytophthora infestans effector AVRblb2 prevents secretion of a plant immune protease at the haustorial interface.* Proceedings of the National Academy of Sciences, 2011.
92. Kaschani, F., et al., *An Effector-Targeted Protease Contributes to Defense against Phytophthora infestans and Is under Diversifying Selection in Natural Hosts.* Plant Physiology, 2010. **154**(4): p. 1794-1804.
93. McLellan, H., et al., *An RxLR effector from Phytophthora infestans prevents re-localisation of two plant NAC transcription factors from the endoplasmic reticulum to the nucleus.* PLoS Pathog, 2013. **9**(10): p. e1003670.
94. Gilroy, E.M., et al., *CMPG1-dependent cell death follows perception of diverse pathogen elicitors at the host plasma membrane and is suppressed by Phytophthora infestans RXLR effector AVR3a.* New Phytol, 2011. **190**(3): p. 653-66.
95. Yaeno, T., et al., *Phosphatidylinositol monophosphate-binding interface in the oomycete RXLR effector AVR3a is required for its stability in host cells to modulate plant immunity.* Proc Natl Acad Sci U S A, 2011. **108**(32): p. 14682-14687.
96. Feng, F. and J.-M. Zhou, *Plant–bacterial pathogen interactions mediated by type III effectors.* Current Opinion in Plant Biology, 2012. **15**(4): p. 469-476.
97. Win, J., et al., *Effector biology of plant-associated organisms: concepts and perspectives.* Cold Spring Harb Symp Quant Biol, 2012. **77**: p. 235-47.
98. Qiao, Y., et al., *Oomycete pathogens encode RNA silencing suppressors.* Nat Genet, 2013. **45**(3): p. 330-3.
99. Wong, J., et al., *Roles of small RNAs in soybean defense against Phytophthora sojae infection.* Plant J, 2014. **79**(6): p. 928-40.
100. Xiong, Q., et al., *Phytophthora Suppressor of RNA Silencing 2 Is a Conserved RxLR Effector that Promotes Infection in Soybean and Arabidopsis thaliana.* Mol Plant Microbe Interact, 2014. **27**(12): p. 1379-89.
101. Qiao, Y., et al., *Phytophthora effector targets a novel component of small RNA pathway in plants to promote infection.* Proc Natl Acad Sci U S A, 2015. **112**(18): p. 5850-5.
102. Wang, X., et al., *A host KH RNA binding protein is a susceptibility factor targeted by an RXLR effector to promote late blight disease.* Mol Plant, 2015.

103. Browse, J., et al., *JAZ repressor proteins are targets of the SCFCO11 complex during jasmonate signalling.* Nature, 2007. **448**(7154): p. 661-U2.
104. Jiang, S., et al., *Bacterial effector activates jasmonate signaling by directly targeting JAZ transcriptional repressors.* PLoS Pathog, 2013. **9**(10): p. e1003715.
105. Gimenez-Ibanez, S., et al., *The bacterial effector HopX1 targets JAZ transcriptional repressors to activate jasmonate signaling and promote infection in Arabidopsis.* PLoS Biol, 2014. **12**(2): p. e1001792.
106. Evangelisti, E., et al., *The Phytophthora parasitica RXLR effector penetration-specific effector 1 favours Arabidopsis thaliana infection by interfering with auxin physiology.* New Phytol, 2013. **199**(2): p. 476-89.
107. Cui, F., et al., *The Pseudomonas syringae type III effector AvrRpt2 promotes pathogen virulence via stimulating Arabidopsis auxin/indole acetic acid protein turnover.* Plant Physiol, 2013. **162**(2): p. 1018-29.
108. Lee, C., et al., *The novel cyst nematode effector protein 19C07 interacts with the Arabidopsis auxin influx transporter LAX3 to control feeding site development.* Plant Physiol, 2011. **155**(2): p. 866-80.
109. Pritchard, L. and P. Birch, *A systems biology perspective on plant,Äìmicrobe interactions: Biochemical and structural targets of pathogen effectors.* Plant Science, 2011. **180**(4): p. 584-603.